DEPOSITION AND COVALENT IMMOBILIZATION OF PORPHYRIN AND MALEIMIDE ON A SI(111) SURFACE

Dissertation

zur Erlangung des akademischen Grades

doctor rerum naturalium (Dr. rer. nat.)

im Fach: Chemie
Spezialisierung: Physikalische und Theoretische Chemie

Eingereicht an der
Mathematisch-Naturwissenschaftlichen Fakultät der Humboldt-Universität zu Berlin
von

M.Sc. Kristina Lovrek

Präsidentin der Humboldt-Universität zu Berlin

Prof. Dr.-Ing. Dr. Sabine Kunst

Dekan der Mathematisch-Naturwissenschaftlichen Fakultät

Prof. Dr. Elmar Kulke

Gutachter*innen: 1. Prof. Dr. Klaus Rademann

2. Prof. Dr. Norbert Esser

3. Prof. Dr. Kannan Balasubramanian

Tag der mündlichen Prüfung: 12.03.2020

ABSTRACT

A growing body of research focuses on developing novel functional materials and their integration in microelectronic and sensing devices. Modern civilization relies on the use of computers and microelectronics in every area of life. Most of these devices are built from silicon, thus making silicon one of the most researched materials in the scope of materials science and technology.

In this thesis, a study on the covalent immobilization of a couple of porphyrin derivatives and a *p*-maleimidophenyl species (*p*-MP) on Si(111) surface is presented to investigate how do reaction parameters influence the deposition and the quality of organic layers. Porphyrins are optically-active, energy-transferring, catalytic materials. Maleimide is a thiol-selective molecule typically used as a cross-linker for the immobilization of biomolecules. As such, they are both essential materials for application in silicon-based sensing and organic electronics. Covalent bonding of the organic materials with the surface increases the stability of the entire organic/silicon system is, therefore, necessary for extending the longevity of the material and transferring the innovation from the lab to widespread commercial use. The thin films are deposited with "wet chemistry" methods, including deposition from solution and electrografting. The prepared structures are analyzed with a variety of surface sensitive techniques, namely, IR ellipsometry, XPS, SEIRA, and IR reflection spectroscopy.

All depositions in this work are conducted in situ, in addition to the ex situ reactions, to gain an understanding of the film growth and deposition rates. The study on porphyrin thin films focused on the conditions of material deposition leading to an established chemical bond. Solution reactions of porphyrin derivatives with (3-aminopropyl)trimethoxysilane indicate that the reaction with the pre-activated porphyrin derivative leads to a better yield than with the in situ-activated porphyrin. However, when this reaction is transferred to the surface by using the layer-by-layer deposition approach, the reaction with the surface-bound aminosilanes molecules takes place at a much slower rate than the same reaction in solution. The key challenge is to identify the amide bond formed between the porphyrin and the organosilane molecules, due to low layer thickness. The combination of surface sensitive methods is utilized for the identification of the amide bond. An alternative synthetic approach, where the product is prepared in solution and then deposited on the oxidized Si substrate, is proposed. The spectral signature of such films is dominated by amide bands with very little contribution from starting materials. A parallel in situ study on *p*-MP electrografting on the H-terminated Si(111) surface provides details on the thin film formation in a monolayer and a sub-monolayer regime. The spectral features of the maleimide film are observed already after less than 1 s of deposition. The spontaneous grafting of *p*-MP is also monitored in situ. It was found that the formation of a monolayer during the electroless deposition takes longer than an electrochemical deposition. A cationic mechanism is proposed as an alternative to a radical mechanism, in which the monolayer formation involves the reaction of an aryl cation with the Si-H instead of an aryl radical.

The synthetic and mechanistic insights from this study contribute to a prosperous research area on surface modification with organic materials and a broader area of organic electronics and their diverse application.

ZUSSAMENFASSUNG

Ein wachsender Forschungsschwerpunkt liegt auf der Entwicklung neuartiger Funktionsmaterialien und deren Integration in mikroelektronische Geräte und Sensorvorrichtungen. Die moderne Zivilisation ist auf den Einsatz von Computern und Mikroelektronik in allen Lebensbereichen angewiesen. Die meisten dieser Bauelemente bestehen aus Silizium, wodurch Silizium einer der am besten erforschten Werkstoffe auf dem Gebiet der Materialwissenschaften und -technologie ist.

In dieser Arbeit wird eine Studie zur kovalenten Immobilisierung einiger Porphyrinderivate und einer p-Maleimidophenyl-Spezies (*p*-MP) auf der Si (111)-Oberfläche vorgestellt. Hierbei lag der Schwerpunkt auf der Untersuchung des Einflusses von Reaktionsparametern auf die Abscheidung und die Qualität organischer Schichten. Porphyrine sind optisch aktive, energieübertragende, katalytische Materialien. Maleimid ist ein Thiol-selektives Molekül, das typischerweise als Vernetzer zur Immobilisierung von Biomolekülen verwendet wird. Als solche gehören Porphyrine und Maleimid zu den wesentlichen Materialien für die Anwendung in der siliziumbasierten Sensorik und in der organischen Elektronik. Die kovalente Bindung der organischen Materialien an die Oberfläche erhöht die Stabilität des gesamten Organik-Silizium-Systems. Es ist daher notwendig, die Lebensdauer des Materials zu verlängern und die Innovation aus dem Labor auf eine weit verbreitete kommerzielle Nutzung zu übertragen. Die dünnen Schichten werden mittels nasschemischer Methoden abgeschieden. Dies beinhaltete die Abscheidung aus der Lösung und die Elektroaufpfropfung. Die hergestellten Strukturen werden mit einer Vielzahl oberflächensensitiver Messtechniken wie der IR-Ellipsometrie, der XPS-, der SEIRA- und der IR-Reflexionsspektroskopie analysiert.

Alle Abscheidungen in dieser Arbeit werden in situ durchgeführt, zusätzlich zu den ex situ Reaktionen, um das Verständnis der Filmwachstums- und Depositionsgeschwindigkeiten zu erhalten. Bei der Untersuchung der Porphyrin-Dünnschichten lag der Fokus auf den Bedingungen der Materialabscheidung, welche zur Ausbildung einer chemischen Bindung notwendig sind. Die Lösungsreaktionen von Porphyrinderivaten mit APTMS zeigen, dass die Reaktion mit dem voraktivierten Porphyrinderivat zu einer besseren Ausbeute führt als mit dem in situ aktivierten Porphyrin. Wenn diese Reaktion jedoch unter Verwendung des Schicht-für-Schicht-Abscheidungsprinzips auf die Oberfläche übertragen wird, findet die Reaktion mit den oberflächengebundenen Aminosilanmolekülen mit einer viel langsameren Geschwindigkeit statt als die gleiche Reaktion in Lösung. Aufgrund der geringen Schichtdicke besteht die zentrale Herausforderung darin, die Amidbindung zwischen den Porphyrin- und den Organosilanmolekülen zu identifizieren. Zur Identifikation der Amidbindung wird die Kombination von oberflächensensitiven Methoden verwendet. Es wird ein alternativer Syntheseansatz vorgeschlagen, bei dem das Produkt in Lösung hergestellt und dann auf dem oxidierten Si-Substrat abgeschieden wird. Die spektrale Signatur dieser Schichten wird von Amidbanden dominiert und der Beitrag der Ausgangsmaterialien ist gering. Eine weitere in situ-Studie zum *p*-MP-Elektropfropfen auf der H-terminierten Si (111) -Oberfläche liefert Details zur Dünnschichtbildung im monolagigen und im sub-monolagigen Bereich. Die spektralen Merkmale der Maleimidschicht werden bereits nach weniger als 1 s Abscheidungsdauer beobachtet. Die spontane Pfropfung von *p*-MP wird ebenfalls in situ überwacht. Es wurde festgestellt, dass die Bildung einer Monoschicht während der stromlosen Abscheidung länger dauert als bei einer elektrochemischen Abscheidung. Als Alternative zum Radikalmechanismus wird ein kationischer Mechanismus vorgeschlagen, bei dem die Reaktion mit dem Si-H und dem Aryl-Kation, anstelle eines Aryl-Radikals, zur Bildung der Monoschicht führt.

Die synthetischen und mechanistischen Erkenntnisse aus dieser Studie tragen zu einem vielversprechenden Forschungsbereich der Oberflächenmodifikation mit organischen Materialien und zu einem breiten Gebiet der organischen Elektronik und ihrer vielfältigen Anwendung bei.

LIST OF ABBREVIATIONS

Abbreviation	Meaning
p-MP	Maleimidophenyl
LbL	Layer-by-layer
XR	X-Ray reflectivity
TPP	Tetraphenylporphyrin
TPyP	Tetrapyridylporphyrin
PPIX	Protoporphyrin IX
Pc	Phtalocyanine
SiNWs	Silicon nanowires
SMP	*N*-Succinimidyl 3-maleimidopropionate
XPS	X-Ray photoelectron spectroscopy
NHS	*N*-Hydroxysuccinimide
IgG	Immunoglobulin G
APTES	(3-Aminopropyl)triethoxysilane
IRSE	Infrared spectroscopic ellipsometry
BSA	Albumin from bovine serum
Con A	Concanavalin A
PL	Poly-L-lysine
EQCM	Electrochemical quartz crystal microbalance
IMFP	Inelastic mean free path
APTMS	(3-Aminopropyl)trimethoxysilane
CTTPS	5-(4-Carboxyphenyl succinimide ester)-10,15,20-(triphenyl)porphyrin
SEIRA	Surface-enhanced IR absorption
EEDQ	*N*-Ethoxycarbonyl-2-ethoxy-1,2-dihydroquinoline
DMSO	Dimethylsulfoxide
ACN	Acetonitrile
NBA	*p*-Nitrobenzoic acid
CTPP	5-(4-Carboxyphenyl)-10,15,20-(triphenyl)porphyrin
MBN	Mercaptobenzonitrile
DMF	Dimethylformamide
iPrOH	*iso*-Propanol
LO	Longitudinal optic
TO	Transverse optic
DFT	Density functional theory

CONTENTS

1 INTRODUCTION

1.1 THESIS STATEMENT AND MOTIVATION

"Deposition conditions influence the quality and the structure of thin organic film on silicon."

This thesis aims to characterize thin films of organic materials on the silicon(111) surface immobilized through covalent bonds by employing different deposition techniques and probing them with surface-sensitive spectroscopic techniques. Furthermore, in situ techniques are used to gain information on the real-time surface attachment and the deposition rates. Deposition parameters like time of deposition, the use of activated forms of molecules, the reaction environment (solution vs. surface), applied voltage, and the way of deposition (layer-by-layer vs. direct) are studied to define their influence on the quality of deposited layers.

Today, nearly all electronics are silicon-based, but they are approaching the limits of miniaturization. Hybrid materials are suggested as a possible alternative to utilize in modern electronic and sensing devices. Hybrid materials are a combination of organic and inorganic material, forming a new material that demonstrates the combined properties of both.[1] Thus, the modification of silicon surface with organic material combines already established properties of bulk silicon with transformed surface chemistry. Such a surface is called "tuned." Tuning can change chemical, biochemical, mechanical, kinetic, optic, or electronic properties of a substrate.[2–4] Molecular bonds, sterics, conjugation, and electronic properties can be manipulated according to the desired function and should provide:

(i) a stable surface,

(ii) modifiable surface properties, and

(iii) the possibility to interact with other molecules or substrates.

This technology, however, is still a subject of a fundamental research, although there are some examples of successful commercial application: organic light-emitting diodes (OLED) and quantum dots for displays, OLED lighting, and organic photovoltaics.[5] Understanding how to achieve the reproducibility of the material, and the events taking place during the molecular surface attachment will contribute to the optimization of material preparation and thus transfer of these materials from the laboratory to industrial-scale production. When hybrid materials are integrated into electronic devices, they are called organic electronics.

At the Chemical Science and Society Summit in 2012, scientists have identified four significant research challenges to overcome before organic electronics can reach peak commercial consumption.[6]

1) Improving control over the self-assembly of organic materials to achieve reproducibility. To meet this challenge, a deep understanding of the electronic properties of organic materials and their change when in contact with other (inorganic) materials is required.
2) To understand the events happening during the material deposition at the interface, like mechanisms of elementary processes and structural and chemical changes, better analytical tools need to be developed. New tools should be sensitive, non-destructive, non-invasive, and high-speed.
3) Improving existing 3D processing technologies for industrial upscaling.
4) Developing multifunctional organic electronics since many organic molecules possess two or more properties.

In this work, two technologically important organic materials, porphyrin and maleimide, are chosen. Porphyrin is chosen in this study due to its versatile properties with potential applications in electronics, while maleimide is chosen as an important linker molecule in constructing biosensing systems.

Porphyrins are a class of naturally-occurring molecules with unique structural and chemical properties. They strongly absorb light in the visible region, have planar, aromatic ring structure with a highly delocalized π-system, and the center of a porphyrin ring has an affinity for coordinating metal cations.[7] As such, they have a potential application in optoelectronic,[8–10] photon harvesting,[11] photovoltaics,[12] molecular information storage,[13] sensing,[9,10,14,15] and catalytic devices,[16,17] as well as medical applications.[18,19]

Porphyrins on silicon have been structurally well-characterized with many different surface analysis techniques.[20–31] Furthermore, scientists have established that they retain their interesting properties when deposited on a silicon surface.[8,11,30–41] When it comes to the immobilization of porphyrin through organosilanes on silicon, halosilanes are mostly used as a linker molecule.[8,20,21,42–44] Halide functional groups (mostly Cl^- and I^-) are reactive and readily undergo further reactions. However, in many cases, halides (especially chlorides) are too reactive and not selective at all, possibly leading to side reactions with other molecules (i.e., solvent) and not just the target molecule. Also, halide chemicals are not suitable for the environment. It would be synthetically advantageous to have the desired functionality deposited directly on the surface. Therefore, using organosilanes with other functionalities for porphyrin immobilization should also be investigated. In this study, (3-aminopropyl)trimethoxysilane is used for the immobilization of porphyrins on a silicon surface through an amide bond.

Maleimide is an organic compound selective towards thiol functional groups. Maleimide and thiol undergo thiol-Michael addition forming a stable thioether bond.[45] Thiol groups can be found in biomolecules in cysteine residues. As such, the thiol-maleimide reaction can be used for site-specific reactions when immobilization of large protein molecules is desired.[46]

In earlier studies of surface modification with maleimide, the covalent, robust attachment is achieved with several different chemistries (silane chemistry, hydrosilylation, phosphonate chemistry, polymers, electrografting).[47–65] The research shows best surface coverage with direct molecular deposition, as well as a tunability of the layers with capping molecules.[52] Electrografting of maleimidophenyldiazonium salt (*p*-MPDS) on the H-terminated Si surface is a quick and reliable way to introduce functionality to an electrode surface. Zhang et al. described a formation of a first maleimidophenyl (*p*-MP) monolayer after 60 s at -2 V and proved the biosensing possibility of a maleimide-modified surface,[62] while Kanyong et al. measured the 50% grafting efficiency after the first potential scan and determined the monolayer thickness.[63] However, a more in-depth look at the events happening at the surface during the formation of a first monolayer is needed towards achieving the reproducibility of the system.

This work aims to contribute to the research of porphyrin and maleimide thin films by looking into their structure, deposition pathways, and reaction mechanisms. The key research question this study addresses is:

- How do reaction parameters influence the quality of the organic thin films?

In addition to the key research question, the research of this study could be broken down in several sub-questions as follows:

- Can we characterize/assign amide bands in a thin layer of a porphyrin/organosilane system with available surface sensitive techniques (IR ellipsometry, XPS, SEIRA, IR reflectometry)?
- Do thin films structurally (and spectroscopically) differ when deposited layer-by-layer (LbL) vs. direct deposition? How robust are those films?
- What is the shortest deposition time for electrochemical deposition of a maleimide at which the ellipsometric signal can be observed?
- What is the time scale of *p*-MP deposition when electricity is not applied to the system? What is the mechanism of such a reaction? Is it feasible to still assume a radical mechanism?

1.2 Silicon surface chemistry and modification

Silicon is one of the best-researched semiconductor materials, well-integrated into existing technologies due to its low cost, tunable electronic properties, and ease of manufacturing.[66] Thus, silicon is an excellent choice as a substrate for research on hybrid materials with the aim of integration in electronic and bioelectronic devices for organic electronics, biosensing, medical diagnostics, organic photovoltaics, and many other applications.[67–72] To construct and utilize novel hybrid materials, it is crucial to understand the interfacial chemistry of the material and how its properties manifest in contact with another material. The interfacial changes have an impact on the device performance, as material properties are intimately related to their surface arrangement. Therefore, a systematic characterization is required, from the primary attachment event and surface coverage to the dynamics of film growth, to

understand the changes in the system. Even though silicon is by no means the only industrial semiconductor, it provides the best compromise between stability, biocompatibility, and the maturity of the semiconductor processing technology.

When developing hybrid materials, it is of interest to understand how the molecular attachment will affect the surface properties and vice versa. A molecule known for particular properties that it exhibits in solution might have changed properties when interacting with the surface. The surface can either enhance or diminish the properties of the deposited material. One of the biggest concerns of materials scientists is how to immobilize the molecule on the surface without diminishing its desired properties.

The silicon surface is reactive towards the oxygen from the air. It is naturally always covered with a few nanometers of native oxide.[73] In existing electronics, the oxide layer is beneficial as it protected against corrosion of the reactive silicon underneath. The semiconductor properties of bulk silicon are strong enough to override the insulating nature of the oxide. However, in microelectronics and hybrid materials, as the silicon substrate gets thinner and smaller, the oxide starts to present a problem, as it presents an additional insulating barrier between the organic layer and bulk silicon.[74]

Native oxide is chemically similar to other silicon oxides (e.g., glass), suggesting inhomogeneity and variability of surface species.[73] Prevailing surface species in silicon surface oxide are siloxane (Si-O-Si) and silanol (Si-OH) groups.[73] Chemical variability of surface species leads to difficulties in the reproducibility and homogeneity of the subsequent modifications. Additionally, the silicon/silicon oxide interface has a high density of electronic defects.

Nevertheless, provided that the silicon oxide layer remains thin (and depending on the final use of the material), the presence of the native oxide affords a convenient route for surface modification. One of the most popular strategies for surface modification is the immobilization of organosilane molecules or silanization. During silanization, organosilanes react with surface Si-OH groups, forming a covalent Si-O-Si network. They become integrated into an existing Si-O-Si network of the native oxide. The downside of this modification routes is that Si-O-Si bonds hydrolyze under neutral or basic pH conditions.[75,76] Nevertheless, it is still used routinely in many applications.

Today, it is possible to bypass surface oxides altogether by attaching materials directly to the silicon. The most promising route of chemical modification is direct Si-C bond formation.[77,78] Si-C bond possesses greater stability than Si-O because of lower bond polarity and high bond strength.[79] Due to its electronegativity, oxygen enhances the nucleophilicity of silicon in the Si-O bond.[80] This is not the case with less electronegative carbon. Organic films immobilized through a Si-C tether ideally have long-term stability, unlike alkoxysilane-modified surfaces.[81]

When the native oxide is removed, a “clean” silicon surface is obtained. The “clean” surface tends to undergo complex reconstructions associated with the loss of coordination of the surface silicon atoms.[73] To preserve the coordination of the silicon surface, it is a common practice to strip away the native

oxide chemically with fluoride ion or thermally under ultrahigh vacuum conditions, and cap silicon atoms with precursors such as hydrides (-H) or halides (-X, X = Cl, I, Br). The chemical replacement creates well-defined, low-defect metastable surface ready to carry out further modifications.[73]

The metastable surface must be stable enough in the atmospheric conditions and the presence of solvent vapors and other impurities, but still reactive enough to undergo further chemical reactions and form a Si-C bond. The H-terminated surface is stable in air for tens of minutes and, therefore, preferably used. The X-terminated surfaces are much more reactive and are handled exclusively under an inert atmosphere.

The electrical and other properties of a hybrid material and the sensitivity of the underlying silicon substrate to oxidation depend on the quality of monolayers. Establishing control over the surface density of the attachment sites leads us one step closer to preparing reproducible, uniform, and well-defined molecular arrays and structures. The complete surface site saturation is very rare and happens only for small organic molecules. Other molecules are big enough to hinder surrounding surface sites.

The deposition of organic material may result in the formation of a molecular monolayer, multilayer, or a polymer.[82] When depositing a monolayer, high packing density is required to create a stable surface. Thus, the goal is to achieve a high uniformity of molecules. Ultimately, the size and the structure of molecules determine the limits of packing density and, accordingly, surface sensitivity. Chidsey et al. showed that on the Si(111) surface linear alkyl chains pack in 2x1 substitution (one molecule for every two Si atoms), which corresponds to about 50% substitution, while the remaining reactive sites are sterically hindered and unreactive.[78,83] The experiments are confirmed with theoretical calculations.[84,85] Figure 1.1 shows a model of a substrate surface with a 50% substitution. One can notice that even with "only" 50% coverage, the surface is densely covered due to molecular tilting and physical interaction with other surrounding molecules. Meanwhile, unreacted surface sites are entirely protected from the environment above the organic monolayer.

For non-linear, bulkier organic molecules, the steric hindering is even greater. Physical forces might also cause the lingering of unreacted material on the surface, either through interaction with surface groups or between molecules, thus hindering both the available surface sites and the functionalities of the already deposited molecules.

If so required, the surface coverage may be completed by inserting chelating agents,[86] capping remaining unreacted sites with small molecules or mixed layers.[87] Mixed monolayers can either be passive or used to introduce new functionalities to the surface.[39]

If a deposited molecule has a functional group attached, the formed layer can be further functionalized in a manner of an LbL deposition. However, due to steric and other factors, not all of the functional groups will undergo a reaction, leading to more defects and non-uniformity of the layer. That is why it is advisable to connect the desired molecules directly to the surface whenever possible.

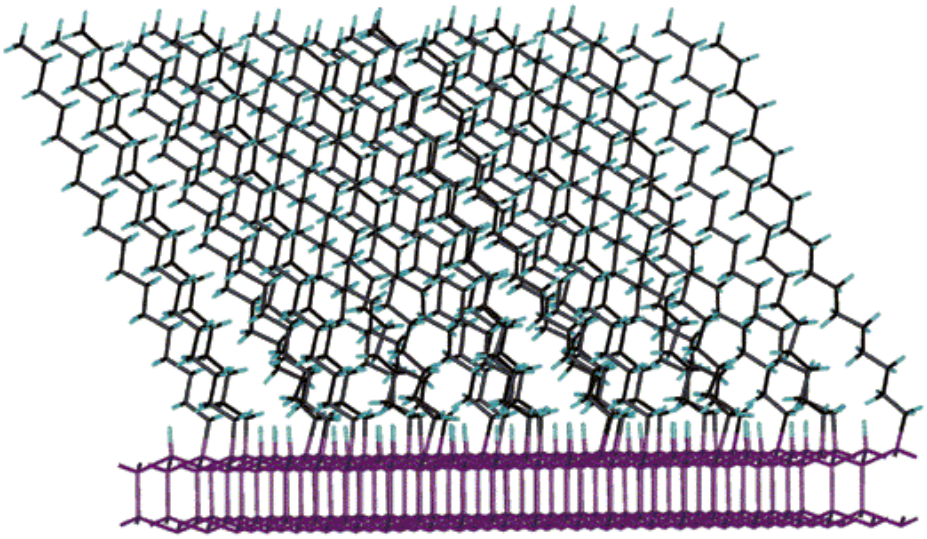

Figure 1.1: *Example of a structure of an alkyl monolayer with 50% coverage as obtained with molecular mechanics simulations using the polymer consistent force field calculations. Reprinted with permission from Sieval et al.[84] © 2001 American Chemical Society.*

Although most of the research on covalent attachment of organic material to silicon is done on flat surfaces, the findings on chemical immobilization may be used as a basis for research on non-planar silicon structures like nanowires, nanoparticles or porous silicon. The non-planar structures have the advantage of having the greater surface area available for the reaction. A greater surface area implies a higher sensitivity of the system, even down to the single-molecule detection.[70,88]

A more detailed account of silicon surface chemistry can be found in the following cited references.[73,89–91]

Organic molecules can attach to the surface covalently or through non-covalent interactions. Non-covalent (physical) interactions happen through directional intermolecular and molecule-surface interactions. Such physical interactions lead to the stacking of the molecules on the surface known as self-assembly. Self-assembly is the tendency of the molecules to create well-ordered and densely packed molecular monolayers on the interface.[3]

Depending on the ultimate application of the material, both physical and chemical attachment can be a valid surface modification option. Covalent attachment is desirable, e.g., when the immobilization of more massive (bio)molecules is needed. Weaker physical bonding is hardly able to keep biomolecules fixed to the substrate under industrial conditions. Covalent attachment is practical and durable, and as such, it provides greater stability of the layer. Covalent attachment of organic molecules to silicon is desirable, especially in the context of large-scale production. Harsh manufacturing conditions require the stability of both the surface and the organic film. Even the smallest imperfection in a microstructure,

a defect or an impurity, can significantly influence the properties of the material. The understanding of the structure-property relationship at the molecular level is, therefore, essential.

1.3 PORPHYRIN AS A FUNCTIONAL MATERIAL

1.3.1 General features

Porphyrins are a group of macroheterocyclic compounds. Each porphyrin derivative has the same core structure called porphine. Porphine consists of four modified pyrrole subunits connected via methine (=CH-) bridges to form an aromatic ring structure (Figure 1.2a).[92] The center of the ring consists of four pyrrolic nitrogens, of which two are hydrogenated in its free form. However, the center can easily be metallated, forming a tetradentate ligand with a metal (Figure 1.2a).[7] Metalloporphyrins are then available to coordinate or react with other species trough metallic center, which can influence reversible changes of electronic configuration like oxidation or spin states.[7,93] The porphine ring can be chemically modified at methine bridges (*meso*-substituents) or pyrrolic carbons (β-substituents) with virtually any functional group, thus providing versatility and tunability of material properties. In Figure 1.2b, the structures of the most commonly used porphyrin derivatives are depicted, namely, tetraphenylporphyrin (TPP), tetrapyridylporphyrin (TPyP), phthalocyanine (Pc), and protoporphyrin IX (PPIX).

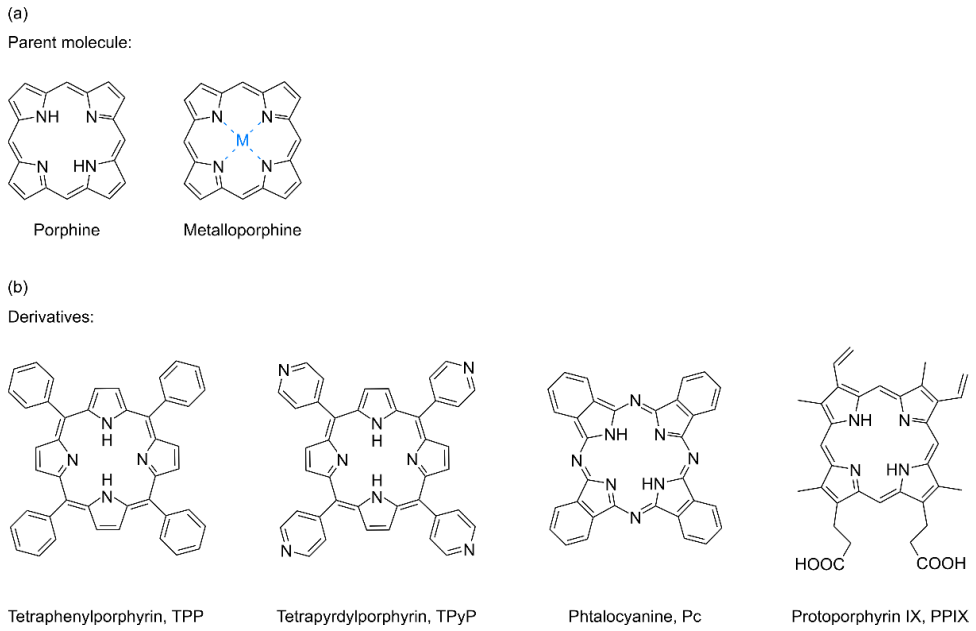

Figure 1.2: *(a) Structures of a porphine, a parent molecule to all porphyrins, and its metal-coordinating counterpart; (b) Structures of the most common porphyrin derivatives used in research.*

The porphyrin structure is aromatic, with an extensive 18π conjugated electron system giving them an intense absorption band in the visible range.[7,94] While the porphine macrocycle is planar in the gas phase, the same is not valid for all its derivatives. When substituents rotate around the bond connected to the porphyrin ring, they often cannot align co-planar with the macrocycle either due to a steric

hindrance or their inherent non-planarity. Experiments showed that for the phenyl substituents in all four *meso*- positions, their planar orientation is energetically very demanding.[93] Especially the *meso*-substituents tend to re-orientate through interactions with other molecules in the solvent.

On the solid substrate, macrocycle may deform during the adsorption, settling into a so-called "saddle-shape" formation.[7] The environment may also influence the electronic structure of porphyrins, that is, deform their molecular orbitals. For example, when porphyrin self-assembled monolayers are deposited on a metal substrate, a charge transfer from the substrate to porphyrin molecules occurs, possibly due to a change in the oxidation state of a metal ion in the center of the molecule.[95]

Electronic and conformational features of porphyrins play a significant role in the dynamic behavior of adsorbed molecules, affecting the functionalities of the molecules and the self-assembly process. This knowledge can be used for fine-tuning of molecular dynamics and thin film properties by choosing the right functional groups, metal ions, surface interactions, or conformational adaptations.[96] Thus, it is of fundamental interest to learn about the impact of those changes on the molecular properties of porphyrins.

Porphyrins are also highly stable, and the redox reactions are reversible under the right conditions.[97] As large aromatic systems, porphyrins have HOMO-LUMO energy gaps in a realistic operational range applicable in electronics.[8] Due to their extended conjugation, they may form π-cation radicals relatively stable under ambient conditions. It is also possible to synthesize porphyrins which display multiple cationic states which operate at relatively low potentials.[98] Porphyrins can also store charge up to several minutes even without the applied potential.[28,98–100] These particular characteristics allow the exploration of porphyrins for multibit information storage with low power consumption while diminishing the refresh rates required in a memory device.[13] The thermal stability of porphyrins allows molecules to easily endure the temperatures of up to 400°C, which is a pre-requisite in the electronics manufacturing industry.[101,102]

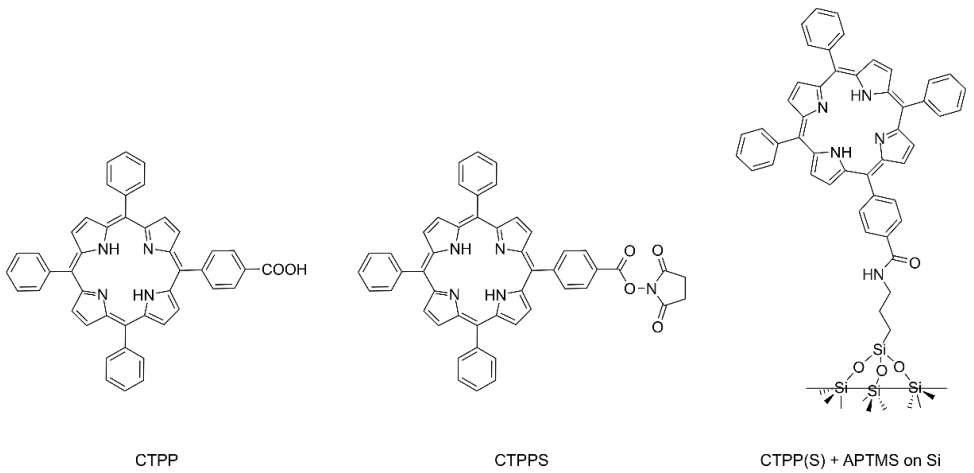

***Figure 1.3**: Schemes of porphyrin derivatives used in this work, CTPP and CTPPS, and their product with APTMS, CTPP(S)+APTMS.*

The aromaticity of the porphyrin macrocycle sets a basis for the semiconducting properties of porphyrins. If the macrocycles are stacked in such a manner that the π-bonding regions are near each other, then that interaction enables electron mobility through molecules resulting in an electron transfer.[103] Also, the conjugation of a molecule may be extended through covalent linkage with other conjugated molecules when aligned in the plane parallel to the macrocycle, assuring a long-range transfer.[104,105]

Due to their specific structural properties, porphyrins are stable compounds capable of absorbing light, transferring electrons, and catalyzing the reactions. Therefore, they are often investigated as molecular diodes, rectifiers, wires, capacitors, solar cells, memory devices, catalysts, and so forth.[12,13,35,39,40,106–109] Basic research on the porphyrin thin film structure on silicon and their properties related to the application are described below.

In this work, two TPP derivatives are used, 5-(4-carboxyphenyl)-10,15,20-(triphenyl)porphyrin (CTPP) and 5-(4-carboxyphenyl succinimide ester)-10,15,20-(triphenyl)porphyrin (CTPPS). Both derivatives are depicted in Figure 1.3. CTPPS is an activated form of a CTPP (activated with *N*-hydroxysuccinimide). Usually, for the coupling of carboxyl and amino groups to form a stable amide bond, an activator is needed to make a better leaving group (activated ester).[110,111] For the reaction with APTMS, CTPP is activated in situ with EEDQ before the reaction, while CTPPS is purchased as a pure activated form.

1.3.2 Literature overview

Porphyrins are known to create highly ordered, closely-packed monolayers when immobilized with an organosilane linker.[20] Mostly, researches have used *meso*-substituted porphyrins, but *β*-substitution is explored as well with a direct attachment to the surface. However, this resulted in only medium coverage and surface oxidation in air.[112] Therefore, *meso*-modified porphyrin derivatives are the preferred choice for silicon surface modification.

Some fascinating research has explored the direction of LbL deposition of multiple porphyrin layers with α,α'-dichloro-p-xylene as a linker (Ln) between porphyrin rings.[21] Spectroscopic characterization of a film structure revealed densely packed monolayers and ten bi-layers which are present even after prolonged sonication experiments in various organic solvents.[21]

Cu(I)-catalyzed azide-alkyne cycloaddition is another example of multilayer formation used both for monolayer immobilization and multilayer growth.[24] Specular X-ray reflectivity (XR) measurements and modeling of ellipsometric data indicated a high degree of linearity in multilayer growth, achieving 19 porphyrin-Ln bilayers, and, notably, their reproducibility across 23 different samples.[24]

Doping of a multilayer porphyrin film with Br_2 caused a redshift in electron absorption spectra of the films, indicating the removal of electron density from the core porphyrin ring rather than from pyridyl groups.[21]

Another immobilization path relies on the transesterification reaction of tetrahydroxy-TPP reacting with an immobilized 10-undecylenic acid methyl ester.[27] Characterization of the film structure indicated a vertical alignment of the porphyrin molecules, with each porphyrin molecule binding to the surface through one or two -OH groups, while others remain available for further modification.

In one instance, the researchers successfully prepared densely packed, long linear porphyrin structures (up to 10 μm) on chlorosilane functionalized Si(100) surface.[42] The structures had an average width of 40-60 nm and a height of ~2.4 nm corresponding to a single monolayer.[42] The linear assembly is rare for silane-functionalized surfaces as they tend to arrange in an amorphous network. However, the choice of a substrate might influence the ordering in deposited films. Additionally, since, in this case, a reaction between individual porphyrin molecules is not expected, one might assign the ordering of the structures also to the π-π stacking interactions, leading to an overlap between the electronic states of individual porphyrin units.

By varying the synthetic conditions, the choice of anchoring atom or moiety, solvent, or even the substrate pre-functionalization, one can influence the process of molecular immobilization and the quality of the resulting structure. Zanoni et al. derivatized porphyrins with different functionalities attached to their structure, different metal centers, and deposited on I-terminated Si(111) and Cl-terminated silicon (100) surfaces.[25] The derivatives are used for XPS studies on the definition of actual electronic states of free-base and metalloporphyrins on silicon by locating their N 1s binding energies.[25]

The N 1s spectra of neat monohydroxy-TPP and tetraethynyl-TPP contain two pairs of unprotonated and protonated nitrogens in a core porphyrin ring at ~398 eV and ~400 eV, respectively. When the porphyrin is metallated, the two peaks converge into one peak at ~399 eV, as the nitrogens are now equally ligated to the metal atom.

However, when deposited on a silicon substrate, the N 1s region becomes a complex peak, even with metalloporphyrins. A thorough investigation revealed that the actual electronic state of immobilized porphyrins (both free-base and metal complex) is at the energy corresponding to demetallated porphyrins after the deposition on the surface (~400.5 eV). The peak is assigned to a diacidic nitrogen derivative carrying a 2+ charge on the ring.[113] Since demetallation requires acidic conditions, it is suspected that protons are produced locally at reaction sites. This discovery is essential for all similar measurements in the future, enabling quick and exact identification of porphyrin species on the surface.

The kinetics of monolayer deposition and film growth vary depending on the type of porphyrin derivative, as well as the type of substrate. For a silicon substrate, a couple of studies are conducted to investigate these dynamics.[26,114]

Lu et al. explored the kinetics of spontaneous grafting of the aryldiazonium porphyrin salts to the H-terminated silicon surface.[114] For this purpose, a TPP derivative bearing a diazonium moiety, as well as its Cu(II), Zn(II), and Co(II) complexes are synthesized. Upon deposition, the film thickness of a free-base analog increased to tens of nanometers with varying concentrations and deposition time.

Meanwhile, the Zn(II)- and Co(II)-analogues showed considerably slower film growth with 4-30 times thinner films for the same concentration and reaction time. The crucial step in the deposition mechanism is the formation of a radical species from the diazonium salts because metalloporphyrin radicals have low stability.[115] It is suggested that due to this low stability, the concentration of the active species is relatively low, leading to slower film growth.

Gadenne et al. looked into the structure and growth mechanism of different porphyrin derivatives, namely of Zn(II)- and Fe(II)-protoporphyrin (Zn(II)-PPIX and Fe(II)-PPIX), and Zn(II)-phthalocyanine (Zn(II)-Pc) on an aminosilane-modified silicon surface.[26] The data revealed that each derivative has a different rate of film formation, the extent of film formation, and the number of mechanism steps.[26]

Adsorption of Zn(II)-PPIX happens in 3 successive steps. The mechanism begins with 20-second adsorption of porphyrin molecules on the surface. Since the thickness of the layer is less than a theoretical length of the molecule, and the UV/vis spectra are similar to those in solution, it is a clear indication of a disordered layer. The first step is followed by a 19-minute latency phase in which molecules re-arrange on the surface, making space for more molecules. The second step creates a Zn(II)-PPIX monolayer, according to thickness measurements. Finally, the third step lasts 150 minutes, during which a second monolayer is formed through a head-to-tail insertion of Zn(II)-PPIX molecules into the first monolayer, thus maximizing the stacking interaction between porphyrin cores.

The film growth for Zn(II)-Pc stops after the formation of a first monolayer, while Fe(II)-PPIX never achieves a full monolayer formation. Instead, they resume in the form of disordered layers, oriented flat on the surface, possibly because Fe atom interacts with surface amine groups.[26]

Due to the ability to complex with the metal atoms, porphyrin properties can be fine-tuned using different metal cations,[44] and are researched as catalysts.[40] Porphyrins on silicon nanowires (SiNWs) demonstrate stable photocurrent behavior when irradiated with white light and recovery to the original state when the irradiation is off.[8] The measured photocurrent value is three times higher as the value obtained for nanowires only and 13 times higher as the value for the porphyrin/flat Si system.[8] Finally, porphyrins are known photosensitizers. The fluorescence decay curves show shorter decay lifetimes demonstrate higher degree of fluorescence quenching with shorter linkers.[11] Combined with gold nanoparticles, porphyrin monolayers on Si exhibit both strong plasmons from nanoparticles and strong luminescence from porphyrins.[43] Porphyrins are mostly known for their application in photodynamic therapy for skin treatments and cancer research. When immobilized on silicon nanoparticles together with mannose, the experiments with cancerous cells result in up to 75% cell death.[32,41]

When a covalent Si-C bond is established between porphyrin molecules bound through the surface through a long alkyl chain (C11), the electron transfer takes place between porphyrin molecules and the silicon substrate in electrochemical measurements.[33] The system exhibits a bistable behavior with two conduction states: a low-current state (*off*) and a high-current state (*on*), revealing a possible application

in molecular memory devices.[33] The linker length influences the electron transfer rate of the substrate. The further the porphyrin ring (redox center) is away from the surface, the slower the electron transfer.[116]

The research on porphyrinic σ-π-σ systems reveals the pronounced reversible negative differential resistance effect, which appears to be intrinsic to the porphyrin molecules.[34] When constructed as a donor-spacer-acceptor (D-s-A) system, the layers exert high rectification ratio.[35]

The electrochemical properties of porphyrins can be utilized in many different ways. The Lindsey and Bocian groups developed a body of knowledge on building porphyrin-based complementary metal-oxide-semiconductor utilizing their redox properties and processing hybrid semiconductor devices. In these devices, the information is stored in oxidative and reductive redox states, which is a basis for the writing/reading process. During a decade-long project, the group synthesized hundreds of porphyrin derivatives with varying structures and investigated the influence of changes in the film properties and structural integrity. The molecular design is crucial for developing and testing different aspects of dynamic random access memory device into which porphyrins will eventually be integrated. Parameters like substrate type, type and length of tethering moiety, or influence of the environment are varied to investigate the influence on attachment, stability, charge transfer, and charge retention properties. The prepared systems are characterized and optimized for the final application. In this literature overview, only findings related to silicon surface modification with porphyrin derivatives are covered. The complete account of all research in this project, including the use other substrates, the influence of porphyrin layer structure on its electronic properties, and the integration of the porphyrin/silicon system into an electronic device is summarized in Lindsey et al.[13]

Jiao et al. studied in detail the adsorption geometry of porphyrins by using spectroscopic labels to investigate the tilt (θ) and rotation (φ) angles of Zn(II)-TPP derivatives on silicon and gold surfaces, allowing for the distinction of two in-plane axes of the porphyrin ring.[23] Either methylthio (-CH_2S-) or benzylthio (-BzS-) moieties are used as an anchor on Au or Si, and a tripodal alkenyl group as an anchor on Si. The CF_3 labels are strategically placed on a porphyrin derivative, so the methyl group of a *p*-tolyl substituent that lies along the molecular axis distal to the tether (R^D) could be distinguished from the *p*-tolyl substituents that lie along the orthogonal in-plane axis lateral to the tether (R^L).

The general trend observed is that both tilt and rotation angles monotonically increase with the decreasing surface coverage.[23] When the surface coverage is lower, the molecules can occupy more space. Since at low coverage, the amount of neighboring molecules is low, the porphyrin molecules may exert greater tilting, aligning more coplanar with the surface.

For all monolayers on surfaces, the rotation and tilt angles are around 45°. From the results, it is not clear if molecules have a tight distribution of angles around 45° or do the molecules have a random distribution of orientations. Since there are no intramolecular steric constraints present that would prohibit φ angles in the range from 0° to 90°, it is entirely plausible that orientations about the molecular

axis are randomly distributed. However, due to steric constraints, the distribution of θ angles is plausible but constrained to a smaller range.

Three sets of rotation angles are determined for all samples.[23] Two sets of angles are calculated using the $\nu_s(CF_3)$ or ν(pyr) absorbances and φ angles determined from the measurements. The third set is calculated using ν(pyr) measured absorbances and $\varphi = 90°$. The 90° rotation angle is chosen due to all previous evaluations in the literature, which required an assumption for the rotation angle. Since at the saturation coverage the tilt is expected to lean to coplanar orientation, the 90° assumption is favored by scientists. This value is often referred to as an average tilt angle, α.

Evaluation of the data revealed that θ angles using ν(pyr) absorbances (58°- 68°) are larger than those using $\nu_s(CF_3)$ absorbances (40-43°). Such large angles are not likely to occur due to steric interactions with the surface. The θ angles determined using the $\nu_s(CF_3)$ angles are more similar to the values of an average tilt angle (33-40°). Even though a couple of control experiments are performed to probe the question of these differences, an adequate explanation is not found. However, the similarity of the results obtained here with earlier reports supports the idea that average tilt angles reflect the actual tilt angles and thus provide a sound assessment of the surface orientation.

Finally, the similarity of surface properties of all porphyrins, no matter the attachment chemistry or a substrate, suggests that the intrinsic macrocycle properties mostly control the adsorption geometry. In Table 1.1, determined average tilt angles of diverse porphyrin derivatives on Si surface across literature are summarized. There are no evident patterns in data, except perhaps that all porphyrins deposited indirectly to surface have somewhat greater tilt angles (between 40° and 70°) compared to directly deposited derivatives (between 33° and 60°). Coincidentally, all indirectly deposited samples are attached to the surface with silane chemistry through the Si-O bond. These results are perhaps to be expected, as it is known that the addition of each successive layer results in a less than ideal surface coverage, contributing to the layer imperfection. Additionally, the deposition of silanes results in an amorphous siloxane network with questionable availability of surface functionalities. All this may contribute to low surface coverage and, thus, a higher tilt angle.

The surface coverage of porphyrins at monolayer saturation coverage is around 1×10^{-10} mol cm^{-2}.[20] In Table 1.1, the surface coverages of porphyrins on the silicon surface are listed. There are no clear trends related to the success of surface coverage, and a few authors focused on elucidating which parameters influence the surface coverage. From work done by Gadenne et al., one can deduce that the surface coverage depends on a type of a porphyrin derivative.[26] However, a more systematic approach is needed to make general conclusions. Some groups can establish control over the film growth and achieve higher coverages with an increasing layer number.[29,117]

The success of the attachment to the surface is assessed by Liu et al., who synthesized a collection of porphyrin derivatives with a variety of hydrocarbon tethers and different substituents on the ring.[118] The

influence of the high-processing temperature conditions (400 °C) on the properties of the film is evaluated.[118]

Table 1.1: *Surface coverage and tilt angles of porphyrin molecules on silicon surfaces in literature.*

Deposition method	Anchoring bond	Type of attachment[a] (direct/indirect)	Surface coverage, Γ[b] [$\times 10^{-10}$/mol cm^{-2}]	Tilt angle[b],α [°]	Ref.
deposition from solution	Si-Ph	direct	10	60	114
hydrosilylation	Si-CH=	direct	0.2 – 75	-	29
hydrosilylation	Si-C, Si-CH=	direct	0.9 – 1.5	37-46	38
hydrosilylation	Si-C	direct	2.0 – 5.1	38	36
hydrosilylation	Si-C	direct	1.6 – 1.9	38-43	119
hydrosilylation	Si-C	direct	1.9 – 3.2	33-42	117
hydrosilylation	Si-C	direct	0.4 – 2.2	36-41	22
hydrosilylation	Si-C	direct	2.2	46	30
silane chemistry	Si-O-Si	indirect	2.0	43	20
silane chemistry	Si-O-Si	indirect	2.0	43	21
silane chemistry	Si-O-Si	indirect	0.04 – 4.2	-	26
electrografting	Si-C	direct	1.7	-	33
drop deposition	Si-O-CH_2	direct	0.3 – 4.2	-	100
drop deposition	Si-O-CH_2	direct	0.4	-	39
hydrosilylation	Si-CH=	indirect	0.6	-	112
hydrosilylation	Si-$(CH_2)_n$-	indirect	0.4	-	27
silane chemistry	Si-O-Si	indirect	0.4 – 0.6	67	42
silane chemistry	Si-O-Si	indirect	0.4	-	43
hydrosilylation	Si-X-CH_2-Ph, Si-X-CH_2-Por (X = O, S, Se)	direct	0.5 – 0.8	34-55	28
hydrosilylation	Si-$(CH_2)_n$-	direct	0.5 – 1.0	37-50	31
hydrosilylation	Si-C, Si-S-CH_2-Ph, Si-S-CH_2-P	direct	0.2 – 1.2	37-59	23
hydrosilylation	Si-C	direct	0.04 – 1.2	-	120
silane chemistry	Si-O-Si	indirect	~0.1	-	44
electrografting	Si-C	direct	<0.1	39-51	34
electrografting	Si-C	direct	0.02-7.5	-	35
hydrosilylation	Si-X-CH_2-Ph, (X = O, S)	direct	0.02-0.7	-	37
silane chemistry	Si-O-Si	indirect	-	40-70	24

Some general trends are observed when porphyrins are baked onto the surface. Namely, the surface coverage increases monotonically with the increasing baking temperature, while the time to reach the highest surface coverage decreases. It is found that the optimal baking conditions to reach saturating coverage are 400 °C for 20 min.[118] Baking at temperatures higher than 400 °C does not result in

improved surface coverage but leads to degrading instead. The increasing porphyrin concentration from 1 to 100 μM in solution led to increasing surface coverage. However, no increase is observed for concentrations above 100 μM. The choice of solvent does not seem to influence the quality of the surface.

The direct attachment is achieved with the following tethers: 2-(trimethylsilyl)ethynyl, vinyl, allyl, and 3-butenyl. When it comes to substituents on the ring, the attachment is achieved with iodo, bromomethyl, 2-(trimethylsilyl)ethynyl, ethynyl, vinyl, and allyl moieties.[118] All attached porphyrins achieved similar surface coverages, while the attachment is not achieved for sterically congested porphyrins (*meso*-iodo, *β*-dibromo, and vicinal *β*-dibromo). The CV experiments demonstrate similar features for both routes of deposition, indicating a robust electrochemical behavior. Furthermore, the relatively narrow voltammetric waves and the absence of visible surface oxidation at high potentials indicate uniform packing and full surface coverage. The tests with electrochemical cycling on one of the prepared samples showed the unchanging voltammetric features for $\sim 10^{10}$ redox cycles.[118]

The influence of different tethering linkers, -Bz- and -CH_2-, and different tethering group VI atoms, O, S, or Se on the quality of the thin films are evaluated next.[28] While both types of linkers achieve surface binding, the -Bz- linker provides a more upright orientation of molecules with respect to the surface normal (37° as opposed to ~50° for -CH_2-), resulting in a higher packing density. The type of tethering atom, O, S or Se, does not affect the electron transfer kinetics.[28] However, molecules with the -CH_2- linker demonstrated faster electron transfer rates by a factor of almost three compared to those with -Bz- linker, presumably because of a shorter distance of a molecule to the surface.[28]

Wei et al. focused only on carbon-tethered porphyrins, investigating their structural and electron-transfer properties when attached to the Si surface.[31] The influence of different linker types on the film properties is examined with two classes of Zn(II)-TPPs. One class is designated ZnPX with an alkyl anchor -$(CH_2)_n$- attached directly to a porphine ring. The other class of derivatives is designated ZnPPhX with phenyl (-Ph-), or phenylalkyl (-Ph$(CH_2)_n$-) anchor attached to the ring. The structural and electron-transfer properties of investigated derivatives are comparable to their analogs with an O, S, or Se tethering atom. The findings suggest that the physicochemical characteristics of monolayers foremost depend on the type of the porphyrin molecule and the linker rather than the anchoring atom.[31] However, the choice of anchoring atom is still relevant when thinking about the chemical stability of the monolayer.

The ZnPPh and ZnPPhCH_2 monolayers demonstrate adsorption geometries and packing densities qualitatively more similar to those of the ZnP$(CH_2)_n$ monolayers, than those with the longer phenylalkyl -PPh$(CH_2)_n$- tethers.[31] The behavior indicates that short alkyl and aryl linkers do not possess torsional flexibility sufficient to optimize the packing of the molecules on the surface. However, adding at least one more methylene group leads to the formation of more densely packed monolayers. The tilt angle

decreases with an increasing number of methylene groups, relating to their ability to stand more upright, possibly due to the larger torsional flexibility of the longer phenylalkyl linkers.[31]

Liu et al. worked on the synthesis of a variety of Zn(II)-TPP derivatives with appended ethyne moieties to promote intermolecular reactions to facilitate polymerization.[29] The results show that almost all unprotected porphyrin derivatives undergo a thermal polymerization producing a multilayered film.[29] The protected derivatives did not form films, only monolayers. The CV measurements reveal 60 times larger surface coverage of polymerized film than of the saturated monolayer.[29] The polymerized films retain their redox activity, but with slower electron transfer rates compared to monolayers. It is also revealed that the surface coverage varies considerably among derivatives but without an observed trend related to the extent of the surface coverage and the molecular structure.

Four sets of experiments are conducted to explore the nature of polymerization:[29]

(i) In the first set, thermally linking of various iodo- and ethynyl-functionalized porphyrins on the surface resulted in a monolayer formation.

(ii) In the second set, the molecules are deposited on SiO_2, gold, and glass surface. On these surfaces, polymerization also occurred, but there is no covalent attachment to these surfaces.

(iii) In the third set of experiments, monolayers of mono-ethynyl- or mono-alcohol-functionalized derivatives are prepared, followed by a deposition of an overlayer containing a multiple-ethynyl-functionalized porphyrin. The electrochemical characteristics of such a system are similar to the one formed by direct anchoring of the overlayer molecule to the surface, indicating the possibility of preparation of multiple mixed layers.

(iv) In the fourth set of experiments, FTIR and resonance Raman spectroscopy are used to research linking between porphyrins and some benchmark molecules (enynes). The enynes are investigated because these might form between neighboring porphyrin during the thermal process. However, the signature C≡C and C=C vibrations could not be observed. The absence of enyne vibrations could be related either to saturation of the bonds between porphyrin molecules due to elevated temperatures, or the conversion of bonds to 1-phenylnaphthalene and 2-phenylnaphthalene, as suggested by the study of ethynyl-benzene pyrolysis.

Presented research sets the basis for porphyrinic film growth with the film thickness control and provides an alternative to polymerization in solution.

Padmaja et al. synthesized and deposited a Zn(II)-TPP derivative with an all-carbon triallyl tripod anchor on an H-terminated silicon surface.[30] Electrical and electrochemical properties of the derivative are investigated, and it is found that redox potentials, charge retention time, electron transfer rates, and tilt angle are all similar to those reported earlier for porphyrins with monopodial tethers. However, the surface coverage is three times higher than for monopodial tethers.

The research related to defining a porphyrin thin film structure on silicon and its correlation to the thin film properties is summarized in this sub-chapter. Porphyrins create highly-ordered, closely-packed thin films that allow further modification with the possibility of building 3D structures. The deposition of porphyrins is reproducible. However, the quality of the thin film and the rate of deposition will depend on the porphyrin bulkiness, attached side-groups and linkers, or type of metal cation. Investigated porphyrinic structures demonstrate good catalytic and electron transfer properties, the on-off switching behavior useful for the construction of molecular memories, rectification properties, and photosensitivity. The electron transfer, and therefore, electronic properties of porphyrins depend on the distance of the porphyrin ring from the surface. Overall, the presented literature provides a solid basis for building research projects on high-quality porphyrin thin film structures and their application in modern electronics and sensing devices.

1.4 MALEIMIDE AS A FUNCTIONAL MATERIAL

1.4.1 General features

Maleimide has a unique role in biosensing in regards to the specific bonding and the preservation of a biomolecular structure. It is selective only towards a thiol group (-SH). In its structure, maleimide has two carbonyl groups demonstrating a withdrawing effect (Figure 1.4a). The withdrawing effect is coupled with the release of ring strain upon reaction with thiol, favoring the formation of a product.[45] Maleimide can be deposited on the surface either directly (Figure 1.4c) or via coupling to the surface functionalized with a linker molecule (Figure 1.4d).

In biomolecules, thiols are found only in one amino acid, cysteine. The natural abundance of cysteine in proteins is low.[121] Because of this reason, the thiol-maleimide reaction is used densely in research on bioconjugates,[122] and is appealing to utilize the same qualities in materials research as a highly specific material for immobilization.[45,123] Furthermore, the proteins themselves can be custom-tailored, so that cysteine is inserted at a specific position suitable for bonding to the surface.[121] In that way, binding sites can be reduced to a minimum, preserving the shape of the protein and with that, its specific function. Thiol moieties can also be inserted into a structure of other biomolecules, like DNA or RNA, manipulating the bonding of the molecule at the specific site (Figure 1.4e).

Except for the selectivity, other advantages of maleimide is that the reaction can undergo in aqueous media and without a catalyst. Besides the reaction of a thiol with the ring, the maleimide ring moiety can be further functionalized through the nitrogen atom, thus attaching different functionalities to a product.

Thiol-maleimide conjugation is a well-established reaction known as thiol-Michael addition, resulting in the formation of a thiosuccinimide bond.[45,123] The mechanism of thiol-maleimide coupling starts with the formation of a thiolate anion (Michael donor).[45] The initiator is most often either a weak base or a nucleophile. The mechanism schemes of both paths are depicted in Figure 1.5a and b.

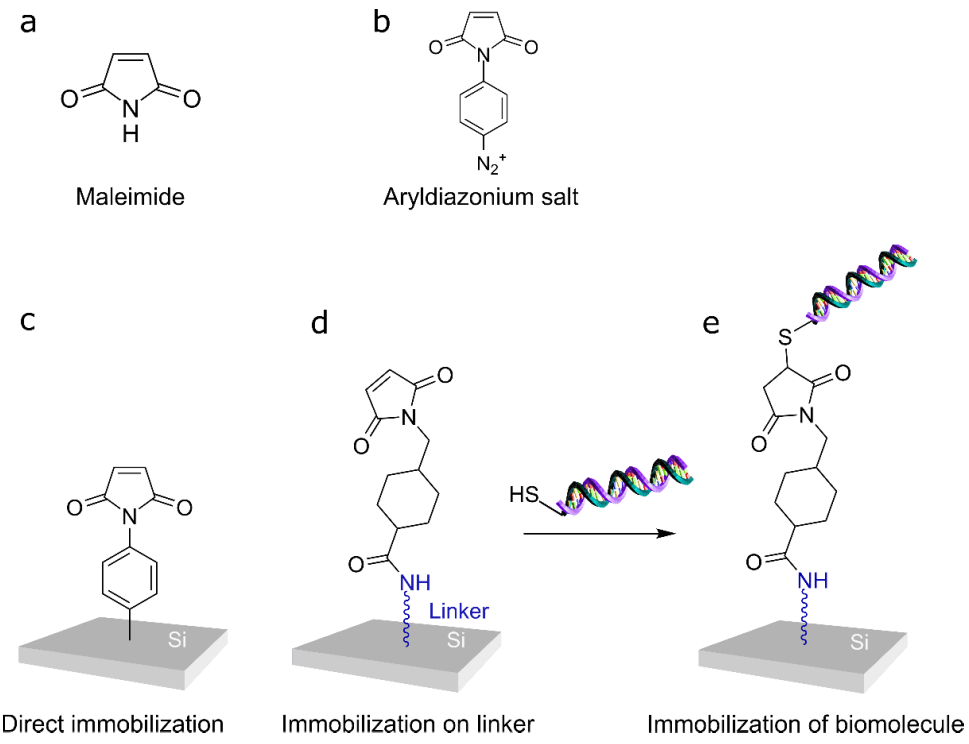

Figure 1.4: *(a) Maleimide. (b) Maleimidophenyldiazonium salt. (c) Direct immobilization of a maleimidophenyl molecule. (d) Immobilization of a maleimide-containing molecule through a linker deposited on the surface. (e) Immobilization of a biomolecule on a maleimide-functionalized surface.*

In the base-initiated mechanism, a weak base abstracts a hydrogen atom from thiol, creating a thiolate anion. Thiolate is a strong nucleophile which then attacks a ring double-bond (Michael acceptor), generating a basic enolate intermediate. The enolate then abstracts hydrogen from another thiol molecule, leading to a product - a thioether and another thiolate molecule, thus continuing the propagation step.[45]

If an initiator is a nucleophile, the reaction starts with a nucleophilic attack on a maleimide double bond, resulting in a zwitterionic enolate (Figure 1.5c). The enolate deprotonates a thiol, and from that point, the mechanism of propagation is the same as for the base-initiated mechanism.[45]

Singh et al. compared covalent immobilization of enzymes on silica beads with two different chemistries.[124] The findings suggest maleimide-chemistry as an excellent alternative to the prevalent aminosilane chemistry in terms of (a) the amount of immobilized enzyme and (b) preservation of the enzyme's specific activity. Thus, maleimide promises good immobilization properties with the advantage of bringing in a high-selectivity, whereas amines react readily with other organic species.

The applications of maleimide's specificity are versatile. In a recently developed paper-based fluorescent sensor, the thiol selectivity of maleimide is crucial for the detection of hydrogen peroxide and glucose.[125] High sensitivity and good selectivity of hydrogen peroxide, as well as glucose, are

achieved both in solution (nanomolar range) and on paper (micromolar range). Thus, this simple set-up has great potential of being used as an in situ assay for the detection of hydrogen peroxide and glucose in real samples like blood.

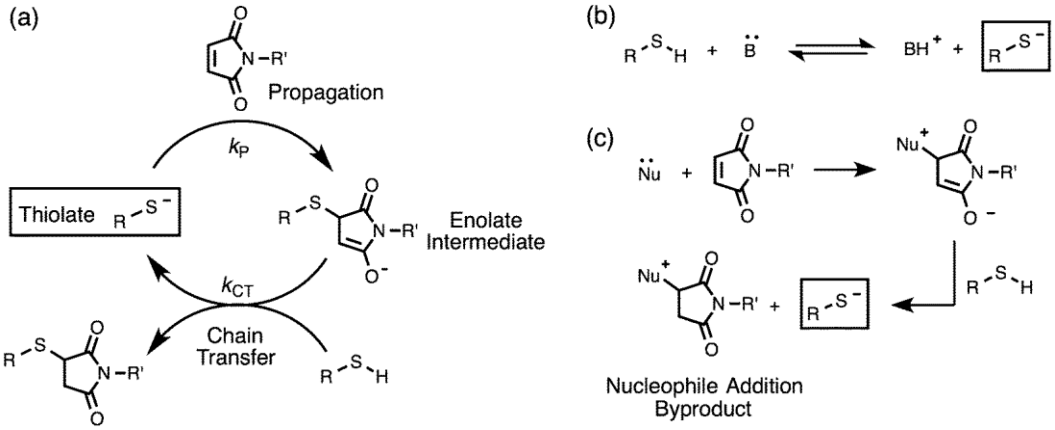

Figure 1.5: *(a) Mechanism for the thiolate-catalyzed addition of a thiol to an N-substituted maleimide. (b) The formation of a thiolate anion from an acid-base equilibrium reaction. (c) Formation of a thiolate anion following a nucleophile-initiated mechanistic pathway. Reproduced from Ref.*[45] *with permission from The Royal Society of Chemistry.*

Thiol-maleimide reaction also found its place in research on modern materials. In a work of Achadu et al. with graphene quantum dots, maleimides are used as sensing units themselves as a fluorescent sensor for thiols.[126] The covalently-functionalized quantum dots showed higher sensitivity than those functionalized non-covalently. The developed system can detect thiols at nanomolar levels in aqueous solution and at physiological pH.

In this work, a maleimide derivative, maleimidophenyldiazonium salt (*p*-MPDS, Figure 1.4b), is used for surface modification via electrografting. The mechanism of the reaction is described in detail in Chapter 2.1.3.

1.4.2 Literature overview

The research on basic structural properties of maleimide-containing organic materials and their interactions with thiols on the silicon interface is limited to a handful of publications. Nevertheless, it shows promising results and outlines the path for further research.

Wang et al. compared four different surface modification approaches for the functionalization of silicon with maleimide-terminated compounds.[47] The methods of direct tethering functionalization of the surface are compared with the earlier established method of layer-by-layer (LbL) deposition [48]

Data analysis indicated the best surface coverage (50%) when the maleimide group attached through a long-alkyl chain modified with chlorosilane head is chosen as a starting material. The single-step

synthesis path is likely to contribute to these excellent results. However, the surface coverages of all four paths are not presented, and therefore the quality of the prepared surfaces could not be compared.

Further experiments with the samples prepared via method 4 reveal surface tunability when mixed with different molar fractions of CH_3-terminated alkyltrichlorosilanes. Prepared surfaces demonstrated successful linking with a series of nucleophiles (nucleophilic heterocycles, alkylthiols, amines, and thiol-tagged DNA oligonucleotides), although no evidence is presented regarding their covalent nature. However, sonication and washing of the samples in solvents point to the strong adhering to the surface.

The immobilization efficacy of two functional groups, maleimide and amine, is investigated in more detail by Böcking et al.[58] Surface is functionalized with aminoalkenes to which *N*-succinimidyl 3-maleimidopropionate (SMP) is coupled and used for thiol immobilization. Several different thiols are immobilized on the surface (decanethiol, 2,2,2-trifluoroethanethiol, and *N*-(2-mercaptoethyl)-^{14}C-acetamide) and evaluated for different properties.

X-ray photoelectron spectroscopy (XPS) investigation of the immobilization of SMP and decanethiol indicates that neither the reactions of the amine monolayer with SMP or SMP with thiols are complete. The reaction of the amine monolayer and SMP resulted in a 50% yield. Furthermore, the fluorine-rich 2,2,2-trifluoroethanethiol and radioactively-labeled *N*-(2-mercaptoethyl)-^{14}C-acetamide are used to detect and quantify the number of formed thioether bonds. The ratio of thiols to aminoalkyl chains in the film is between 1:3 and 1:7. The XR data indicate a densely packed monolayer and no significant degradation of the quality of the layers during all modification steps. Also, the ratios of 1:1.5 of SMP and aminoalkyl chains and 1:2 of decanethiol and aminoalkyl chains are estimated. The results outline the problem of LbL deposition, contributing to a loss of thin film quality with each deposition step. Thus, direct deposition is desirable whenever possible.

Three functional groups, (i) maleimide, (ii) *N*-hydroxysuccinimide (NHS) ester, and (iii) hydrazide, are compared in work by Kim et al.[59] to evaluate their efficiency in immobilizing a protein, monoclonal rabbit immunoglobulin G (IgG). The measurements with UV/vis spectroscopy and fluorescence microscopy revealed a ~40% and 50% surface coverage of succinylated and maleimidylated (3-aminopropyl)triethoxysilane (APTES) thin films, respectively. Infrared spectroscopic ellipsometry (IRSE) results indicate significantly greater surface coverage (80%) for succinylated APTES. The difference in coverage originates from the choice of measured parameters. In UV/vis measurements, the coverage is determined based on unreacted amino groups. In ellipsometry, the surface coverage calculation is based on the estimated film thickness.

The IgG protein is immobilized according to each surface's chemistry. The NHS-, hydrazide-, and maleimide-surface groups are each coupled with primary amines (-NH_2) in IgG, the aldehyde (-CHO) of an oxidized carbohydrate residue in IgG, and the sulfhydryl (-SH) of fragmented half-IgG, respectively. Their biological activities are estimated as well by measuring fluorescence intensities before and after the adsorption of the antibody FITC-labeled goat anti-rabbit IgG (FITC-Ab).

At FITC-Ab concentrations of less than or equal to 0.01 mg mL^{-1}, fluorescence intensities of half-IgG immobilized with maleimide and hydrazine are comparable. At FITC-Ab concentrations greater than 0.02 mg mL^{-1}, a 10% larger amount of FITC-Ab accumulates on the surface with half-IgG immobilized with maleimide. Meanwhile, fluorescence intensities of half-IgG immobilized with NHS are 50-70% lower than both maleimide and hydrazine. The long-term biological activity and hydrolytic stability of immobilized protein systems are similar, with fluorescence intensities of all three samples reduced by ~25% after seven days of incubation in phosphate-buffered saline.

The results indicate that biological activity indeed depends on the choice of chemical linkers by dictating the availability of active sites in a protein. Out of the three tested linkers, maleimide shows superior bonding capacity over NHS and hydrazine.

Seto et al. proposed an innovative technique for the immobilization of polymers on siliceous surfaces using maleimide-thiol chemistry.[60] Maleimide groups are introduced to the surface with SMP and used to immobilize various polymers. Several polymers with distinct properties [polystyrene (hydrophobic polymer), poly(acrylic acid) (anionic polymer), poly(*N*-isopropylacrylamide) (temperature-responsive polymer), and poly(*p*-acrylamidophenyl-α-mannoside) (glycopolymer)] are introduced on three different substrates (silicon wafer, glass slide, and silica-sputtered substrate) to demonstrate a broader applicability. All but one polymer (hydrophobic polymer) produced smooth, thin layers.

Glycopolymer (PMan) is selected as a platform for research on protein microarrays and micropatterning by photolithography. FITC-labelling is used for comparison of thiol-terminated polymers immobilized covalently through a thiol-maleimide bond with non-covalently deposited (spin-coated) counterparts. Fluorescence microscopy measurements are performed on two FITC-labeled proteins (albumin from bovine serum (BSA) and concanavalin A (Con A)) adsorbed to PMan-functionalized glass slides and compared with spin-coated PMan-glass slides. Covalently immobilized PMan thin films demonstrated a higher intensity than their spin-coated counterparts. It is assumed that the spin-coated PMan is eluted from the glass slide during incubation in a protein solution due to its physisorbed nature.

The prepared surfaces are further tested for the protein-recognition ability and compared with a commercially available, poly-L-lysine-coated (PL-coated) glass slide. The coating of the commercial glass slide is based on electrostatic interactions. The PMan-immobilized glass slide allowed detection of up to 0.005 g L^{-1}, while the commercial glass slide allowed the detection of only 0.01 g L^{-1}. Especially for Con A protein, the slide demonstrates specific and strong bonding to the surface, indicating a better detection with covalent bonding.

Electrochemical grafting is another route used for the immobilization of organic material on H-terminated silicon surfaces. Maleimide is first immobilized using this method by Sun et al.[61] The surface is first functionalized with carboxyl- groups using carboxybenzyl diazonium salt, creating a stable Si-C tether. The carboxyl groups are then used to introduce amine functionalities through reaction with 1,3-

diaminopropane. Finally, maleimide moiety is introduced to the surface by depositing *N*-(2-carboxyethyl)maleimide. The experiment is performed on both Au and Si(111) surfaces.

The carboxybenzyl-covered Au surface is mapped using the FTIR synchrotron mapping ellipsometer, revealing surface inhomogeneity. The film inhomogeneity might be caused by variations in morphology or structural changes caused by having many deposition steps, resulting in a disordered layer. The findings are in agreement with other experiments with the LbL deposition path.

Zhang et al. approached this problem by synthesizing *p*-MPDS and deposited it directly to the Si-H surface.[62] Chronoamperometric measurements revealed that a first monolayer is formed after 60 s of electrodeposition at -2 V. The formation of a second monolayer is estimated at around 250 s, based on the amount of charge consumed and assuming a two-electron process. The slowed-down formation of a second monolayer is due to a steric hindrance of available *ortho*- position by a bulky maleimide group in *para*- position on the benzene ring.

The prepared substrate is tested for its biosensing capabilities. A cysteine-peptide is immobilized on the maleimide-functionalized surface and tested for binding of specific and non-specific antibodies. Spectroscopic measurements showed a successful deposition of specific antibody through an increase in the intensity of amide bonds, while the non-specific antibody is only loosely attached.

The same experiment is repeated in situ with quartz crystal microbalance - flow injection analysis to explore the immunosensing label-free potential of the prepared samples. The surface demonstrates a higher affinity towards a specific antibody. Its concentrations exceeding 10 μg ml^{-1} show a binding activity, with the greatest mass change (Δm) occurring at 50 μg ml^{-1}. The non-specific antibody shows non-specific binding at a concentration of 10 μg mL^{-1}. However, the surface shows no further affinity towards non-specific antibody at higher concentrations.

Immunoelectrode potentiometric response measurement on Si at zero current showed a 40 mV change in potential at the specific antibody concentration of 22.5 μg mL^{-1}. There is no significant change for a non-specific antibody, thus confirming the selectivity of the surface as a biosensor.

The research on *p*-MPDS thin films is continued by Kanyong et al., who looked into the kinetics of the deposition mechanism by quantifying the amount of electrografted maleimide material on Au-QCM and μc-Si-Au-QCM, and c-Si(111) surfaces with in situ electrochemical quartz crystal microbalance (EQCM) and spectroscopic measurements.[63] The EQCM measurements reveal a ~0.5 grafting efficiency after the first potential scan for Au-QCM, μc-Si-Au-QCM sensors. However, after the following four potential scans, the mean grafting efficiency (η_{mean}) is ~0.6 and ~0.25 for Au-QCM and μc-Si-Au-QCM, respectively. This behavior is once again explained with the steric hindrance of bulky maleimide molecule, consistent with the earlier reports. Correspondingly, a formation of about 3 (Au-QCM) and 6 (μc-Si-Au-QCM) monolayers is calculated after the first potential scan, and 5 and 8 monolayers after five cycles followed by removal of loosely bound molecules. The microcrystalline structure of silicon

is speculated as a reason for a thicker layer on μc-Si-Au-QCM. The electrochemical deposition is also studied with in situ ellipsometry. A comparison of amplitudes of the C=O band for in situ measurements indicates a thickness of 3.5 nm ± 0.5 nm.

Application-wise, immobilization of maleimide on the silicon surface has mostly been utilized in research on DNA hybridization as a crosslinker between a surface and thiol-bearing DNA oligonucleotides.[48–53,55,57,64,65,127,128] DNA (or RNA) hybridization is a measure of the degree of genetic similarity between two DNA sequences and has its application in genetics. The technique usually involves the coupling of a labeled DNA (e.g., with a fluorescence tag) strand with an unlabeled one. The more complementary the unlabeled strand is to the labeled DNA, the stronger the bonds between them and, thus, will require more energy to separate them. The less complementary sequences will dissociate or "melt" away faster. The DNA strands usually do not contain thiol group, but may be chemically modified to have them.

The covalent nature of the bond between the organic material and silicon improved the stability of the surface.[129] The stability is kept even when this way of modification is transferred to H-terminated SiNWs.[64] Passivation of the remaining unreacted surface sites with 1-octadecanethiol between deposited maleimide-alkyl chains resulted in well-ordered alkyl monolayers.[52] Some researchers resorted to using polymers to achieve a "matrix isolation" of oligonucleotides to diminish the molecular interaction between oligonucleotide molecules and oligonucleotides and the surface and thus improve their biosensing selectivity.[55,57,128] The use of polymers resulted in a drastically reduced non-specific adsorption of oligonucleotides during the hybridization experiments.[55,57]

The presented summary of research on the functionalization of silicon surface with maleimide-containing moieties reveals that the best surface coverage with maleimides is achieved with direct coupling of the molecule to the surface via deposition techniques such as hydrosilylation or electrografting. The maleimide-covered surface can further be tuned by mixing of the layers with non-reactive molecules (i.e., alkyl chains) to achieve spacing of the maleimide groups on the surface. When tested against other functional groups, maleimide showed superior results in biological activity due to the availability of active sites in a protein molecule. Additionally, a better sensitivity of the biosensors was achieved when maleimide was immobilized covalently on the surface, as opposed to non-covalent attachment in biosensors, which are used as a commercial standard.

2 EXPERIMENTAL METHODS

2.1 CHEMICAL SURFACE MODIFICATION

2.1.1 Pre-treatment of a Si(111) surface

Depending on the chosen surface modification route, the substrate surface needs to be prepared accordingly. In this work, two surface terminations were used: (i) oxidized with OH-termination and (ii) H-terminated Si.

To obtain Si-OH groups on the surface, the passive siloxane network of a native silicon oxide must be oxidized in strong acids. In the present work, the silicon substrate is oxidized as follows:

1) **Cleaning** the substrate in an ultrasonic bath in an organic solvent to get rid of any loosely attached organic molecules that might come from packaging or environment.
2) **Etching** of the substrate in a 1% HF solution to peel off the native oxide layer and any other molecules that might still be present on the surface.
3) **Oxidizing** the substrate in piranha solution ($H_2SO_{4(conc)}$:$H_2O_{2(conc)}$ = 1:1) to obtain silanol bonds (Si-OH).

To establish a Si-C bond between the organic layer and the silicon, the native oxide should be removed from the surface, and the surface silicon atoms capped with hydrogen atoms (H-terminated Si). To obtain the H-terminated Si surface, the following steps were taken:

1) **Cleaning** the substrate in an ultrasonic bath in the organic solvent to rid off any loosely attached organic molecules that might come from packaging or environment.
2) **Etching** of the substrate in 1% or 10% HF solution to rid off any remaining organic molecules and to peel off the native oxide layer.

Such OH- or H-terminated substrates were immediately used in the reaction.

2.1.2 Silanization with (3-aminopropyl)trimethoxysilane (APTMS)

The most popular strategy for the covalent attachment on silicon is through silane chemistry. Silanization provides quick covalent bond formation with the surface by integrating into the existing siloxane network of the native oxide. Silanes form a siloxane network that stabilizes the monolayer. However, even though there has been extensive research on silane deposition and characterization, it remains a challenge to create uniform monolayers.[130] The silanization reaction is complex, and the mechanism is still under debate. However, three steps are known and expected to occur.

1) **Hydrolysis** of organosilane molecules (Figure 2.1) in solution or close to the surface.

2) **Hydrogen bonding** between organosilane molecules from the solution and surface silanols is established. Organosilane molecules are still capable of moving laterally across the surface (Figure 2.1). The movement leads to aggregation driven by attractive forces such as van der Waals forces between the pendant hydrocarbon chains, hydrogen-bonding, and dipole-dipole interactions. The aggregation ultimately leads to lower mobility of siloxane molecules.

3) **Condensation** to Si-O-Si network between organosilane molecules and surface Si-OH groups (Figure 2.1). In the case of trifunctional organosilanes, all three hydrolyzed groups can react with the surface or laterally with each other, but often leads to oligomerization in solution, leading to a disordered structure.[131]

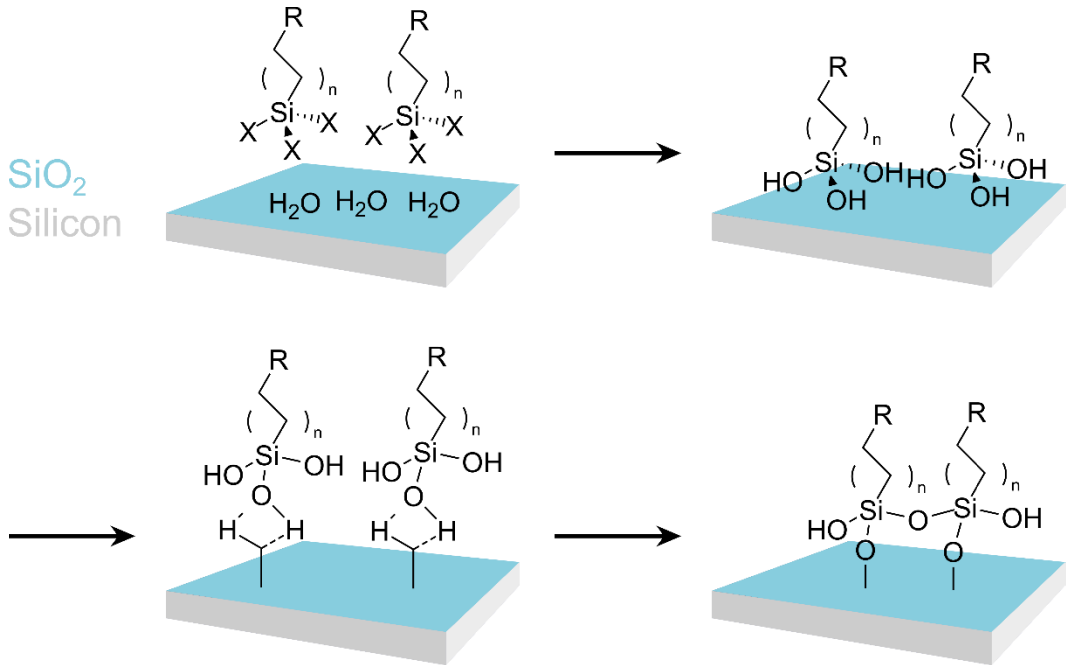

Figure 2.1: *Silanization mechanism.*

Many reaction parameters play a role in the outcome of the layer structure and the attachment kinetics. The amount of water has a crucial role in these steps. Too much water will cause polymerization of organosilanes in solution and aggregation on the surface, leading to disordered layers (Figure 2.2e). On the other hand, too little water will lead to incomplete monolayers. Thus, this crucial parameter in the first step will influence all other steps and the quality of the monolayer.[132–134] The choice of solvent,[135,136] silane concentration, reaction time,[136] the length of aliphatic chains,[134] reaction temperature,[134,137] and curing conditions[138,139] also have an impact on the quality of the produced layers and should be carefully optimized.

Often-used aminosilanes have a very reactive basic amine head group which self-catalyzes the hydrolysis reaction, promoting a more aggressive monolayer formation (Figure 2.2e and f).[140–142] The amine group and other polar head groups may also form hydrogen bonds with silanol groups coming from the surface, from other silane molecules in solution, or with other amine heads (Figure 2.2c and

f).[140,141] In atmospheric conditions, the amine group may also react with CO_2 from the air (Figure 2.2d), which upon reduction converts to imine (Figure 2.2b).[143]

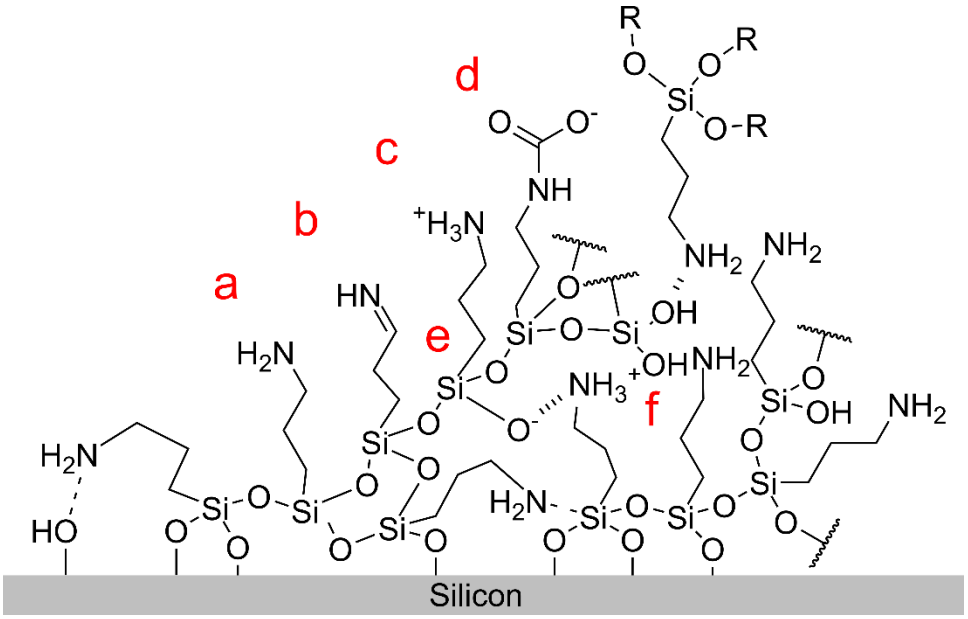

Figure 2.2: *Scheme of aminosilanes layer and possible interactions within.*

Trifunctional alkoxysilanes will form only one or two bonds with the surface of other deposited molecules. The third group will most likely stay loose either in hydrolyzed form or as an alkoxy group.[144] Thermal curing of the layers promotes the formation of the siloxane network by bonding together these loose groups with each other or the remaining Si-OH groups on the surface, thus strengthening the siloxane network.[138,139] The heat also converts protonated and hydrogen-bonded amine groups in their free base form (Figure 2.2a), thus increasing the number of functionalities on the surface.[139,145]

2.1.3 Electrografting of diazonium species

Electrochemical deposition or electrografting uses electricity to drive the redox-based surface grafting of a selected material. Electrochemical surface reactions are much faster than chemical reactions and are completed in a matter of seconds. A substrate is used as an electrode (usually a cathode) placed in an electrochemical cell and in contact with an electrolyte solution of a material one wishes to deposit. Electrografting is easy to control and reproduce. This method uses a cathodic current, providing an electron-rich surface which can exclude oxidation and hydrolysis of the surface. Thus, one can produce a hybrid material modified exclusively with the chosen organic molecule. The electrografting process can be monitored in situ by monitoring the changes in the intensity of spectroscopic labels with IR ellipsometry.

Electrografting of aryldiazonium salts is a powerful technique to covalently attach organic material on metals and semiconductors.[146] Consistent literature reports all point towards an established covalent bond when using this approach as well as the stability of the created structures.[147–150] Electrografting of

aryldiazonium species usually takes place in an aprotic solvent or acidic aqueous medium.[151] The aryl moiety bears a diazonium species on one side and a reactive R group in *para*- position for further surface modification. The resulting aryl films show stability in a range of treatments, including sonication in solvents, boiling in chloroform, boiling in water, etching with fluoride and hydroxides.[151,152]

The mechanism of aryldiazonium deposition (Figure 2.3) proceeds with a one-electron transfer from the surface to the molecule, leading to a homolytic dediazonation of a diazonium cation.[153] The diazonium cation ($-N_2^+$) is electrophilic and, during the reduction of the salt, releases a stable leaving group (N_2). One aryl radical plucks a hydride radical from the H-terminated surface, leaving a dangling bond, while the other reacts with a dangling bond on the surface. The aryl radicals also may react with each other in solution.

Aryl radicals also proceed to react with the already deposited molecules towards a formation of a multilayer.[154–157] The kinetics of a multilayer growth depend on the electron-withdrawing and steric properties of *para*-substituents.[158,159] Larger substituents like maleimido- and carboxyl- groups in *para*-position produce thinner layers (1.5-3 monolayers) than a smaller nitro group (15 monolayers under the same conditions).[158]

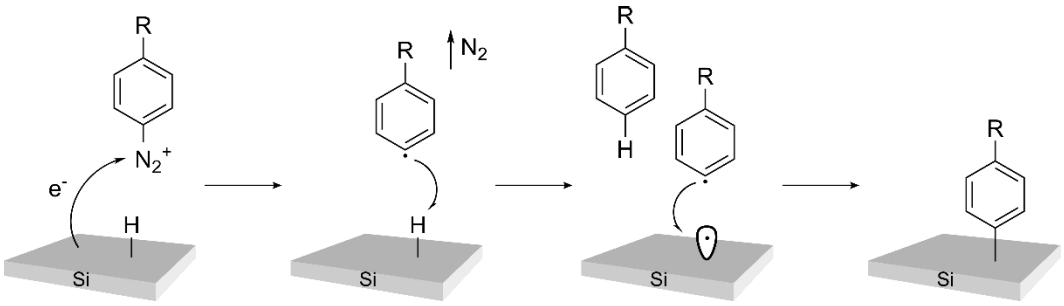

Figure 2.3: *Electrografting mechanism. Adapted from Ref.*[151] *with permission from The Royal Society of Chemistry.*

The electronic activation/deactivation properties of a substituent group greatly influence the mechanism, and therefore, the formation of multilayers. The strongly electron-withdrawing substituents favor the radical mechanism of a multilayer growth, while the less electron-withdrawing groups (i.e., carboxyl) can additionally activate secondary mechanisms like electrophilic aromatic substitution mechanism by diazonium ion or the dediazoniated carbocation.[153,159–161] Neutral and activating groups can be grafted by secondary mechanisms.[159] The choice of solvent also influences the film growth.[158,159] Furthermore, when the substituents are in the *meta*- position, only a monolayer is formed.[157] When the substituents are in the *ortho*- position, the multilayer formation proceeds only when the substituents are small.[162]

The deposition of aryl diazonium species may also proceed without the use of electricity. Instead, the reaction may be initiated photochemically, chemically, ultrasonically, or thermally. Cao et al. give an excellent overview of research done on the electroless deposition.[146]

2.2 SURFACE ANALYSIS METHODS

2.2.1 Infrared spectroscopic ellipsometry (IRSE)

Ellipsometry is a powerful non-destructive, contact-free spectroscopic technique for thin film analysis. The sensitivity of the technique allows the detection of ultrathin films with thicknesses as little as a few nanometres. In ellipsometry, a change of the polarization of light reflected from the surface of the thin film is measured as a function of wavelength and angle of incidence. The name "ellipsometry" comes from the elliptically polarized reflected light, which is used to obtain information about the interface.

The experiments measure two ellipsometric parameters, Ψ and Δ, where tanΨ is the amplitude ratio between the s- and p-polarized components of the reflected light, and Δ is their phase difference.[163] The ellipsometric parameters are measured as the ratio of the complex reflection coefficients for parallel, r_p, and perpendicular light polarization, r_s with respect to the plane of incidence:

$$\frac{r_p}{r_s} = \tan\Psi\, e^{i\Delta} \tag{2-1}$$

With these two parameters and by applying the Fresnel equations, one can define the optical constants *n* (refractive index) and *k* (absorption index), as well as information on surface roughness, crystallinity, anisotropy, or dielectric function.[163] With optical modeling, it is possible to determine the film thickness down to a sub-monolayer.[164]

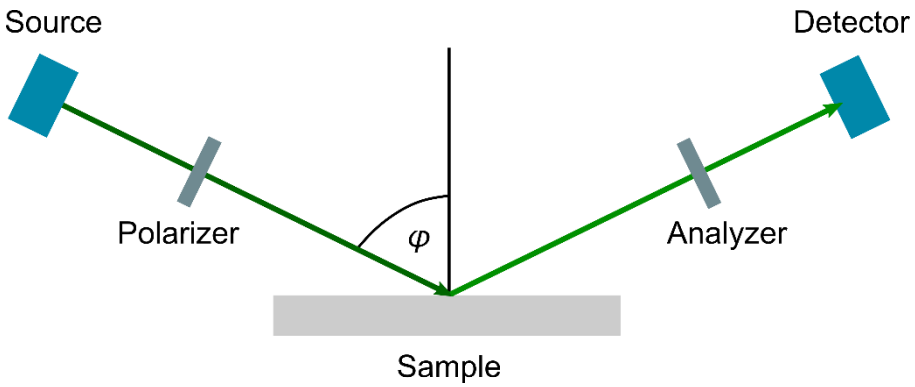

Figure 2.4: *Scheme of a simple ellipsometric setup.*

In Figure 2.4, the scheme of an ellipsometric measurement setup is presented. The beam of light passes from a source through a polarizer onto the sample and is there reflected. Then, the beam passes through another polarizer and falls onto the detector.

IR ellipsometric spectra give information on the thin film structure by identifying the vibrational bands of functional groups and interactions between molecules (i.e., hydrogen bonding), as well as how the sample interacts with the environment (liquid or air).[163,165]

If the organic layers are very thin, their IR signature bands will be small and might overlap with the bulk substrate bands. To cancel out the bands coming from the substrate, the ratio of tanψ spectra of the

organic layer and the uncoated substrate is used for the thin film spectra interpretation. All spectra in this work are also normalized unless otherwise stated.

2.2.2 In situ ellipsometry

In situ ellipsometry is used for real-time monitoring of processes taking place at the solid-liquid interface by recording the spectral signature of the interface over time.[166] The schematic of in situ cell for ellipsometric measurements is shown in Figure 2.5. With the in situ monitoring, it is possible to evaluate film growth, interactions with the liquid, or adsorption processes of molecules.[166–169]

The in situ ellipsometry cell is a specially designed flow cell or an electrochemical cell. The cell is connected to a pump that pumps in and out the reactant solution. The cell consists of a frame, lined on one side with a quartz window, while on the other, the substrate is mounted (the IR-transparent silicon wedge) with the side-to-be-functionalized turned towards the inside of a cell. The outer side of the wedge is cut under a 1.5° angle to induce a divergence between the outer and inner reflex of the wedge. The detector is aligned to capture the reflection from the solid/liquid interface. Additionally, such wedge shape minimizes the interferences caused by multiple reflections between the silicon surfaces are minimized.[170] Finally, this setup also minimizes the contribution from a solvent, as spectra of a beam going through the substrate are recorded. The penetration depth of IR light in such a setup (in water) is only a few micrometers.[170]

In a flow cell, spectra are collected regularly after allowing a specific reaction time. In an electrochemical cell, spectra are collected after applied electricity. All spectra are collected at the 50° angle of incidence.

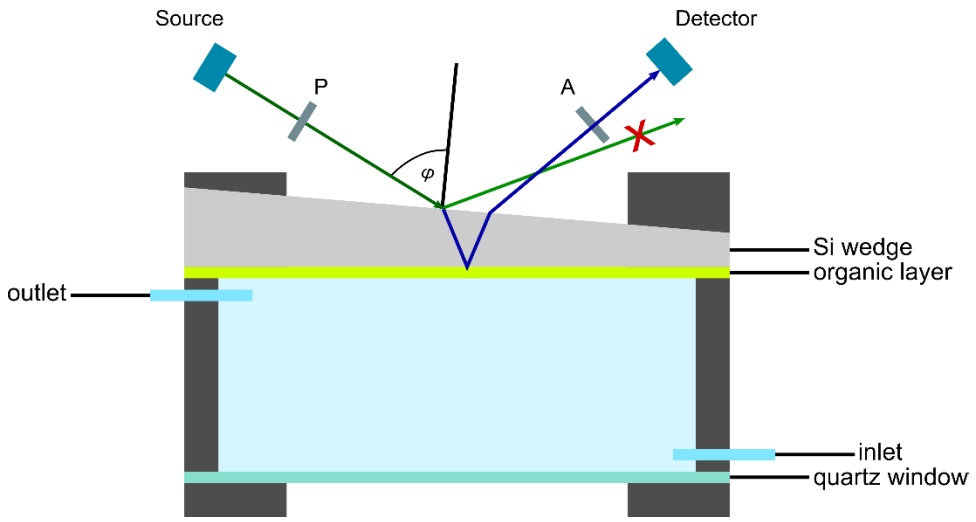

Figure 2.5: *A schematic cross-section of an in situ cell.*

2.2.3 X-ray photoelectron spectroscopy (XPS)

X-ray photoemission spectroscopy is a surface analysis technique based on the photoemission phenomenon in which the absorption of a photon by a material takes place, followed by the immediate emission

of a (photo)electron into vacuum.[171] The technique is used to determine the binding energies of an electron by measuring the energy spectrum and photoelectron yield, often as a function of photon energy.

Because of the high-energy X-rays, the electrons that end up being ejected are the core electrons. Their bandwidths are very narrow, so each level may be approximated as having single energy, E_{core}.[171] The kinetic energy of the emitted electron, E_K, is

$$E_K = h\nu - E_{core} - \varphi \tag{2-2}$$

where $h\nu$ is the energy of a photon and φ is a work function.[171]

Thus, for a given incoming photon of an energy $h\nu$, there will be a sharp peak in the energy distribution curve (h = Planck constant, ν = frequency). The exact value of the E_{core} is sensitive to the distribution of valence electrons surrounding the core. The core electron may only be photoionized if it has enough energy to exit the atom by passing through the valence shells.

In solid materials, the electron path is limited to a few nanometers depth from the material surface because the inelastic scattering events also contribute to the photoemission process. The inelastic mean free path (IMFP) is the distance which an electron will, on average, travel through a solid before losing its energy. Thus, the XPS analysis enables the study of surface atoms. In the XPS spectra, chemical shifts of surface chemical species and their respective core levels are observed. In the studies of organic materials on inorganic substrates, the information on the chemical structure of organic materials, the interface between the layer and the substrate is gathered, and the layer thickness can be estimated.

In this work, XPS was used to acquire information on the nature of bonding between porphyrin and organosilane layers on the silicon surface, i.e., the identification of an amide bond. Besides the product layers, additional spectra of pure samples of (3-aminopropyl)trimethoxysilane (APTMS), CTPPS, and *N*-hydroxysuccinimide (NHS) were collected to obtain a fuller picture of the system.

2.2.4 IR reflection spectroscopy

In IR reflection spectroscopy, the intensity of the reflected IR light at the interface is used for surface characterization. In this work, IR reflection spectroscopy is used as a support to ellipsometric measurements. Because ellipsometry is such a sensitive technique, it detects the vibrational signature of a bulk substrate, the interpretation of ellipsometric spectra might sometimes be confusing and ambiguous, especially with the ultra-thin films. With IR reflection spectroscopy, it is not possible to detect the vibrational signature of the substrate, as it does not use polarized light. Therefore, even though it is less sensitive than ellipsometry, this technique might provide valuable information about structures of the organic material on the surface, which would otherwise be missed.

2.2.5 Surface-enhanced IR absorption (SEIRA)

Surface-enhanced infrared absorption is a highly sensitive technique based on a phenomenon of molecular infrared signals being increased in the proximity of metal island structures as a result of

collective electron resonances. In this work, a gold gradient is deposited on the prepared porphyrin thin film and then analyzed with IR microscopy to support the findings acquired with IR ellipsometry.

3 EXPERIMENTAL DETAILS

3.1 SAMPLE PREPARATION

3.1.1 Materials

Table 3.1: *List of chemicals and materials used in this work.*

Chemicals and materials	Specification	Vendor
Ethanol	absolute, ≥99,8%	Sigma-Aldrich
(3-aminopropyl)trimethoxysilane (APTMS)		Sigma-Aldrich
H_2SO_4	95-98%	Sigma-Aldrich
H_2O_2	30 wt% in H_2O	Sigma-Aldrich
N-Ethoxycarbonyl-2-ethoxy-1,2-dihydro-quinoline (EEDQ)	≥99%	Sigma-Aldrich
Dimethylsulfoxide (DMSO)		Merck
Acetonitrile (ACN)		Merck
p-Nitrobenzoic acid (NBA)		Fluka
Hydrofluoric acid (HF)	10%	Bernd Kraft
5-(4-carboxyphenyl)-10,15,20-(tri-phenyl)porphyrin (CTPP)		PorphyChem
5-(4-carboxyphenyl succinimide ester)-10,15,20-(triphenyl)porphyrin (CTPPS)		PorphyChem
Silicon(111) wafer	p-boron type, ~0.1 Ωcm	MaTeck
DI water	18.2 MΩ ultrapure (Type I) at 25°C	
Maleimidophenyldiazonium tetrafluoroborate (*p*-MPDS)	Synthesized and purified at Fraunhofer-Institut für Angewandete Polymerforschung	
Tetrabutylammonium tetrafluoroborate (Bu_4NBF_4)		Sigma-Aldrich
Mercaptobenzonitrile (MBN)		Synchem
Dimethylformamide (DMF)		Sigma-Aldrich

3.1.2 Preparation of APTMS-modified substrates

3.1.2.1 In situ deposition of APTMS in a flow cell

A solution of 2% APTMS in EtOH was prepared. Si(111) wedge was cleaned by ultrasonication in EtOH for 15 minutes and then oxidized in the piranha (1:1) solution for 20 minutes. Oxidized wedge was mounted on a flow cell and introduced into an ellipsometric chamber. The flow cell was connected to a pump. The system was purged for 1 h with dry air, and then the APTMS solution was pumped into

a cell. Spectra are collected after the first hour, and 15 and 16 hours. After 17 hours, the solution was pumped out. The cell was flushed with EtOH and then purged with dry air. The flow cell was taken out of the chamber, and the wedge was unmounted from the cell. The wedge was ultrasonically cleaned for 10 minutes.

3.1.2.2 Deposition of APTMS on oxidized silicon

Si(111) wedge was cleaned by ultrasonication in EtOH, etched in 1% HF, and then oxidized in piranha (1:1) solution. The oxidized substrate was dipped in a 2% APTMS solution overnight. The substrate was then taken out, washed in a copious amount of water, ultrasonicated in EtOH, and then baked at 110°C for 30 min.

3.1.3 Modification of the substrate with NBA

3.1.3.1 Immobilization of NBA with EEDQ as an activator on an APTMS-modified silicon substrate

A solution of the NBA in ACN was prepared (1.1 mM) and mixed with EEDQ (3.1 mM) for one hour. An APTMS-covered Si substrate was immersed in a solution for five days. As a post-modification workup, the substrate was ultrasonically cleaned two times for 5 minutes each time in a fresh solvent (ACN).

3.1.3.2 In situ deposition of NBA in a flow cell

The APTMS-covered Si(111) wedge was mounted on a flow cell and introduced into an ellipsometric chamber. The flow cell was connected to a pump. The system was purged for 1 h with dry air. A solution of the NBA in ACN was prepared (0.5 mM). An activator, EEDQ, was added to an NBA solution in surplus (0.9 mM), and the mixture was stirred for 1 h. The solution was pumped into a flow cell, and spectra are collected for the first 3 hours. The flow cell with a solution was left mounted over the weekend. Spectra are collected again, after which the solution was pumped out, the cell was rinsed with ACN, and purged in dry air. The wedge was ultrasonically cleaned for 6 min in ACN.

3.1.4 Deposition of porphyrins on the APTMS-modified substrate

3.1.4.1 Immobilization of CTPP with EEDQ as an activator through LbL deposition

A solution of CTPP in DMF (0.3 mM) was prepared with EEDQ in a surplus (4 mM). The solution was mixed for 1 h before dipping in the APTMS-modified substrate. The substrate was dipped for five days. The samples are ultrasonically cleaned two times for 5 min, each time in fresh ACN.

3.1.4.2 Immobilization of CTPPS through LbL deposition

A solution of CTPPS in DMSO (0.7 mM) was prepared. The APTMS-modified substrate was dipped in solution for two days. The samples are ultrasonically cleaned for 2 min in DI water.

3.1.4.3 Solution reaction of CTTPS and APTMS

A solution of CTPPS in DMSO (1.1 mM) was prepared. APTMS (1.15 mM) was added to the mixture and stirred. Drops of product mixture are deposited on a substrate and let dry.

3.1.4.4 Solution reaction of CTTPS and APTMS and bonding to the oxidized Si substrate

A solution of CTPPS (1 mM) and APTMS (1.15 mM) in DMSO was stirred for 3.5 h. To the mixture, 10 μL of water was added. An oxidized substrate was immersed in a solution and left over the weekend. As a test of the film adherence to the surface, the substrate was ultrasonicated in various solvents (water, DMSO, EtOH, iPrOH, and acetone) and etched for 2 minutes in 10% HF solution. As a control, the experiment was repeated with the Si substrate covered with the native oxide.

3.1.4.5 In situ deposition of CTTPS+APTMS

A solution of CTPPS in DMSO (0.56 mM) was prepared. The solution was mixed for 1 h. APTMS (0.69 mM) was added to the solution, and the mixing was continued for 2 h. Then, 0.01% of water was added to the solution. Oxidized Si(111) wedge was mounted on a flow cell and introduced into an ellipsometric chamber. The flow cell was connected to a pump. The system was purged for 1 h with dry air, and then the CTPPS+APTMS solution was pumped into a cell. Spectra are collected for the first 4 h, and from 16th to 23rd hour. After the solution was pumped out, the cell was flushed with iPrOH and then purged in dry air. The sample was ultrasonically cleaned for 2 min in water and additionally washed with iPrOH and water.

3.1.5 Electrografting of diazonium salt substances

3.1.5.1 Deposition of p-MPDS

Solutions for all *p*-MPDS depositions, both electrochemical and electroless, are prepared in the same way. MPDS was dissolved in ACN (2 mM), and Bu_4NBF_4 (0.1 M) was added as an electrolyte. MPDS was deposited on H-terminated Si(111) wedge. The H-termination is achieved in the following way: the substrate was ultrasonicated in an organic solvent (acetone or EtOH), oxidized in piranha (2:1) solution. The oxide layer was finally removed with the dipping of the substrate in a 10% HF solution. The substrate was washed in ACN, water, and iPrOH to remove loosely attached molecules.

3.1.5.2 Thiol deposition

A solution of MBN in EtOH (10 mM) was prepared. The *p*-MP-covered Si substrate was ultrasonically cleaned in water, ACN, and iPrOH before dipping into the MBN solution. The substrate was left in the solution for two days.

3.1.5.3 In situ thiol deposition

A solution of MBN in EtOH (2.2 mM) was prepared and pumped into a flow cell with an already mounted *p*-MP-modified Si(111) wedge. The solution was left overnight with measurements performed every hour for 7 h and after 23 and 24 h. The solution was then pumped out, and the flow cell was

washed with DI water and purged with dry air. The wedge was unmounted and was ultrasonically cleaned in water and ethanol.

3.2 INSTRUMENTAL ANALYSIS

3.2.1 IR reflection and ellipsometric spectroscopy

IR ellipsometric measurements were performed in a photometric ellipsometer chamber attached to a TENSOR 37 (Bruker) FTIR spectrometer, while the reflection measurements were performed inside TENSOR 37 spectrometer. The spectra were collected with a 4 cm^{-1} resolution using a mercury cadmium telluride (MCT) detector. All spectra were collected at a 65° angle of incidence. To reduce the contributions of H_2O and CO_2 in spectra, the chamber with the mounted sample was purged for 0.5-1 h with dry air before the measurement.

3.2.2 In situ IR ellipsometry

For in situ measurements, a flow cell was mounted in the ellipsometric chamber attached to a pump. For electrochemical deposition, the flow cell was connected into a circuit. The potential is measured between a working and counter electrodes in a three-electrode system (working electrode (WE), counter electrode (CE), reference electrode (RE)) connected to a potentiostat. The redox reaction takes place at the WE (Si wedge) by electron transfer from the electrode to the analyte (aryldiazonium species). The CE must have a known potential, and its job is to balance the current observed at WE. The RE (Pt wire) acts as a reference in measuring and controlling of WE potential and in itself does not pass the current.

3.2.3 SEIRA

The CTPPS+APTMS samples were covered with a gold gradient and analyzed with IR microscopy (Bruker Hyperion 3000 IR-Microscope). The gold gradient was deposited by electron beam slow thermal evaporation for 15 min.

3.2.4 XPS

Spectra were recorded at room temperature, using non-monochromatized Al Kα (1486.6 eV) excitation and a hemispherical analyzer (Phoibos 150, SPECS). The binding energy (BE) scale was calibrated by the standard $Au4f_{7/2}$ and $Cu2p_{3/2}$ procedure. All spectra are shown without any binding energy corrections. To calculate the elemental composition, theoretical cross-sections from Yeh and Lindau were used.[172]

To remove the background coming from the inelastic electron scattering, the Shirley background subtraction method is used.[173] The Shirley background subtraction method assumes that the background arises from the scattering of electrons of higher kinetic energy at any point of measurement. From this assumption stems that the background is proportional to the integrated area above the higher kinetic energy side of the peak.

4 SURFACE MODIFICATION WITH APTMS

In this work, APTMS is used to introduce amine functionality to the surface and use them to immobilize porphyrin derivatives.

4.1 DEPOSITION FROM SOLVENT

APTMS is deposited from the EtOH solution on the oxidized silicon surface. In Figure 4.1.a, an IR spectrum of bulk APTMS film is presented. The bulk spectrum points to the specific vibrational bands important for the identification of the material. Aissaoui et al. describe the APTMS spectra on oxidized silicon in detail.[174] Briefly, the two most important bands for the identification of APTMS are the band at ~1578 cm^{-1} belonging to an NH_2 scissor vibration, and the band at ~1150 cm^{-1} belonging to the LO stretching in the organosilane layer. These bands are clearly distinguishable in the spectrum of bulk APTMS. In the thin film spectrum, the amine vibrational bands are often weak or invisible. In Figure 4.1.b, a spectrum of one such film is presented. The NH_2 scissor vibration band is low in intensity and overlaps with another band at ~1597 cm^{-1} and is ascribed to N-H bending mode of the NH_2 group, which is hydrogen-bonded to silanol groups (Si-O-H---NH_2-).[175]

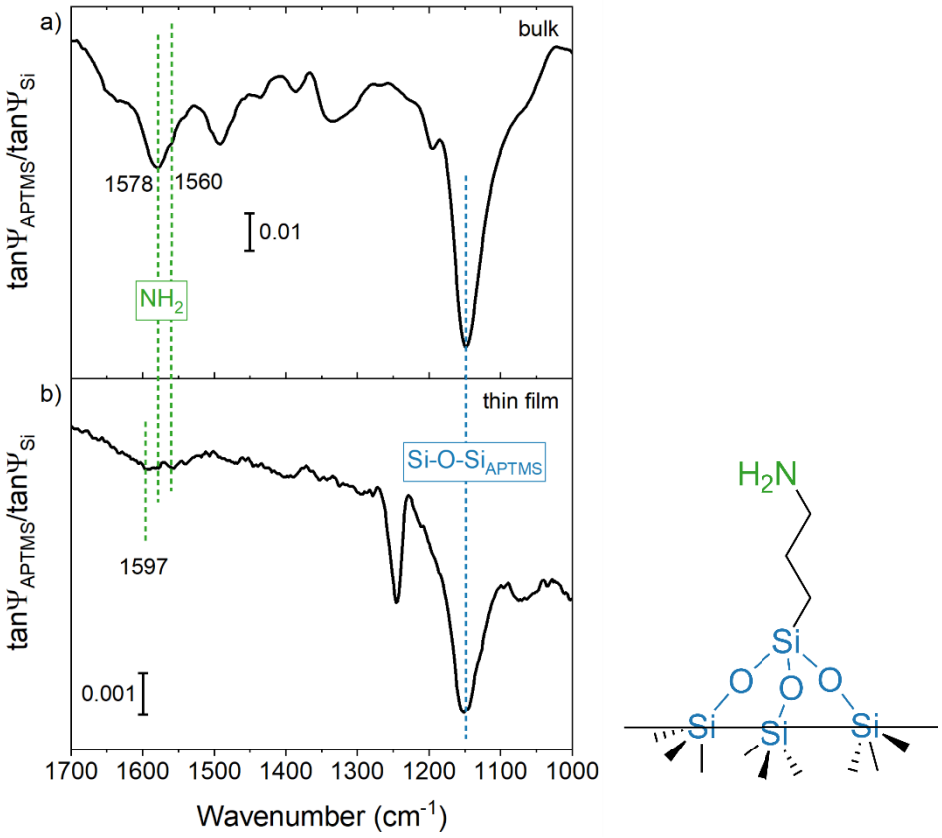

Figure 4.1: *IR ellipsometry spectra of a) bulk APTMS on Si (physisorbed) b) thin APTMS film (chemisorbed).*

However, some conflicting information has been found in the literature regarding this band assignment. Kim et al. claim that the band found at ~1575 cm^{-1} belongs to the stated hydrogen bond (Si-O-H---NH_2-), while the neutral amine band is found at ~1550 cm^{-1} after curing of the films.[139] While both groups had similar methods of deposition, Kim et al. have nevertheless dedicated 24 h to the curing of the films, while Aissaoui et al. cured the films for only 2 hours, allowing more time for structural changes caused by heat and breaking of hydrogen bonds.[139,174] These conflicting findings imply the shift of the amine band in 1600-1550 cm^{-1} area with different amounts of hydrogen bonding within the film structure. Repeated measurements in this work have shown that the results are in agreement with Aissaoui et al., implying hydrogen bonding between APTMS molecules and a portion of amine groups being in a protonated form.

4.2 In situ deposition

The deposition of APTMS is investigated with in situ ellipsometry for the first time. The oxidized silicon wedge was mounted on a flow cell, and the solution of APTMS in EtOH was pumped in. The changes in the spectra over 20 hours of deposition are presented in Figure 4.2. The development of the Si-O band at ~1150 cm^{-1} is the most apparent change in the spectra, indicating a successful integration of APTMS siloxane onto the native oxide structure. The C=O band at 1740 cm^{-1} has also developed but is removed after ultrasonication in the solvent after the deposition (Figure 4.3). Most of the other bands come from the solvent and are no longer present after the substrate is unmounted from the cell and ultrasonicated in the solvent. Since the amine group is weakly absorbing, this area in the in situ spectra is unchanged.

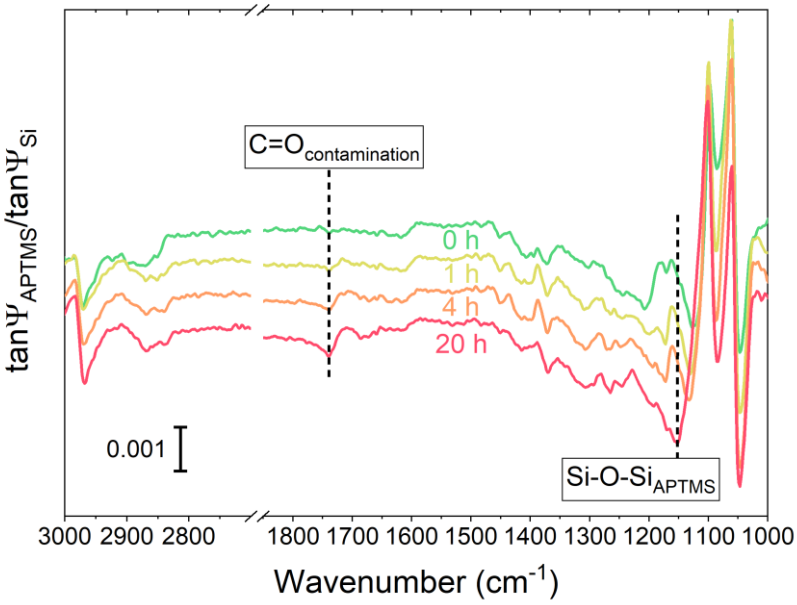

Figure 4.2: *In situ spectra of APTMS after 0 h, 1h, 4 h, and 20 h of deposition.*

The amine band is, however, present in the ex situ spectrum of the same substrate, and after 10 min of ultrasonication (Figure 4.3). In this area, an assemble of unassigned structures with peaks at 1592 cm^{-1}, 1581 cm^{-1}, and 1569 cm^{-1}, and shoulders at 1600 cm^{-1} and 1554 cm^{-1} is observed, indicating a significant contribution of hydrogen bonding in the thin film structure. The sample was not thermally cured.

The asymmetrical and symmetrical stretching of CH_2 groups originating from the propyl chains are present at 2933 cm^{-1} and 2865 cm^{-1}, respectively,[137] while there are no contributions from CH_3 groups originating from methoxy- ($-OCH_3$) groups (area above 2950 cm^{-1}). The lack of CH_3 vibrations, together with a sharp peak at ~1150 cm^{-1} coming from the organosiloxane network, indicates successful chemisorption of APTMS on the substrate.

The two peaks at ~1650 cm^{-1} and ~1500 cm^{-1} are assigned tentatively to silicon surface vibrations. They appear only in the spectra of very thin films. Milekhin et al. describe a peak at 1620 cm^{-1} as being related to multiphonon processes in silicon dioxide coming from the native oxide layer grown at the surface of the sample after annealing and is assigned as $2TO_2$ mode.[176] The calculated peak frequency of this mode is 1632 cm^{-1}. On the other hand, the band at 1650 cm-1 might arise from water molecules trapped in a silane layer,[177] while the band at 1500 cm-1 is a non-specific band which might also come from hydrocarbon species, i.e., propyl chain or contamination. Alternatively, these bands might be some effect from the detector.

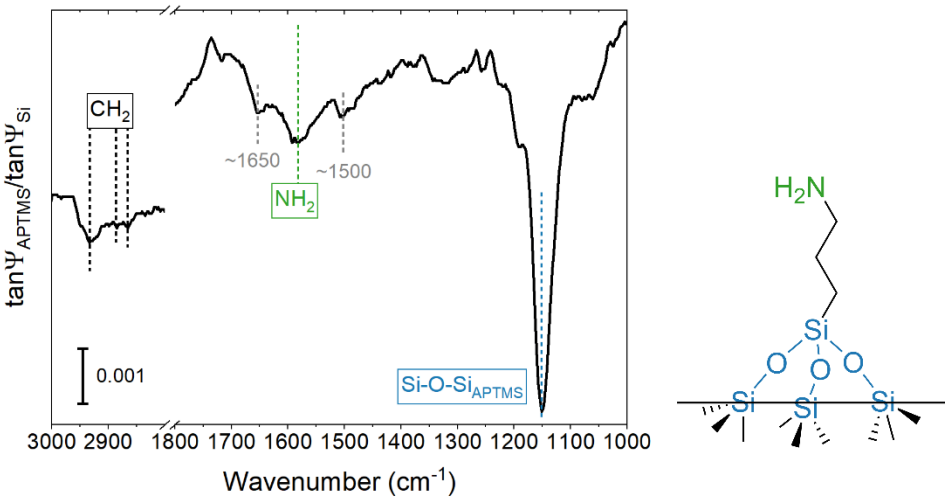

Figure 4.3: *APTMS thin film spectrum after in situ deposition and ultrasonication in a solvent.*

In summary, it was demonstrated that the growth of APTMS films can be monitored in situ. Further research is needed to clarify the issues regarding the position of the amine band, i.e., the influence of hydrogen bonding and the length of thermal curing on the position of the band. In research on some other linker groups with amine functionality, it was demonstrated that the surface modification is improved if the amine group was protected when introducing it to do surface.[48,49,58,64,65] Due to these

findings, it would be worthwhile to research the quality of aminosilane-modified surfaces when the amine group is protected before the deposition.

5 SURFACE MODIFICATION WITH PORPHYRINS

Porphyrins on silicon have been structurally well-characterized with many different surface analysis techniques.[20–26,28,29,31,34,35,42,112,114] Furthermore, scientists have established that they retain their interesting properties when deposited on silicon surface.[8,11,32–35,41,116]

When it comes to the immobilization of porphyrin using organosilanes deposited on silicon, halosilanes are mostly used as a linker molecule.[8,20,21,42–44] Halide functional groups (mostly Cl^- and I^-) are reactive and readily undergo further reactions. However, in many cases, halides (especially chlorides) are too reactive and not selective at all, possibly leading to a reaction with other molecules (i.e., solvent) and not just the target molecule. Also, halide chemicals are not good for the environment. Therefore, using organosilanes with other functionalities (like APTMS) for porphyrin immobilization should also be investigated.

Alternatively, immobilizing porphyrins directly to the surface would be beneficial in creating conductive hybrid silicon surfaces. This idea has been utilized in creating porphyrin-modified surfaces in Lindsey and Bocian groups via hydrosilylation of alkenes,[22,23,28–31,36–38,117,119,178] with triazine directly attached to Si,[114] or with OH-substituted porphyrins and oxidized silicon surface (Si-OH).[39] Given that the electrografting of diazonium salts has proven to be an efficient path for surface passivation with organic molecules, it is worthwhile to explore it with porphyrins as well.

5.1 PROVING THE SURFACE FUNCTIONALIZATION (REACTION WITH *P*-NITROBENZOIC ACID)

To prove the surface modification with $-NH_2$ groups and its ability to further react with other organic materials, the functionality was briefly tested with the immobilization of nitrobenzoic acid (NBA). NBA is used because it gives two easily identifiable spectral bands of appended nitro (NO_2) group.

In Figure 5.1a, the spectrum of bulk NBA is presented, which shows NO_2 bands at 1533 cm^{-1} and 1350 cm^{-1}. They are easily identified in the spectrum of the deposited NBA on an amino-functionalized surface (Figure 5.1b). The amide I and II bands are found at 1655 cm^{-1} and 1554 cm^{-1}, indicating a successful formation of a peptide bond. The C=O band at 1707 cm^{-1} in Figure 5.1a drastically diminishes in Figure 5.1b, further supporting the evidence of an amide formation. Only small traces of the C=O group are present, indicating loosely attached starting material.

The amide I band at 1655 cm^{-1} is broad and positioned in the area 1680-1620 cm^{-1} with shoulders at ~1670 $cm^{-1}$and ~1640 cm^{-1}, implying more bands overlapping each other (Figure 5.1b). The half-width is 32 cm^{-1}. This broad area shows up in all subsequent measurements and modifications with more complex porphyrin structures and in different shapes, thus making the unambiguous identification of amide I band a challenge.

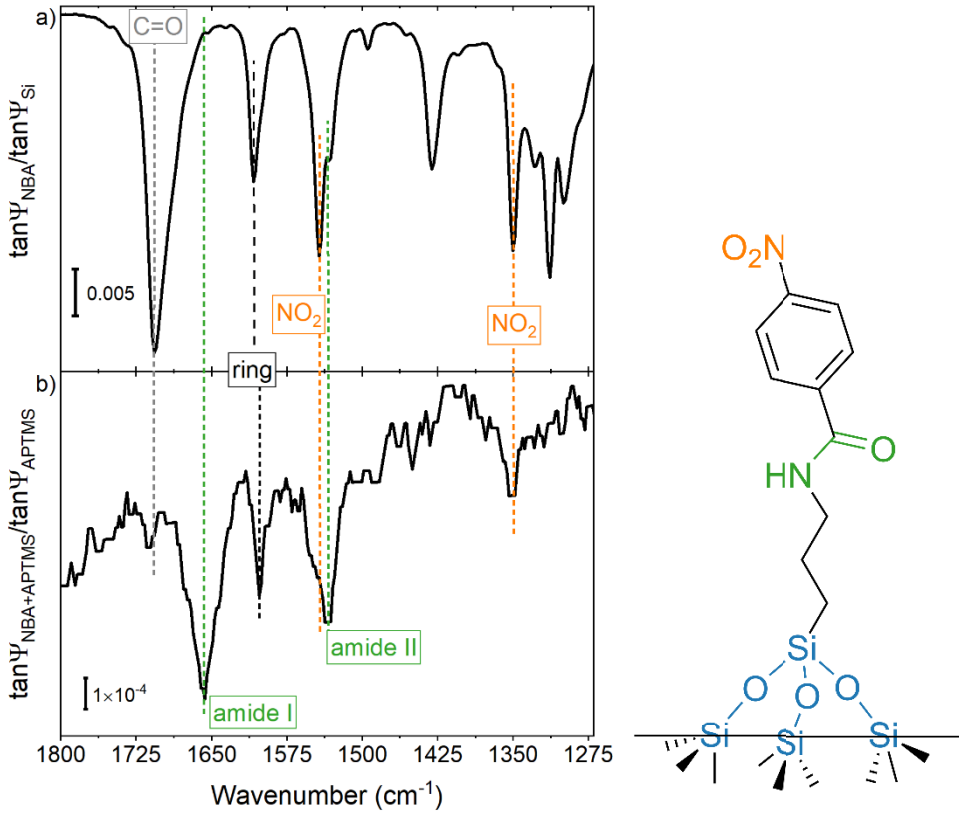

Figure 5.1: *a) Spectrum of pure bulk NBA on Si; b) Spectrum of NBA+APTMS thin film referenced to the APTMS-modified Si.*

The coupling of the NBA with APTMS is also monitored with in situ ellipsometry. In Figure 5.2, we see the spectra of NBA+APTMS thin film development over time. After 3 h reaction time, there is no evidence of NBA attachment, except for the slight oxidation of the surface. However, after two days, a change in the baseline is visible, and one can distinguish C=O, amide I, and NO_2 bands. However, signals remain somewhat weak, indicating a very thin film. Since it is not expected that NBA molecules react with each other and form multilayers, it is probable that a monolayer formed. The peak intensity is comparable with that of a maleimidophenyl monolayer on Si (Chapter 6.1). Being that NBA+APTMS and maleimidophenyl are of similar dimensions and assuming a very thin APTMS layer below the NBA, the peak intensity may relate to a monolayer.

In Figure 5.3a, ex situ tanψ spectra of Si surface, APTMS film on Si, and NBA+APTMS film from the in situ experiment are presented. There are changes in the baseline in the Si-O-Si area (~1150 cm^{-1}), NO_2 areas (1350 cm^{-1} and 1530 cm^{-1}), and amide I area (~1660 cm^{-1}). In Figure 5.3b, the same spectra of APTMS film on Si and NBA+APTMS film on Si referenced to Si spectrum are presented, where we can better see the changes in spectra before and after NBA deposition. Important note: in the APTMS spectrum, H_2O bands in the 2100-1200 cm^{-1} area are visible due to insufficient purging of the ellipsometric chamber with dry air. Therefore, one should take special care in interpreting this area.

Meanwhile, there is no significant presence of the C=O band in NBA+APTMS film, a strong indicator that the NBA is present on the surface only through amide chemistry.

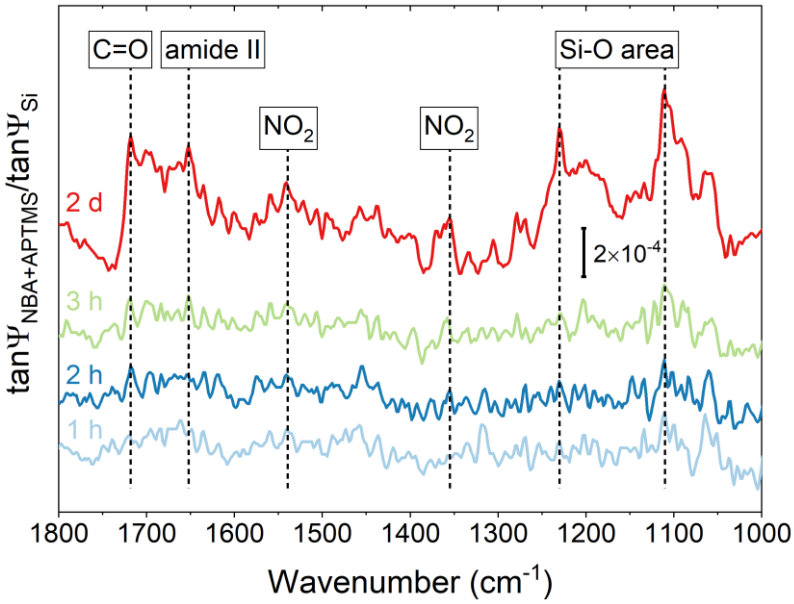

Figure 5.2: *Spectra of in situ NBA deposition over time, referenced to a cell with solvent (ACN).*

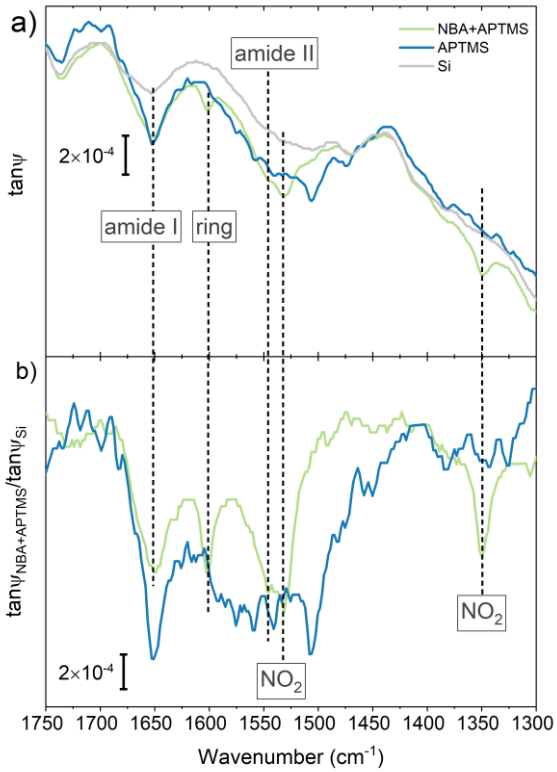

Figure 5.3*: a) Spectra of Si, APTMS on Si, and NBA+APTMS on Si; b) Spectra of APTMS and NBA+APTMS thin films referenced to Si.*

The presented results demonstrate that the spectra from in situ and ex situ measurements are in agreement with each other. The reproducibility of the results also points to APTMS being an adequate choice as a linker molecule for further functionalization.

5.2 IMMOBILIZATION OF CTPPS ON AN APTMS-MODIFIED SURFACE (LBL APPROACH)

CTPPS is an activated form of CTPP, activated with NHS. In the reaction with APTMS, CTPPS and CTPP give the same product, CTPP(S)+APTMS. Since CTPPS is already in its activated and pure form, that means that its activation barrier is lowered, and it readily reacts with other reactants. Using the pre-purchased activated form of the material eliminates an additional step of the in situ synthesis and improves the yield.

5.2.1 IR ellipsometry

The reaction of CTPPS with APTMS in solution is successful and resulted in an almost completed reaction, which can be seen in Figure 5.4a. After 30 min reaction time, a reaction solution is drop deposited on the Si+SiO_x surface. A sharp decrease of 1740 cm^{-1} and 1767 cm^{-1} C=O bands is evident after the reaction with the APTMS (Figure 5.4a, dark blue curve) as compared to a starting material (light blue curve). The structure of CTPPS (Figure 1.3) has three inequivalent C=O bands. This might explain the spectrum of pure CTPPS compound (Figure 5.4a, light blue curve), which has two C=O bands at 1767 cm^{-1} and 1740 cm^{-1} and a shoulder at ~1720 cm^{-1}.

After the reaction, only a small band at ~1720 cm^{-1} remained, possibly indicating the minute presence of a starting material. In the product spectrum (Figure 5.4a, dark blue curve), an appearance of overlapping 1662 cm^{-1} and 1649 cm^{-1} bands in the amide I region and a 1535 cm^{-1} band in the amide II region is observed, thus confirming the successful reaction. For more details, in Figure S5.1, the spectra of all starting materials and products are presented.

The reaction is then transferred to a silicon surface. APTMS is immobilized chemically, and CTPPS is added by LbL deposition. In Figure 5.4b, one observes the C=O bands of an unreacted physisorbed CTPPS, but also there are new bands in the amide region, as well as amine band at 1575 cm^{-1}, indicating a partial reaction. Considering that the reaction time is two days, the results point to much slower reaction times than the same reaction in solution.

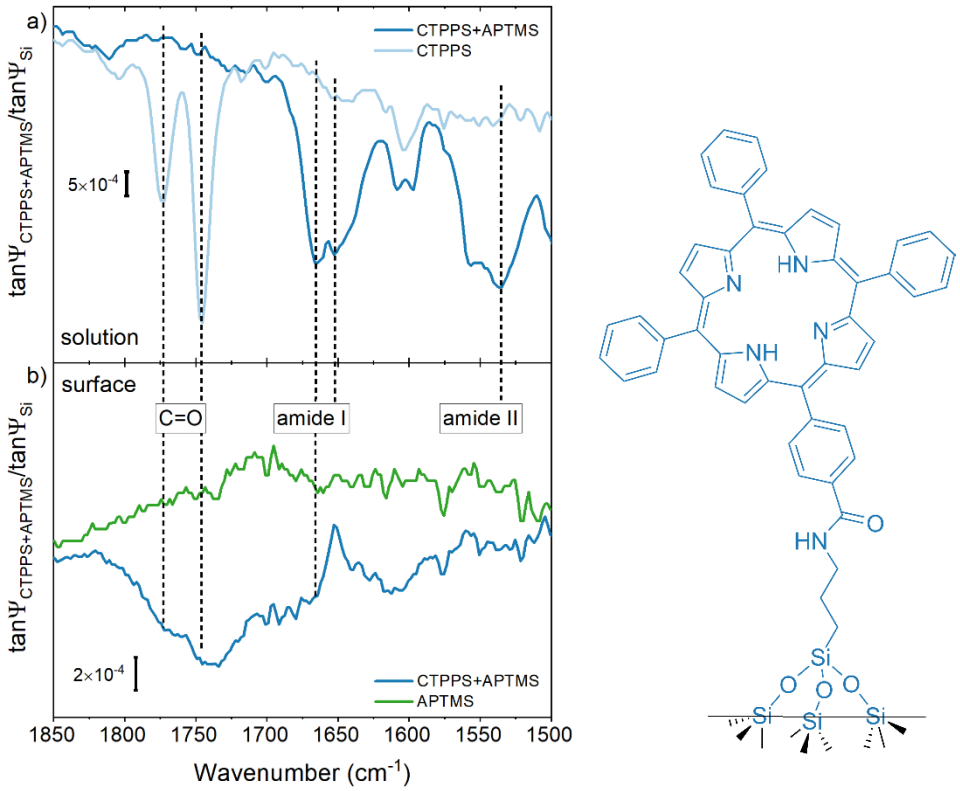

Figure 5.4: *a) Spectra of pure CTPPS and CTPPS+APTMS product in solution (DMF); b) Spectra of APTMS and CTPPS+APTMS thin films deposited by LbL deposition.*

5.2.2 SEIRA

The sample is also probed with SEIRA. In Figure 5.5, the SEIRA spectrum of APTMS indicates that any contribution coming from this material will be weak. Thus, the change in spectra from CTPPS (Figure 5.5a) to CTPPS+APTMS (Figure 5.5b) is attributed to the formation of amide bonds.

The carbonyl, the amide I, and the ring vibration areas are changed in such a way that the entire 1750-1500 cm^{-1} area looks like one broad band (Figure 5.5b), suggesting an overlap of multiple bands, indicating a change in the structure. Two shoulders are observed at 1714 cm^{-1} and 1658 cm^{-1}, indicating C=O and amide I bands, respectively, signaling the presence of both unreacted and reacted CTPPS in support of ellipsometric measurements. The carbonyl peak at ~1710 cm^{-1} decreases in size while amide I and ring bands seem to increase, which would correspond to the formation of an amide bond and increased presence of CTPPS molecules in general, respectively, since every CTPPS molecule has four benzene rings and a core =CH- skeletal structure (Figure 1.3).

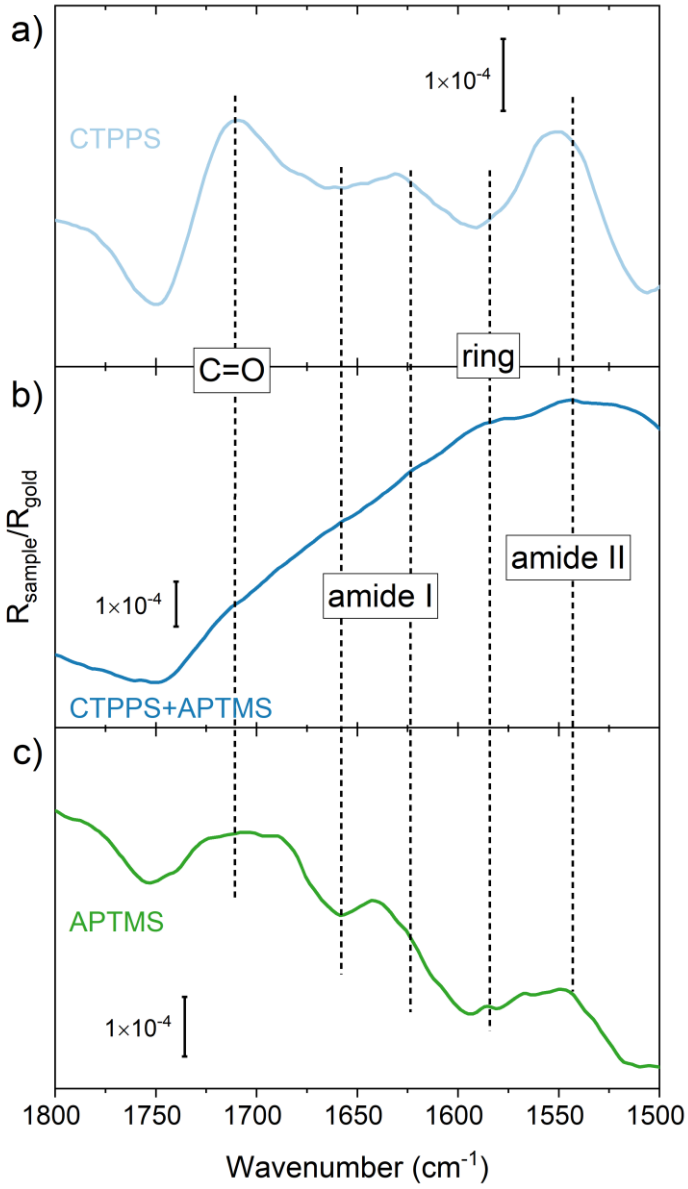

Figure 5.5: *SEIRA spectra of a) CTTPS, b) CTPPS+APTMS, c) APTMS.*

5.2.3 XPS

It is well known for aminosilanes, that surface amine groups oxidize in contact with air[145] or otherwise interact inter- and intramolecularly.[140] XPS measurements of the sample also confirm this.

The XPS ray photoelectron spectroscopy was used to evaluate the composition of the materials on the silicon surface, and to assess the chemical state of the contributing species. Table 5.1 shows the quantitative information, whereas Figure 5.6 depicts the main core levels.

Survey spectra (not shown) reveal only the expected Si, O, N, and C species, with no contribution from any other elements. The elements of interest all have low photoionization cross-sections at their characteristic core levels; thus, their spectrum intensity is in general low. This is especially problematic at the N1s spectra, as the amount of N in the samples is low. This is especially true for the NHS sample.

Table 5.1: *Surface near-molar ratios according to XPS.*

	APTMS	NHS	CTPPS	CTPPS+APTMS
N/C	0.095	0.072	0.092	0.085
C/Si	0.25	0.086	0.17	0.58
N/Si	0.024	0.006	0.016	0.049
O/Si	0.38	0.36	0.36	0.39
O/Si(ox.)[a]	2.75	2.9	2.84	2.5

[a]: Si2p was fitted to extract the portion of oxidized Si

The N/C elemental ratios are always smaller than those expected based on the stoichiometry of the entity intended to deposit onto the Si surface. This is, however, most probably because all materials contain some carbonaceous deposits on the surface. The best agreement in the N/C ratio is for the sample CTPPS+APTMS (0.085 vs. the stoichiometric 0.104).

Based on the C/Si and N/Si values, the least amount of organic molecules were deposited in NHS, followed by CTPPS. APTMS attachment seems to be more successful compared to NHS and CTPPS, which makes sense with its silicon chemistry. In the target reaction, after attaching APTMS to the surface, CTPPS can be linked to the amine group. In this sample (CTTPS+APTMS), the largest amount of C and N was observed. This is the first indication that CTPPS indeed attaches to APTMS.

The Si2p spectrum shows the strong elemental Si peak at ~99.55 eV. The native oxide peak is positioned at ~103.4 eV, except that of CTPPS+APTMS, which is shifted to 103 eV. Fitting also suggests a peak at ~101.3 eV, which can be related to some Si-suboxide.

There is some variation in the O1s peak binding energy (532.6-532.8 eV), but this energy fits well with oxidized Si. Nevertheless, when the amount of oxygen observed (O1s) is related to the amount of oxidized Si (Si2p), the values are higher than 2, suggesting the presence of some other oxygen species on the surface. This is probably the presence of water and organic contamination, except for APTMS, which also contains oxygen.

In general, the samples appeared to be not overly beam-sensitive, as N1s and C1s spectra were reasonably reproduced over time.

The N1s spectra were analyzed assuming only 4 N species, even though the possibility of more N species involved cannot be ruled out.

APTMS should have only one type of N1s species (amine), but the spectrum clearly indicates two species. The peak at ~400.3 eV is related to the amine group.[179] The second peak is situated at higher binding energy (402.3 eV), which can be assigned to some oxidized N functional group.[179]

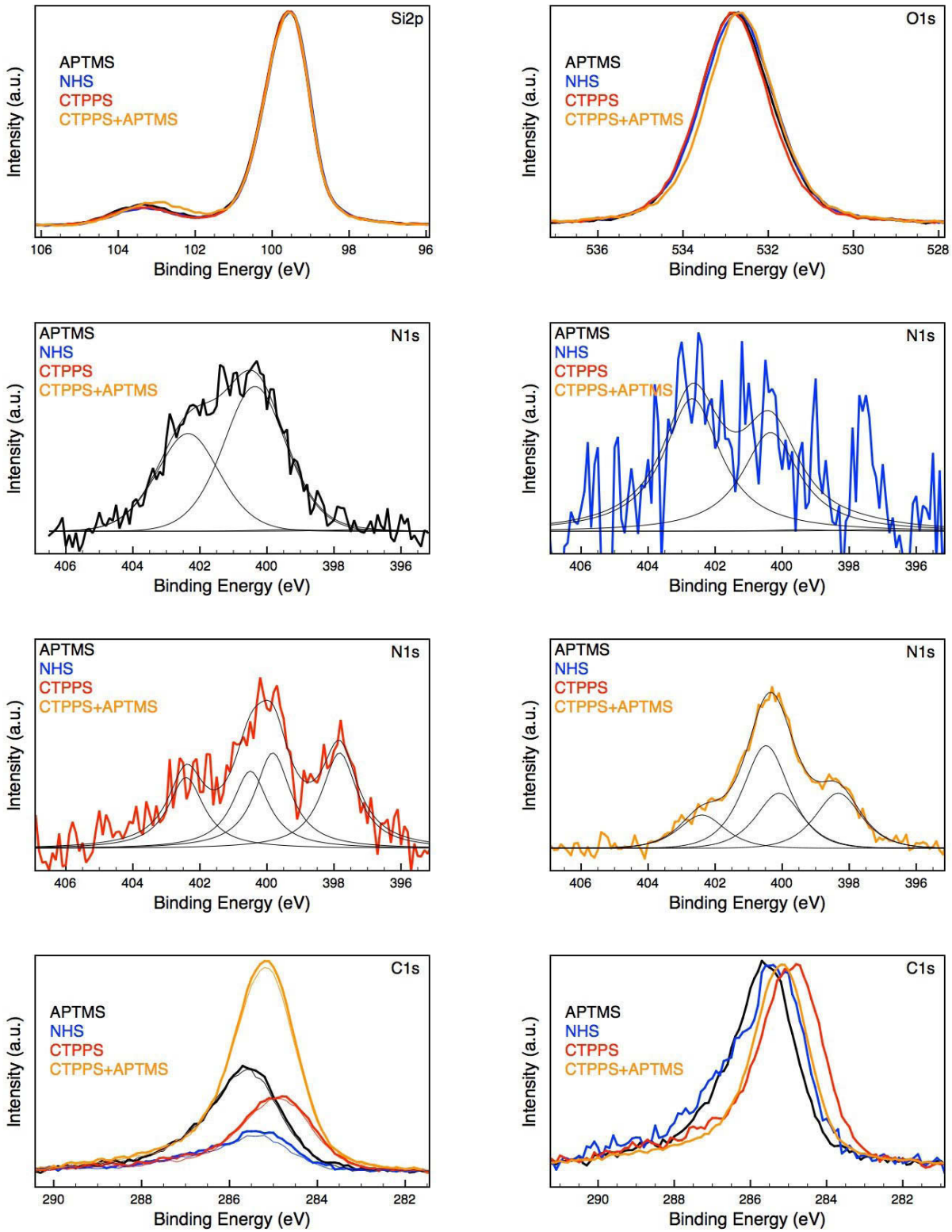

Figure 5.6: *The main core-level regions of the samples after Shirley background subtraction and intensity normalization. C1s spectra are also shown without normalization (the thin line is a second spectrum recorded some time later). All binding energies are shown as collected.*

Even though the NHS spectrum is mostly noise, the largest contribution appears to be at a similar high binding energy (402.7 eV), which is assumed to be related to the intended hydroxysuccinimide. Nevertheless, there is some lower binding energy N1s contribution in this sample, too, indicating the presence of some reduced N functional groups.

CTPPS should contain three different types of N: a non-protonated (397.8 eV) and a protonated N in the porphyrin structure (399.8 eV), as well an oxidized N of the imide (402.4 eV). Ideally, the ratio of the protonated and non-protonated N in the porphyrin structure is 1. Furthermore, the main N1s line at ~400 eV seems to be asymmetric. Thus, four peaks were used in the fitting, with the constraint of two equally sized peaks related to the porphyrin. The fitting results in ~21% oxidized N, ~2x28% N in the porphyrin structure, and an additional 21% contribution, which might be some NH_x species. If the ratio of protonated and non-protonated N in the porphyrin structure is assumed to deviate from 1, and thus all the ~400 eV peak can be related to the protonated N in the porphyrin, the ratio of oxidized N to porphyrin N is 21/79, that is close to the expected 1:4.

In the N1s spectrum of CTPPS+APTMS, a ~13% oxidized N (402.4 eV) is observed. As this peak also appears in the APTMS spectrum, it is possible that some part of amino groups oxidizes and then it remains on the surface as a spectator. This proposition corresponds well with the general scheme of APTMS layers being protonated and interconnected with hydrogen bonding, as described in Chapter 2.1.2. That is, this part will not react with CTPPS. Alternatively, this oxidized peak can be unreacted imide functional groups from CTPPS. Furthermore, two similar lower binding energy peaks as in CTPPS are present, but the binding energies are slightly different. The peak of non-protonated (398.3 eV) and protonated (400.1 eV) porphyrin are upshifted, suggesting some sort of modification. Note, the magnitude of the binding energy shift of the protonated porphyrin N is difficult to estimate with high certainty. This will depend upon the assumptions one makes in constraining the fit. Nevertheless, the shift suggests some change in comparison to CTPPS. The porphyrin rings may interact with each other, or with the substrate surface, depending on the actual geometry on the surface and the underlying APTMS structure. The fitting result indicates that 22% of the total N of the sample belongs to the non-protonated porphyrin N. Ideally, this should be 40%, and was 28% in CTPPS. Since in CTPPS+APTMS it is only 22%, the oxidized species is assumed to come not from the unreacted CTPPS but rather the oxidized APTMS.

The C1s spectra are displayed in both an unscaled and scaled way. As mentioned above, the samples have much more C as compared to N, and hence some part of the C1s intensity is not related to the targeted organic entity. Nevertheless, one can see that the binding energy of the main line shifts; the lowest binding energy is found for CTPPS and CTPPS+APTMS, whereas the highest binding energy is found for APTMS. This is related to the degree of hydrogenation of the carbon species. In APTMS, all carbon atoms are fully hydrogenated, while in the porphyrin structure, all carbon atoms are dehydrogenated (sp^3 vs. sp^2). NHS has a clear higher binding energy shoulder, which can be related to

the carbonyl groups in the succinamide. Since the CTPPS+APTMS sample has the least intensity at the C=O binding energy, there is probably no or very little unreacted CTPPS in that sample.

In conclusion, it is not certain that the CTPPS+APTMS sample contains only the targeted organic entity. Rather, hints of unreacted APTMS, and/or oxidized APTMS are present. Furthermore, there is some indication that the ratio of protonated and non-protonated porphyrin N is not unity, but is shifted towards protonation.

5.3 Immobilization of CTTPS+APTMS directly to the surface (Si-OH)

An alternative synthetic approach to the LbL deposition is proposed. The reaction of CTPPS and APTMS is allowed to take place in solution, followed by a product deposition on an oxidized silicon surface (schemes of both methods of deposition are depicted in Figure 5.7). In this way, two unwanted side-effects are avoided:

(i) the degradation of thin film quality due to LbL deposition, and

(ii) the loss of available surface amine groups due to oxidation or hydrogen bonding.

The spectra of such surfaces correspond to the spectra of the drop-deposited reactant from a previous experiment (Figure 5.8a and b).

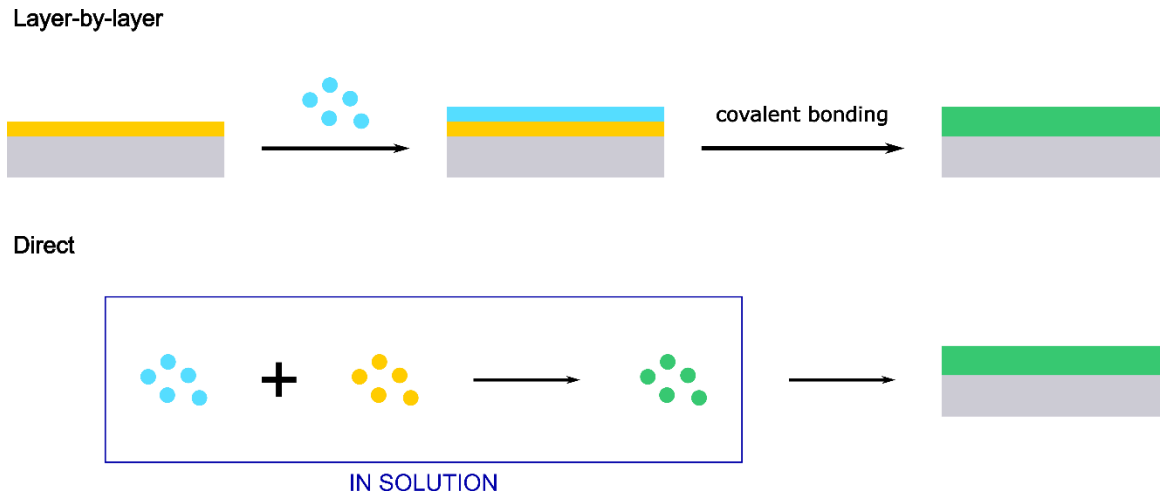

Figure 5.7: *Scheme of a layer-by-layer deposition and direct deposition from solution, as used in this work.*

The blank experiment on non-oxidized silicon ($Si+SiO_x$) is also performed. In both cases, the product stays bound to the surface, even when the substrates undergo ultrasonic treatment in several different solvents (water, DMSO, ethanol, isopropanol, and acetone). The spectra of both are shown in Figure 5.9. However, the sample on $Si+SiO_x$ shows the greater contribution of C=O bands than the sample deposited on the Si-OH surface, indicating a greater presence of loosely attached material on the surface.

The dark blue curve in Figure 5.9 depicts a CTPPS+APTMS film on Si-OH after a 1-minute etching in 10% HF. Despite these harsh conditions, the amide bands are still present, indicating strong adhering to the surface.

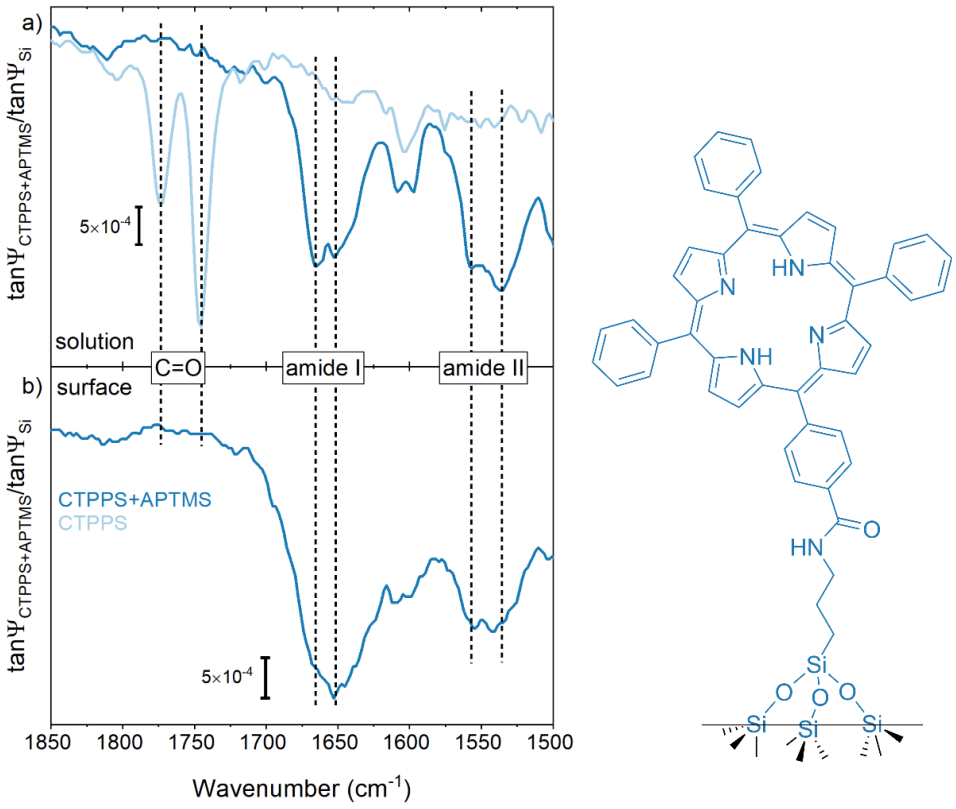

Figure 5.8: *Direct deposition of a product, CTPPS+APTMS, on Si (b) is spectrally similar to the spectrum of the product in solution (a).*

The same deposition approach on oxidized silicon (Si-OH) was tried in situ. The in situ spectra in Figure 5.10 show physisorption in the first 4 h of the reaction.After leaving the cell with the solution and the sample overnight, and pumping in a fresh solution in the morning, all of the material washed off the substrate. There is no further film growth after this event. In the siloxane area, a reduction of the Si-O-Si band at 1066 cm^{-1} over time is observed (the reduction is marked with the red arrow in Figure 5.10).

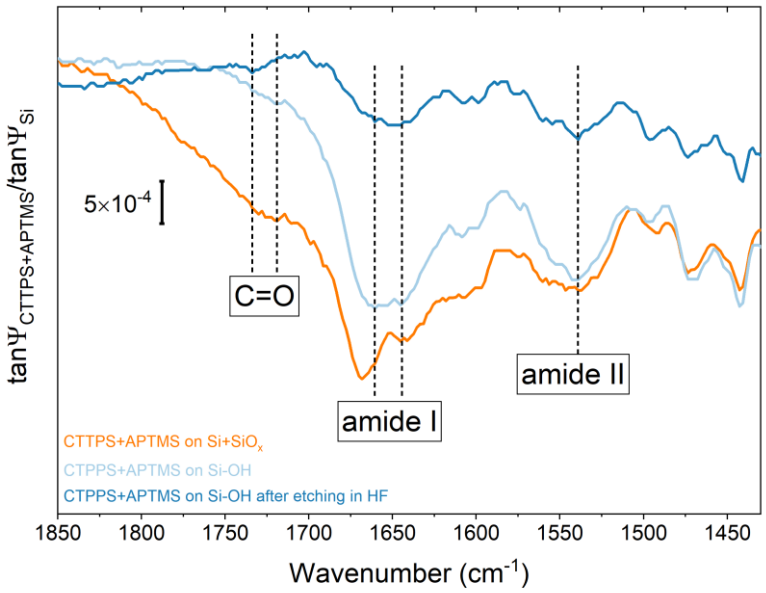

Figure 5.9: *Spectra of CTPPS+APTMS films deposited on oxidized (light blue curve) and non-oxidized (orange curve) silicon substrate. The dark blue curve is the spectrum of CTPPS+APTMS film on oxidized Si after 1-minute etching in 10% HF.*

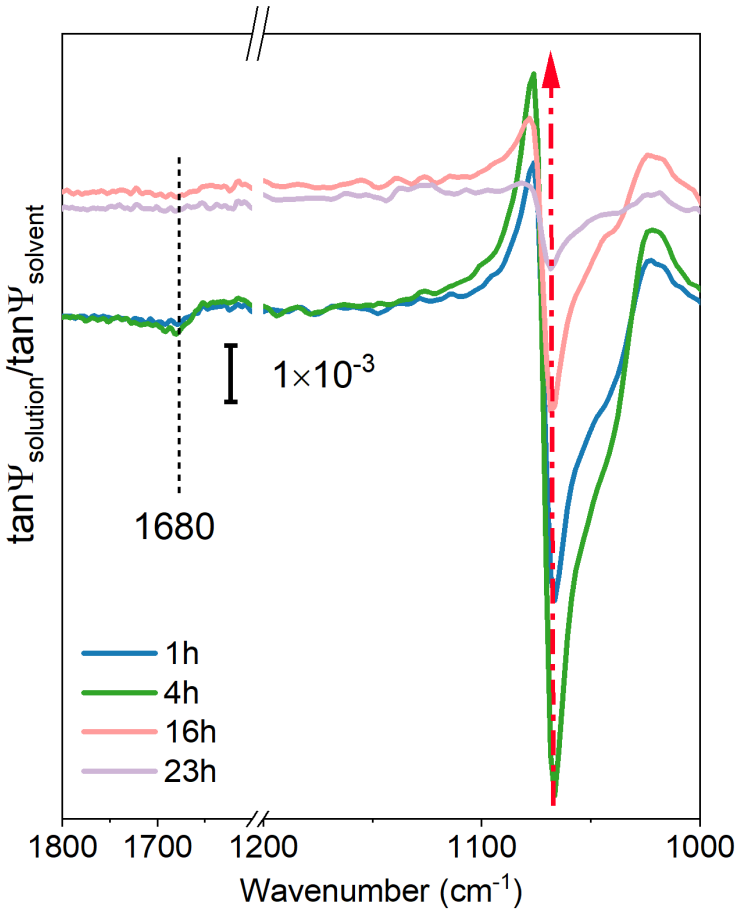

Figure 5.10: *In situ spectra of CTPPS+APTMS deposition on Si-OH over time, referenced to a cell with the solvent (DMSO).*

5.4 IMMOBILIZATION OF CTPP ON AN APTMS-MODIFIED SURFACE

CTPP is a non-activated form of CTPPS. For the reaction to take place, the CTPP is activated in situ with EEDQ.

The reaction of EEDQ-activated CTTP with APTMS to form an amide bond is tested in solution. EEDQ is added to the CTTP solution in surplus amount with DMF as a solvent and is mixed for 1 hour before adding APTMS. All reactants and products are prepared in solution, drop deposited on Au substrates, and analyzed with IR reflection spectroscopy.

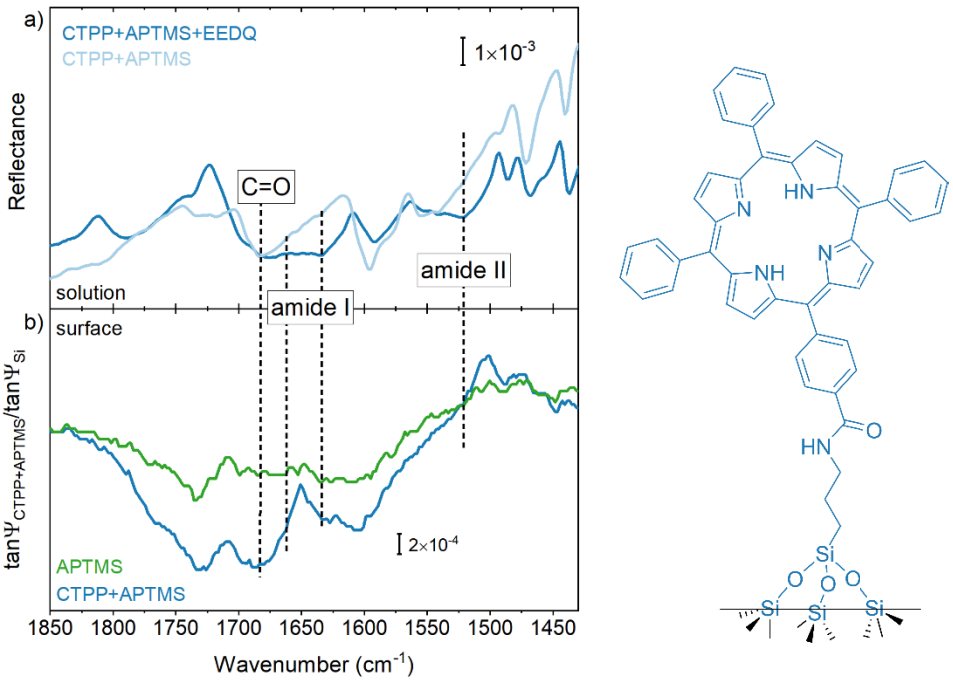

Figure 5.11*: a) IR reflection spectra of CTPP+APTMS mixture without an activator (light blue curve) and CTPP+APTMS with EEDQ as an activator (dark blue curve) in solution); b) Spectra of APTMS and CTPP+APTMS (activated with EEDQ) thin films deposited via LbL technique.*

Especially for the mixtures of CTPP and APTMS with and without EEDQ (dark and light blue curves in Figure 5.11a, respectively), we see a development of amide peaks in 1680-1610 cm^{-1} and 1530-1500 cm^{-1} areas in the dark blue spectrum, assigned to amide I and amide II vibrations, respectively, evidencing a more successful reaction with the help of an activator. Even so, unlike in the reaction of CTPPS and APTMS, the contribution of C=O bands at ~1680 cm^{-1} from the starting material is still significantly large. The slower or unfinished reaction probably comes from the fact that the EEDQ and CTPP need to be mixed and allowed to react before the reaction with APTMS. This extra step presents

a limitation in synthesis since more synthetic steps mean a lower yield of the final product. With CTPPS, however, we already have an activated form of a starting material with a lower activation barrier and ready to react with other reactants.

For a detailed picture, in Figure S5.2, the spectra of all starting materials and products are presented.

The solution experiment provided valuable insight into the identification of the vibrational bands of reactants and products when converted on the surface (Figure 5.11). The silicon substrate is modified with APTMS in a standard way and then dipped into a mixture of CTTP and surplus EEDQ in DMF for five days. The peaks of vibrational bands are broad, but a change in the baseline is evident. A shoulder of amide I band is present at ~1660 cm^{-1}, while the amide II band is too weak to be clearly observed. The presence of a physisorbed starting material is evident with bands at 1724 cm^{-1} and ~1685 cm^{-1}.

In summary, two porphyrin derivatives, CTPP and CTPPS, are successfully attached to the APTMS-modified silicon substrate. Identification of the successful chemical bonding through the detection of amide bands in IR spectra proved challenging. Already with the simple molecule like NBA, there are multiple peaks in the amide I area, making the detection of amide band challenging, and this is even more prominent with larger porphyrin molecules that have a more complex spectral signature (especially on a monolayer level). Additionally, the in situ experiments of NBA binding to the APTMS-modified surface shows no observable attachment in the first 3 hours of deposition and a formed monolayer after 48 hours.

It is observed that the amidation reaction happens much faster in solution than on the surface. Solution reactions also indicate that the reaction of APTMS with the pre-activated porphyrin derivative (CTPPS) has a higher yield than in situ activated porphyrin (CTPP activated with EEDQ).

The identification of amide bands in samples deposited by the LbL approach with IR ellipsometry and reflectometry is challenging and ambiguous due to incomplete surface reactions and the complex IR signature of porphyrin molecules. The XPS and SEIRA measurements of the same system contribute to the identification of amide I bond by providing additional evidence of the amide group.

Another synthetic approach, where the product CTPPS+APTMS is prepared in solution and then deposited on the oxidized Si substrate, is proposed. Such synthesis results in a strongly adhering thin film with minimal contribution from unreacted molecules, resistant to ultrasonication in various solvents and etching in 10% HF for at least one minute. The preliminary evidence on this synthetic approach demonstrates that it is a good alternative to the LbL approach, avoiding the degradation of the surface and the oxidation of amino groups on the surface and, thus, the unwanted surface species.

The findings contribute to a better understanding of porphyrin attachment to siliceous materials, illuminate the necessary synthetic conditions for the successful attachment, and provide insight into the kinetics of bulky molecules at the solvent/solid interface.

6 SURFACE MODIFICATION WITH MALEIMIDE

Electrografting of *p*-MPDS on an H-terminated Si surface is a quick and reliable way to introduce maleimide functionality to an electrode surface. Zhang et al. described a formation of a first maleimidophenyl (*p*-MP) monolayer after 60 s at -2 V and proved the biosensing possibility of a maleimide-modified surface,[62] while Kanyong et al. measured the 50% grafting efficiency after the first potential scan and determined the monolayer thickness.[63]

However, a more in-depth look at the events happening at the surface during the formation of a first monolayer is needed to construct more robust surfaces successfully. Here, we zoom-in on the surface events taking place during the maleimide immobilization.

6.1 ELECTROGRAFTING OF *P*-MP: IN SITU IRSE STUDY

Figure 6.1 shows the ex situ *p*-MP spectrum after 10 s of electrochemical deposition at -2 V normalized to a non-modified Si(111) surface. In Figure 6.1a, the tanΨ spectra of unmodified and modified Si substrate are presented, accentuating the changes that take place after the *p*-MP deposition. As anticipated, the spectrum is in agreement with the literature reports for maleimide deposited on the surface. Briefly, the strong peak at 1734 cm^{-1} is attributed to vibrations of two C=O groups in the maleimide ring. The peak at 1541 cm^{-1} is assigned to benzene ring vibrations, while the peak at 1385 cm^{-1} is assigned to C_{aryl}-N bond.[63]

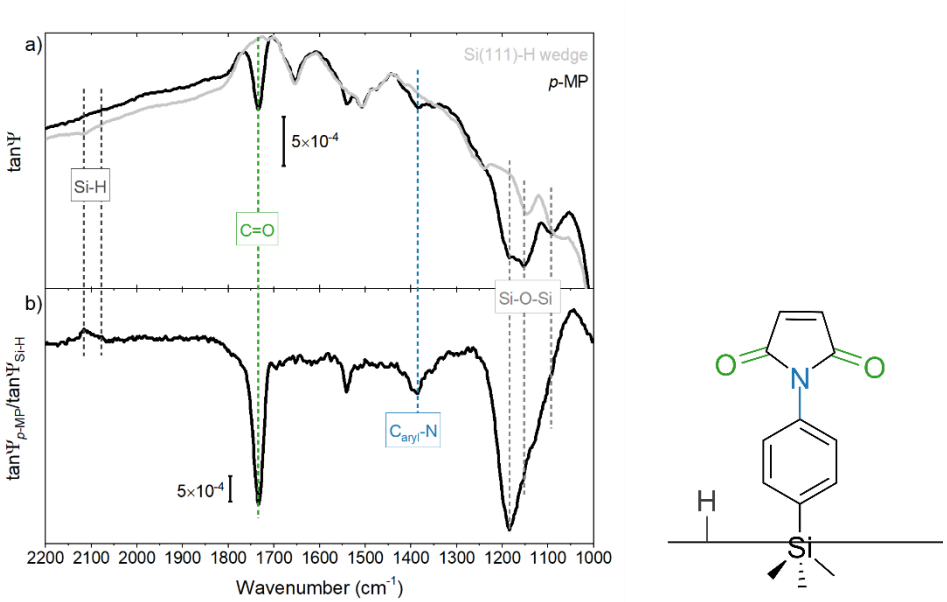

Figure 6.1: *a) ex situ tanψ spectra of H-terminated Si(111) substrate and p-MP thin film on a Si(111) substrate; b) tanψ spectra of p-MP thin film normalized to H-terminated Si(111) substrate.*

When films are thicker (with more prolonged deposition), the C≡N, CH_2, and CH_3 peaks also appear around ~2300 cm^{-1}, 2880 cm^{-1}, and 2970 cm^{-1}, respectively (Figure S6.5), which are generally assigned to solvent molecules (ACN).[63] Solvent molecules are easily removed with sonication.

According to the optical model developed by Kanyong et al., we can estimate the number of *p*-MP monolayers from the C=O peak amplitude of the in situ measurement.[63] An amplitude of ~8×10^{-4} relates to ~3.5 monolayers. In the present experiment, the amplitude is about ~6×10^{-4} after 600 s deposition at -2 V, indicating the formation of roughly two monolayers.

The two Si-H peaks present in the Si(111)-H wedge spectrum, are no longer present in the *p*-MP spectrum (Figure 6.1a). When the *p*-MP spectrum is normalized to that of a Si(111)-H wedge (Figure 6.1b), the peaks appear inverted, which is an indication of the loss of Si-H species at the surface, or they are below the limit of detection.

Additionally, there is a development of siloxane peaks at 1184 cm^{-1}, 1153 cm^{-1}, and 1091 cm^{-1}. Since the cathodic current is used in anhydrous acetonitrile, there should be no oxidation of the surface. It is found that purging the electrochemical cell with dry air for 2 h to remove atmospheric water before pumping in of the solution in the cell contributes to the diminishing of siloxane peaks (Figure S6.2). However, even with the purging, some of the oxide still develops (peaks at ~1090 cm^{-1} and 1070 cm^{-1} attributed to TO in Figure S6.2).[180] Another possibility is that the oxidation happens due to a trace amount of water or dissolved air bubbles in the *p*-MPDS solution. In the case of air bubbles, it would help that the solution is bubbled with an inert gas such as N_2 to rid of any air molecules.

Etching of the samples with a 10% HF solution for 10 minutes removes entire oxide while the maleimide layer is still present (Figure S6.3). This finding indicates a covalent bonding of *p*-MP to the surface, with the oxide forming on top of the organic layer or in between the *p*-MP islands.

The samples also showed resistance to ultrasonic treatment in various solvents (water, ACN, i-PrOH), with the solvents removing physisorbed molecules, indicating a robust binding of an underlying organic layer to the surface (Figure S6.4). There is yet no direct way of confirming the formation of the Si-C bond at the interface, but the experiments with etching in HF and ultrasonic treatment in solvents give a significant indication of a stable, robust binding to the surface silicon atoms.

6.2 PULSE CHRONOAMPEROMETRIC DEPOSITION

In a typical electrochemical deposition at -2 V, most of the *p*-MP monolayer is deposited already after the 30 s (Figure S6.6). A study was conducted to observe the film growth when short electric pulses are applied to the system. In this experiment, ten 1-second pulses are applied to the electrochemical system. In situ IRSE spectra are collected after each pulse. By monitoring the change in the amplitude of a C=O, a formation of this band is already observed after 4 s (Figure 6.2). Across further six depositions, the

C=O band becomes more prominent. The C=O band amplitude of ~2×10^{-4} suggests the formation of an incomplete monolayer.

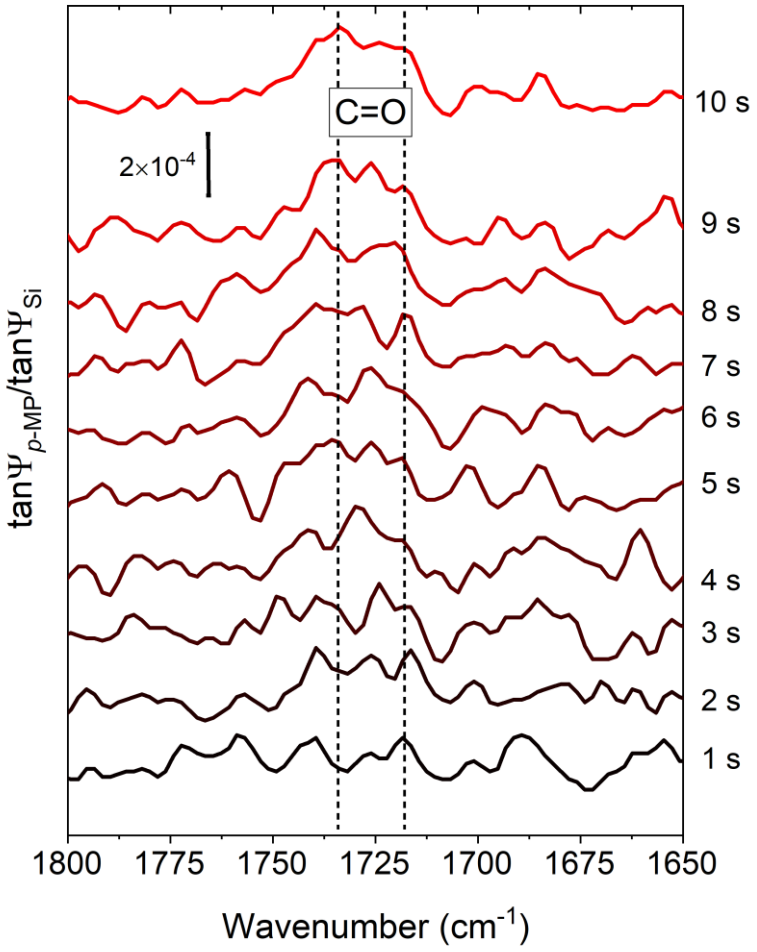

Figure 6.2: *In situ spectra of the formation of a p-MP thin layer on a silicon substrate is taken after each 1-second pulse.*

In further experiments, the deposition times are dropped down to the millisecond level with capturing of IRSE spectra between each deposition. At first, a 100 ms deposition is performed, and the spectra are collected. An indication of a C=O band is immediately noticeable, but due to the S/N ratio of a baseline, it could not be confirmed. Therefore, higher quality measurements are collected. After taking these measurements, it is noticed that the film grew over time (the intensity of the bands changed) even though the charge is no longer applied. In Figure 6.3, spectra are shown after the first measurement (which lasted ~30 min), then the second (~1 h), and finally, the third measurement (~8 h). An intensity change in the amplitude of a C=O band is clearly visible after each measurement. Furthermore, the intensity change of the bands is not linear, as evidenced in Figure 6.3. Since the change in the spectra is rapid in the first 1.5 h, it is concluded that the first measurement (after ~30 min) does not truly reflect the state of the interface after 100 ms deposition. This finding also implies that due to fast film growth, it is not possible to capture high-quality spectra of silicon interface after such short times with this

instrumentation because due to the radical nature of the mechanism, the film growth cannot be paused and collecting high-quality spectra takes time.

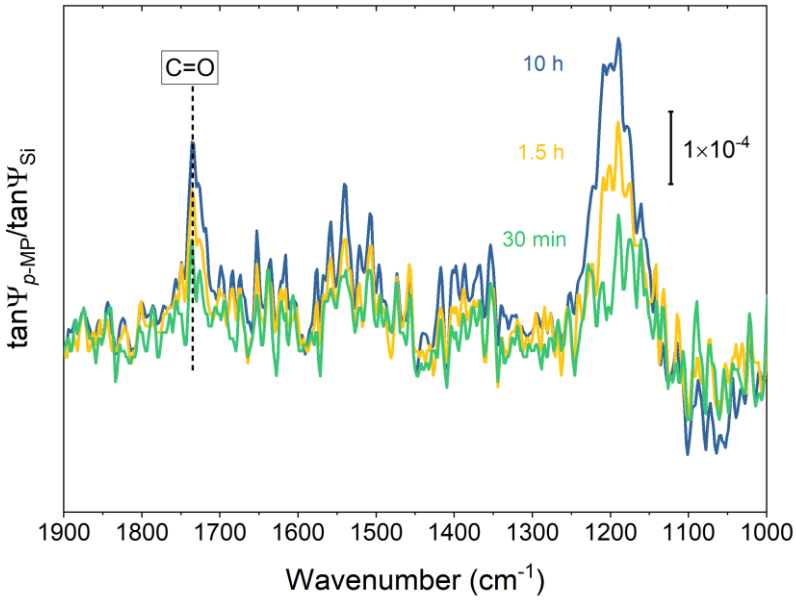

Figure 6.3: *In situ spectra of the p-MP layer on a silicon substrate, taken after a) 30 min, b) 1.5 h, c) 10 h since the deposition (t = 100 ms, V = -2 V).*

In the next experiment, short electric millisecond pulses are applied with shorter IRSE measurements (~10 min) after each deposition. In Figure 6.4, the spectra of millisecond depositions after 40 ms and 940 ms are shown (there are five pulses in total: 40 ms, 100 ms, 100 ms, 200 ms, and 500 ms). Finally, after a total of 940 ms, a C=O band visibly emerges with an amplitude of ~0.8×10^{-4}, proving the presence of the maleimide material even when short pulses are applied, with sub-monolayer forming in less than 1 second of deposition. Overnight, the amplitude triples in intensity, reaching a monolayer thickness, proving again that the reaction continues even without electricity.

This set of measurements also accentuates the limits of the instrumentation. In situ IRSE is a sensitive and non-destructive technique for monitoring the film deposition by directly probing the vibrational modes of organic molecules. Coupled with electrochemistry, this technique is a reliable way to prepare functionalized surfaces. However, due to S/N ratio, there is a limit of detection of thin film spectroscopic bands after millisecond-scale deposition when the film formation is independent of applied potential, and the rate of film formation is too fast to obtain real-time spectra.

The rate of aryldiazonium salt deposition and the final layer thickness depend on the substituents on the aryl moiety.[158,181] Depending on the substituent, the rate of the deposition may be influenced by its electron-withdrawing properties or its size, increasing with the greater electron-withdrawing character of the substituent,[181] while the bulky substituents limit the reactivity of the layers and result in thinner multilayers.[158] Maleimide is a bulky substituent, but also has two electron-withdrawing C=O groups in its structure. In our measurements, longer deposition (t = 600 s) resulted in ~2.5 monolayers.

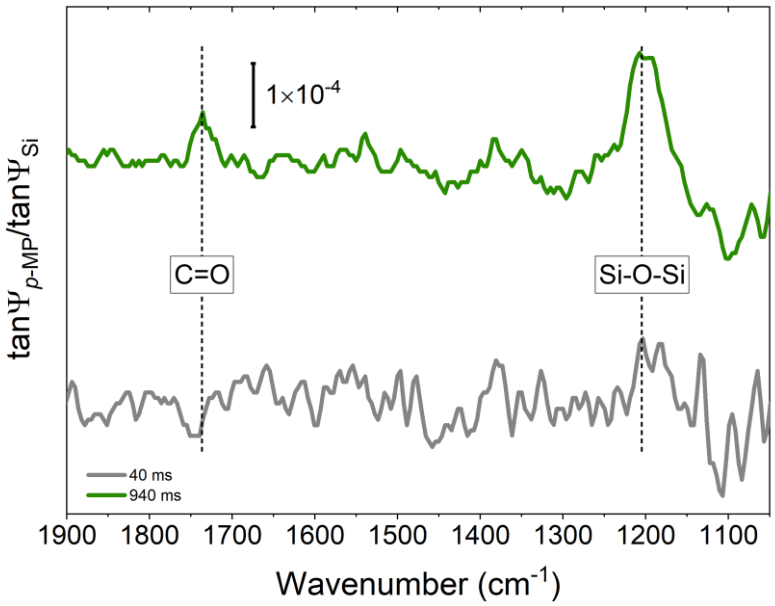

Figure 6.4: *In situ spectra of the p-MP on a silicon substrate after a) 40 ms, b) 940 ms deposition.*

Even though an unwanted silicon oxide developed, the work-up with solvent wash and etching in HF suggests that this does not necessarily present a problem since the oxide can be removed in its entirety while still preserving some *p*-MP material on the surface. The unreacted sites can be, i.e., capped with unreactive molecules or polymers. More research is needed on the reactivity of such surfaces. Especially when binding large-area biomolecules, it is not necessary to have every surface site modified with maleimide, since the goal is to bind biomolecules to the least possible number of attachment sites to preserve their reactivity and specificity.

Eventually, immobilizing biomolecules like proteins or DNA can lead to the construction of biosensing devices. Silicon presents an excellent alternative to gold and glass substrates in this regard since it is a well-researched material and provides a route for easy integration in existing electronic devices. The existing research suggests better sensitivity for covalently immobilized maleimides/biomolecules,[60] the possibility of transferring the reaction to silicon nanostructures such as SiNWs,[64] and their integration into electronic devices,[56] or the possibility of constructing DNA-field effect transistor devices by immobilizing shape-restricted DNA through thioether bond on silicon.[49,50]

The electrografting of maleimide functionality directly on the surface provides another alternative path to existing modification strategies for creating a robust modified surface, while electrochemical deposition presents a simple and reproducible method of deposition.

6.3 In situ electroless deposition of *p*-MPDS

The electroless deposition of *p*-MPDS is investigated in more detail by in situ ellipsometric measurements in a flow cell with freshly prepared maleimide solution over the 24 h period during which

no current is applied. The results are presented in Figure 6.5. There is an apparent increase of the C=O signal, with the first sign of binding after 1.5 hours of reaction and reaching the plateau of the reaction after 20 h. After 24 h of reaction, the height of the C=O band is ~2.8×10^{-4}, suggesting a monolayer formation.

The electroless (or spontaneous) grafting has been reported earlier with various methods of deposition (ultrasonic,[182] photochemistry,[183] microwave-induced,[184] reducing agents,[185–187] reducing substrates[188,189], mechanical scribing[190]), and on various surfaces,[115,182–184,188,189,191] including silicon.[115]

Since the electroless grafting was discovered, the mechanism of deposition is assumed to happen through spontaneous electron transfer at the open circuit potential, followed by homolytic dediazonation and the formation of an aryl radical.[115,151] To induce a spontaneous grafting, a reducing substrate (metals) or a reducing agent are usually needed. That is why scientists find it curious that spontaneous grafting also happens on gold and other non-reducing substrates. Berisha et al. propose an alternative mechanism for spontaneous grafting of diazonium species on gold, involving a heterolytic dediazonation, with the formation of a carbocation instead of a radical.[192] They used density functional theory (DFT) calculations to support their experimental findings.

The DFT calculations of aryldiazonium species with a gold cluster in the water suggest that the heterolytic cleavage of the Au-Ph bond is energetically disfavored. This implies that for the reverse reaction, the driving force is greater than for the analogous radical reaction.

Heterolytic cleavage: $Au\text{-}Ph \rightarrow Ph^{+} + Au^{-}$ (energetically disfavoured)

Cationic reaction: $Ph^{+} + Au^{-} \rightarrow Au\text{-}Ph$ (energetically favoured)

Radical reaction: $Ph\bullet + Au \rightarrow Au\text{-}Ph$

In sum, the findings suggest that in the presence of both a carbocation and a radical, Au will react preferentially with the carbocation.

Their experiments support the calculations.[192] Two experiments are conducted under heterolytic (pH = 1) and homolytic (pH = 9) dediazonation conditions in water/alcohol mixtures. The results showed that, under heterolytic conditions, the thin films indeed form on a gold surface. Furthermore, the heterolytic dediazonation results in the formation of thinner films, presumably because carbocations are much less reactive than radicals. Therefore, the carbocation mechanism is another possibility for surface grafting of diazonium salts. However, other mechanisms of spontaneous grafting (without a radical) should also be considered, i.e., the cleavage of the Ar-N bond or the diazohydroxide, Ar-N=N-OH, catalyzed by the gold surface.

Their findings give mechanistic implications to the results within this project, where each electroless deposition stops after the monolayer formation, wherein the case of an electrochemical (radical) deposition, the reaction would proceed to the formation of multilayers.

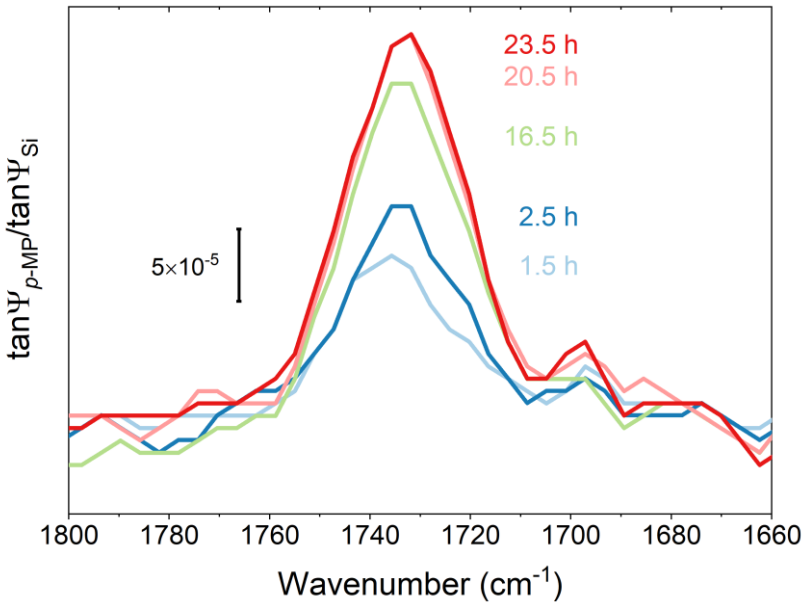

Figure 6.5: *In situ spectra of electroless grafting of p-MP on a silicon substrate are taken over 24 h.*

The findings in this work suggest another way of modifying Si with aryldiazonium salts when the goal is a monolayer deposition. However, the stopping of the reaction at the monolayer level might be limited to the choice of a *para*- substituent on an aryl ring. Menanteau et al. investigated secondary mechanisms of film growth during the deposition of diazonium salts with different *para*- substituents.[159] The secondary mechanisms are the film growth through an electrophilic attack of aryl carbocation or aryldiazonium cation on deposited phenyl rings. They found that the strongly electron-withdrawing substituents drive only the radical mechanism. With the neutral or electron-activating groups, the secondary mechanisms are plausible, and in fact, result in thick films. Mildly electron-withdrawing groups (-COOH) drive the radical, as well as secondary mechanisms, the latter with the limited impact, further supporting the findings of Berisha et al.

Control experiments with light and ultrasonic treatment as initiators of spontaneous grafting

Since it is described in the literature that the spontaneous grafting could be initiated with ultrasonic treatment[182] and visible light,[183] two control experiments are conducted to explore this matter further. In the first control experiment, an H-terminated Si(111) substrate is dipped in a solution of *p*-MPDS overnight, with no access to light. The maleimide solution is prepared in ACN, using the ultrasonic treatment for a few seconds to break down and dissolve solid *p*-MPDS (this procedure is done because, in all our previous preparations of *p*-MPDS for in situ experiments, the *p*-MPDS would be ultrasonicated in a solvent to speed up its dissolution in a solvent). The sample spectra in Figure 6.6 is marked as **M2**. In the second control experiment, the same protocol was performed, but the ultrasonic treatment was not used (**M1** in Figure 6.6). Both experiments resulted in a formation of a *p*-MP layer on the surface (Figure 6.6). Thus, neither light nor ultrasonic treatment have an effect on the *p*-MPDS deposition on

Si(111)-H surface. Note that the two experiments are performed ex situ on a silicon wafer, while the in situ experiment is performed on a silicon wedge. In Figure 6.6, the **M2** sample has less organic material deposited than **M1**. After etching in 1% HF, both samples demonstrate that the *p*-MP is still present.

The Si-H peak at 2083 cm^{-1} is present because both substrates are etched for 5 minutes with 1% HF to prove the chemical bonding of the molecules to the substrate. This also indicates that not all available binding sites react with MP. However, due to intrinsic differences of a silicon wafer and a silicon wedge, to confirm these experiments, they have to be performed in situ, on silicon wedge. More research on attachment mechanism is needed to support these claims. However, the control experiments demonstrate the reproducibility of the reaction, even with changing parameters.

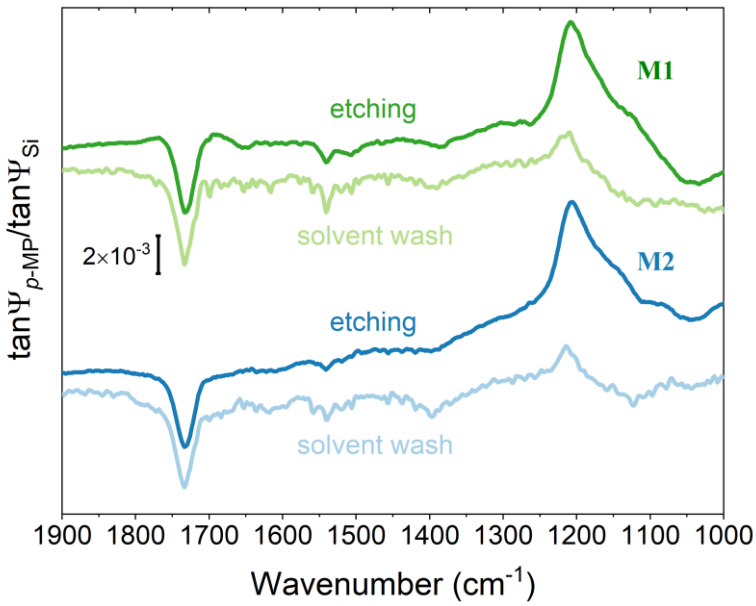

Figure 6.6: *Spectra of the ex situ deposition of p-MP on a silicon substrate. Deposition in solution without the access of light and a) with and b) without ultrasonic treatment.*

6.4 BINDING OF THIOL ON MALEIMIDE-COVERED SURFACE

The functionalization of prepared *p*-MP-modified surfaces is tested by coupling with model thiol molecules with spectroscopic labels attached.

The *p*-MP-modified silicon substrate was immersed in the 4-mercaptobenzonitrile (MBN) solution in ACN. The nitrile group serves as a spectroscopic label as it has a peak in otherwise spectroscopically inactive areas. In Figure 6.7, the spectra of immobilized MBN on *p*-MP is presented. A small nitrile peak at 2229 cm^{-1} is present, indicating a low amount of MBN attached to the surface. The peak remained even after washing in solvents, indicating a robust bonding to the *p*-MP layer and thus confirming the functionality of maleimide-immobilized surfaces.

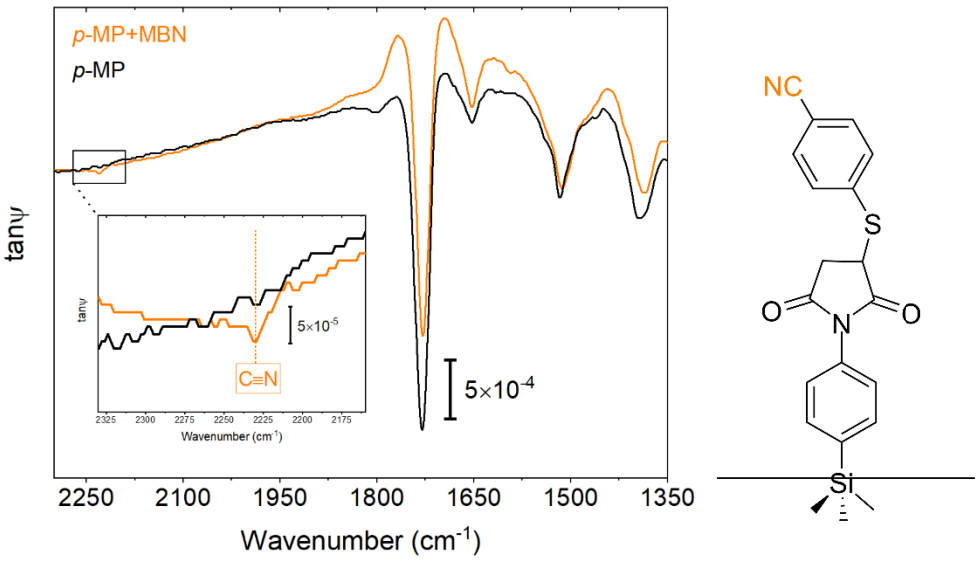

Figure 6.7: *Spectra of ex situ MBN coupling with the p-MP-modified surface.*

The experiment was transferred in a flow cell to conduct an in situ experiment of MBN binding to the surface. The experiment resulted in the physisorption of MBN molecules. However, after sonication in a solvent, the physisorbed layer is removed (Figure 6.8).

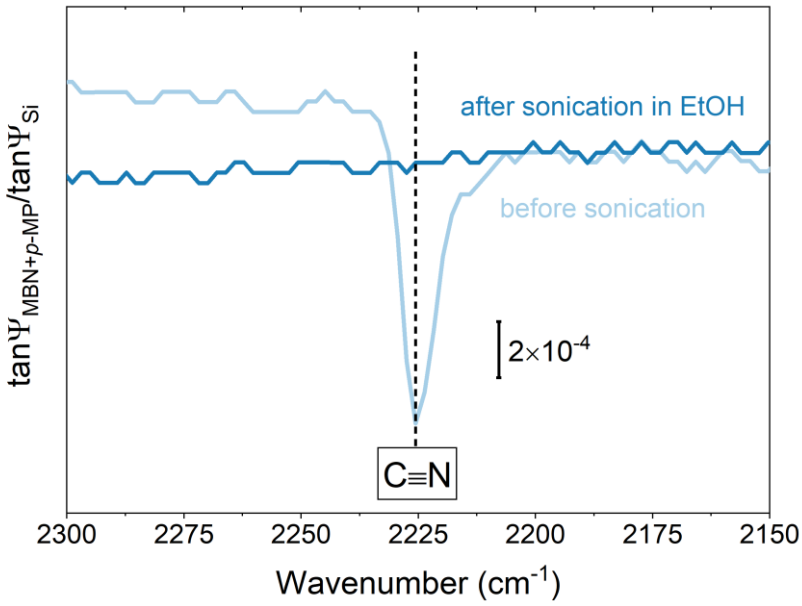

Figure 6.8: *Physisorbed MBN molecules are washed away when sonicated in a solvent (EtOH).*

In sum, study results provide compelling insight into the mechanism of *p*-MP attachment on the H-terminated Si(111) surface via electrochemical or electroless deposition.

The electrochemical study finds that the almost complete monolayer formation happens after 30 s of deposition (at V = -2 V), while after 600 s, the thickness increases to about two monolayers. The reason

for the formation of such thin multilayers is the bulkiness of maleimide moiety, which obstructs the approach of the radical species to *ortho*- position on the aryl ring.

The shortest time of deposition, after which we can observe the C=O band, is 940 ms. At this point, we reach the limit of detection with in situ IR ellipsometry. At shorter times, we cannot observe bands due to the noise. Longer measurement times, which would lower the noise level, are not possible since the electrografting competes with spontaneous grafting of *p*-MP on silicon.

In situ electroless deposition demonstrated that the film growth reaches a plateau after 20 h with a film thickness of approximately one monolayer. Even though longer measurements are needed to confirm that the film growth indeed stopped, the fact that the film thickness did not change between 20th and 24th hour of deposition suggests that maybe some other mechanisms take place at the interface instead of a well-known radical mechanism.

The functionality of the surface is confirmed by the coupling of the *p*-MP layer with the thiol molecule.

The mechanistic insights from this study contribute to a prosperous research area on surface modification with aryldiazonium salts and a broader area of organic electronics.

7 CONCLUDING REMARKS AND FUTURE DIRECTIONS

In this thesis, the covalent surface modification of silicon with two technologically interesting materials, porphyrin and maleimide, is studied. The study aims to better understand their bonding to the surface by employing in situ monitoring techniques. The central question was to illuminate which parameters influence the deposition of the material and the film growth. Thus, a study on the deposition of both materials is conducted with particular care for deposition conditions and synthetic parameters, with insight into the deposition mechanism. Two porphyrin derivatives, 5-(4-carboxyphenyl)-10,15,20-(triphenyl)porphyrin (CTPP) and 5-(4-carboxyphenyl succinimide ester)-10,15,20-(triphenyl)porphyrin (CTPPS) are deposited on the (3-aminopropyl)trimethoxysilane-modified (APTMS-modified) silicon substrate. The prepared structures were characterized with surface-sensitive analytical techniques. Furthermore, the electrochemical silicon surface modification with maleimidophenyl diazonium salt (*p*-MPDS) is also studied. The kinetics of the film formation in a monolayer and sub-monolayer regime in real-time using in situ ellipsometry are researched.

The present research on silicon surface modification with porphyrin and maleimide can be summarized by following five points:

i. Porphyrins are immobilized on an APTMS-modified silicon surface, and the binding was proved by the identification of a covalent amide bond. Evidence of a successful bonding is provided by three independent surface-sensitive methods: IR ellipsometry, XPS, and SEIRA.

ii. The corresponding reactions in solution (to the ones taking place on the surface) reveal that the reaction of APTMS with the pre-activated porphyrin derivative (CTPPS) leads to a better yield than an in-situ-activated porphyrin derivative (CTTP). However, the surface modification with porphyrin by layer-by-layer deposition takes place at a much slower rate than the same reaction in solution.

iii. An alternative synthetic approach to the layer-by-layer deposition, where the product is quickly formed in solution and then deposited on the oxidized Si substrate through the process of silanization, is proposed. Such synthesis results in a spectral signature of a product dominated by amide vibrational bands and a strongly adhering thin film resistant to washing in various solvents and etching in 10% HF solution.

iv. The surface modification with maleimidophenyl species (*p*-MP) reveals almost complete monolayer formation after 30 s of electrografting, while the first evidence of maleimide on the surface is observed already after 940 ms. At this point, the limit of detection with in situ IR ellipsometry is reached. At shorter times, the background noise is too strong to observe the bands. The growth of multilayers is slow due to the steric hindrance of *p*-MP.

v. The in situ observation of a spontaneous deposition of *p*-MPDS resulted in the formation of a monolayer after one day of reaction. Due to different kinetics of the film growth of

electrochemical and electroless depositions, a cationic mechanism is proposed as an alternative to a previously presumed radical mechanism of *p*-MPDS deposition. The functionality of prepared *p*-MP monolayers is confirmed by coupling with the thiol molecule.

We conclude that the presented work demonstrates the compatibility of porphyrins with a common, widespread material (organosilanes) for the immobilization on the silicon by establishing an amide bond between layers. The approach to the synthesis of the layers influences the structure and the quality of prepared thin films. It is demonstrated that porphyrins with a non-specific functional group like COOH give better reaction yield when pre-activated with an activator molecule like NHS, as opposed to in situ activation before the reaction. Even so, it is found that the surface reaction is too slow with the layer-by-layer mode of deposition, leading to the development of an alternative synthetic approach. The new way of synthesis resulted in a formation of a robust thin film, providing a promising new path for surface modification with porphyrins.

The observation of the maleimide film growth at an applied potential demonstrates that the immobilization is noticeable already after a short deposition of 940 ms. However, due to the fast film growth caused by radical mechanism, it is not possible to capture high-quality spectra of silicon interface after shorter times with current instrumentation, because the film growth cannot be paused and collecting high-quality spectra takes time. The kinetics of electroless deposition is much slower with the monolayer formation ending after one reaction day. Different kinetics of electrochemical and electroless depositions lead to a proposal of cationic mechanism taking place during electroless deposition, instead of radical mechanism.

Experimentally, future research directions in this area would benefit from looking into the geometry and molecular stacking of porphyrin monolayer deposited via the proposed new synthetic way, the possibility of the film growth, and testing of their electronic and optical properties. As a promising alternative, one could also prepare a porphyrin diazonium salt and use electricity to attach the porphyrin ring directly to the surface. Continuing on our findings on the spontaneous mechanism, the research into the nature of the electroless deposition might provide new conclusions for the achievement of a single monolayer film with implications of integrating biosensors into electronic devices. The transfer of the technology to novel substrates potentially relevant for future materials (Si nanowires, porous Si, nanoparticles, graphene) and comparing them with properties of prevalent silicon might reveal new research and technological directions. Eventually, the optimization of synthetic conditions of monolayer formation and film growth will lead to research on the integration of prepared surfaces into electronic and biosensing devices.

BIBLIOGRAPHY

(1) Faustini, M.; Nicole, L.; Ruiz-Hitzky, E.; Sanchez, C. History of Organic-Inorganic Hybrid Materials: Prehistory, Art, Science, and Advanced Applications. *Adv. Funct. Mater.* **2018**, *28* (27), 1704158.

(2) Gao, F.; Teplyakov, A. V. Challenges and Opportunities in Chemical Functionalization of Semiconductor Surfaces. *Appl. Surf. Sci.* **2017**, *399*, 375–386.

(3) Ulman, A. Formation and Structure of Self-Assembled Monolayers. *Chem. Rev.* **1996**, *96* (4), 1533–1554.

(4) Bent, S. F. Organic Functionalization of Group IV Semiconductor Surfaces: Principles, Examples, Applications, and Prospects. *Surf. Sci.* **2002**, *500* (1–3), 879–903.

(5) Das, R.; He, X.; Ghaffarzadeh, K. Printed, Organic and Flexible Electronics 2020-2030: Forecasts, Technologies, Markets https://www.idtechex.com/en/research-report/printed-organic-and-flexible-electronics-2020-2030-forecasts-technologies-markets/687.

(6) Zhang, X.; Bäuerle, P.; Aida, T.; Skabara, P.; Kagan, C. Organic Electronics for a Better Tomorrow: Innovation , Accessibility , Sustainability. *A White Pap. from Chem. Sci. Soc. Summit* **2012**, No. September, 34.

(7) Auwärter, W.; Écija, D.; Klappenberger, F.; Barth, J. V. Porphyrins at Interfaces. *Nat. Chem.* **2015**, *7* (2), 105–120.

(8) Wen, L.; Liu, X.; Yang, N.; Zhai, J.; Huang, C.; Li, Y.; Jiang, L. Photoelectric Conversion Behavior Based on Direct Interfacial Charge-Transfer from Porphyrin Derivative to Silicon Nanowires. *Appl. Phys. Lett.* **2010**, *97* (25), 253111.

(9) Lu, H.; Kobayashi, N. Optically Active Porphyrin and Phthalocyanine Systems. *Chem. Rev.* **2016**, *116* (10), 6184–6261.

(10) Suslick, K. S. An Optoelectronic Nose: "Seeing" Smells by Means of Colorimetric Sensor Arrays. *MRS Bull.* **2004**, *29* (10), 720–725.

(11) Alderman, N.; Danos, L.; Fang, L.; Grossel, M. C.; Markvart, T. Light Harvesting in Silicon(111) Surfaces Using Covalently Attached Protoporphyrin IX Dyes. *Chem. Commun.* **2017**, *53* (89), 12120–12123.

(12) Cai, J.; Chen, H.; Huang, J.; Wang, J.; Tian, D.; Dong, H.; Jiang, L. Controlled Self-Assembly and Photovoltaic Characteristics of Porphyrin Derivatives on a Silicon Surface at Solid-Liquid Interfaces. *Soft Matter* **2014**, *10* (15), 2612–2618.

(13) Lindsey, J. S.; Bocian, D. F. Molecules for Charge-Based Information Storage. *Acc. Chem.*

Res. **2011**, *44* (8), 638–650.

(14) Biesaga, M.; Pyrzyńska, K.; Trojanowicz, M. Porphyrins in Analytical Chemistry. A Review. *Talanta* **2000**, *51* (2), 209–224.

(15) Ding, Y.; Zhu, W.-H.; Xie, Y. Development of Ion Chemosensors Based on Porphyrin Analogues. *Chem. Rev.* **2017**, *117* (4), 2203–2256.

(16) Ladomenou, K.; Natali, M.; Iengo, E.; Charalampidis, G.; Scandola, F.; Coutsolelos, A. G. Photochemical Hydrogen Generation with Porphyrin-Based Systems. *Coord. Chem. Rev.* **2015**, *304–305*, 38–54.

(17) Zhang, W.; Lai, W.; Cao, R. Energy-Related Small Molecule Activation Reactions: Oxygen Reduction and Hydrogen and Oxygen Evolution Reactions Catalyzed by Porphyrin- and Corrole-Based Systems. *Chem. Rev.* **2017**, *117* (4), 3717–3797.

(18) Alves, E.; Faustino, M. A. F.; Neves, M. G. P. M. S.; Cunha, Â.; Nadais, H.; Almeida, A. Potential Applications of Porphyrins in Photodynamic Inactivation beyond the Medical Scope. *J. Photochem. Photobiol. C Photochem. Rev.* **2014**, *22*, 34–57.

(19) Singh, S.; Aggarwal, A.; Bhupathiraju, N. V. S. D. K.; Arianna, G.; Tiwari, K.; Drain, C. M. Glycosylated Porphyrins, Phthalocyanines, and Other Porphyrinoids for Diagnostics and Therapeutics. *Chem. Rev.* **2015**, *115* (18), 10261–10306.

(20) Li, D.; Swanson, B. I.; Robinson, J. M.; Hoffbauer, M. A. Porphyrin Based Self-Assembled Monolayer Thin Films: Synthesis and Characterization. *J. Am. Chem. Soc.* **1993**, *115* (15), 6975–6980.

(21) Li, D.; Buscher, C. T.; Swanson, B. I. Synthesis, Characterization, and Properties of Covalently Bound, Self-Assembled Porphyrin Multilayer Thin Films. *Chem. Mater.* **1994**, *6* (6), 803–810.

(22) Schmidt, I.; Jiao, J.; Thamyongkit, P.; Sharada, D. S.; Bocian, D. F.; Lindsey, J. S. Investigation of Stepwise Covalent Synthesis on a Surface Yielding Porphyrin-Based Multicomponent Architectures. *J. Org. Chem.* **2006**, *71* (8), 3033–3050.

(23) Jiao, J.; Thamyongkit, P.; Schmidt, I.; Lindsey, J. S.; Bocian, D. F. Characterization of Porphyrin Surface Orientation in Monolayers on Au(111) and Si(100) Using Spectroscopically Labeled Molecules. *J. Phys. Chem. C* **2007**, *111* (34), 12693–12704.

(24) Palomaki, P. K. B. B.; Krawicz, A.; Dinolfo, P. H. Thickness, Surface Morphology, and Optical Properties of Porphyrin Multilayer Thin Films Assembled on Si(100) Using Copper(I)-Catalyzed Azide-Alkyne Cycloaddition. *Langmuir* **2011**, *27* (8), 4613–4622.

(25) Zanoni, R.; Aurora, A.; Cattaruzza, F.; Decker, F.; Fastiggi, P.; Menichetti, V.; Tagliatesta, P.; Capodilupo, A.-L.; Lembo, A. Metalloporphyrins as Molecular Precursors of Electroactive

Hybrids: A Characterization of Their Actual Electronic States on Si(100) and (111) by AFM and XPS. *Mater. Sci. Eng. C* **2007**, *27* (5–8), 1351–1354.

(26) Gadenne, V.; Porte, L.; Patrone, L. Structure and Growth Mechanism of Self-Assembled Monolayers of Metal Protoporphyrins and Octacarboxylphthalocyanine on Silicon Dioxide. *RSC Adv.* **2014**, *4* (110), 64506–64513.

(27) Gulino, A.; Lupo, F.; Condorelli, G. G.; Mineo, P.; Fragalà, I. Viable Synthetic Route for a Luminescent Porphyrin Monolayer Covalently Assembled on a Molecularly Engineered Si(100) Surface. *Chem. Mater.* **2007**, *19* (21), 5102–5109.

(28) Yasseri, A. A.; Syomin, D.; Loewe, R. S.; Lindsey, J. S.; Zaera, F.; Bocian, D. F. Structural and Electron-Transfer Characteristics of O-, S-, and Se-Tethered Porphyrin Monolayers on Si(100). *J. Am. Chem. Soc.* **2004**, *126* (47), 15603–15612.

(29) Liu, Z.; Schmidt, I.; Thamyongkit, P.; Loewe, R. S.; Syomin, D.; Diers, J. R.; Zhao, Q.; Misra, V.; Lindsey, J. S.; Bocian, D. F. Synthesis and Film-Forming Properties of Ethynylporphyrins. *Chem. Mater.* **2005**, *17* (14), 3728–3742.

(30) Padmaja, K.; Wei, L.; Lindsey, J. S.; Bocian, D. F. A Compact All-Carbon Tripodal Tether Affords High Coverage of Porphyrins on Silicon Surfaces. *J. Org. Chem.* **2005**, *70* (20), 7972–7978.

(31) Wei, L.; Syomin, D.; Loewe, R. S.; Lindsey, J. S.; Zaera, F.; Bocian, D. F. Structural and Electron-Transfer Characteristics of Carbon-Tethered Porphyrin Monolayers on Si(100). *J. Phys. Chem. B* **2005**, *109* (13), 6323–6330.

(32) Secret, E.; Maynadier, M.; Gallud, A.; Gary-Bobo, M.; Chaix, A.; Belamie, E.; Maillard, P.; Sailor, M. J.; Garcia, M.; Durand, J.-O.; Cunin, F. Anionic Porphyrin-Grafted Porous Silicon Nanoparticles for Photodynamic Therapy. *Chem. Commun.* **2013**, *49* (39), 4202.

(33) Koiry, S. P.; Aswal, D. K.; Chauhan, A. K.; Saxena, V.; Nayak, S. K.; Gupta, S. K.; Yakhmi, J. V. Electrical Bistability in Electrografted 5-(4-Undecenyloxyphenyl)-10,15,20-Triphenylporphyrin Monolayer on Si. *Chem. Phys. Lett.* **2008**, *453* (1–3), 68–72.

(34) Garg, K.; Majumder, C.; Gupta, S. K.; Aswal, D. K.; Nayak, S. K.; Chattopadhyay, S. Stable Negative Differential Resistance in Porphyrin Based σ-π-σ Monolayers Grafted on Silicon. *RSC Adv.* **2015**, *5* (62), 50234–50244.

(35) Garg, K.; Majumder, C.; Gupta, S. K.; Aswal, D. K.; Nayak, S. K.; Chattopadhyay, S. A Novel Design for Porphyrin Based D-s-A Systems as Molecular Rectifiers. *Chem. Sci.* **2016**, *7* (2), 1548–1557.

(36) Jiao, J.; Anariba, F.; Tiznado, H.; Schmidt, I.; Lindsey, J. S.; Zaera, F.; Bocian, D. F. Stepwise Formation and Characterization of Covalently Linked Multiporphyrin-Imide Architectures on

Si(100). *J. Am. Chem. Soc.* **2006**, *128* (21), 6965–6974.

(37) Jiao, J.; Nordlund, E.; Lindsey, J. S.; Bocian, D. F. Effects of Counterion Mobility, Surface Morphology, and Charge Screening on the Electron-Transfer Rates of Porphyrin Monolayers. *J. Phys. Chem. C* **2008**, *112* (15), 6173–6180.

(38) Thamyongkit, P.; Yu, L.; Padmaja, K.; Jiao, J.; Bocian, D. F.; Lindsey, J. S. Porphyrin Dyads Bearing Carbon Tethers for Studies of High-Density Molecular Charge Storage on Silicon Surfaces. *J. Org. Chem.* **2006**, *71* (3), 1156–1171.

(39) Li, Q.; Mathur, G.; Gowda, S.; Surthi, S.; Zhao, Q.; Yu, L.; Lindsey, J. S.; Bocian, D. F.; Misra, V. Multibit Memory Using Self-Assembly of Mixed Ferrocene/Porphyrin Monolayers on Silicon. *Adv. Mater.* **2004**, *16* (2), 133–137.

(40) Eriksson, K. L. E.; Chow, W. W. Y.; Puglia, C.; Bäckvall, J.-E.; Göthelid, E.; Oscarsson, S. Performance of a Biomimetic Oxidation Catalyst Immobilized on Silicon Wafers: Comparison with Its Gold Congener. *Langmuir* **2010**, *26* (21), 16349–16354.

(41) Secret, E.; Maynadier, M.; Gallud, A.; Chaix, A.; Bouffard, E.; Gary-Bobo, M.; Marcotte, N.; Mongin, O.; El Cheikh, K.; Hugues, V.; Auffan, M.; Frochot, C.; Morère, A.; Maillard, P.; Blanchard-Desce, M.; Sailor, M. J.; Garcia, M.; Durand, J.-O.; Cunin, F. Two-Photon Excitation of Porphyrin-Functionalized Porous Silicon Nanoparticles for Photodynamic Therapy. *Adv. Mater.* **2014**, *26* (45), 7643–7648.

(42) Cristaldi, D. A.; Motta, A.; Millesi, S.; Gupta, T.; Chhatwal, M.; Gulino, A. Long Range Order in Si(100) Surfaces Engineered with Porphyrin Nanostructures. *J. Mater. Chem. C* **2013**, *1* (32), 4979.

(43) Contino, A.; Maccarrone, G.; Fragalà, M. E.; Spitaleri, L.; Gulino, A. Conjugated Gold-Porphyrin Monolayers Assembled on Inorganic Surfaces. *Chem. - A Eur. J.* **2017**, *23* (59), 14937–14943.

(44) Gera, B.; Manna, A. K.; Chandra Mondal, P. Metal-Ions Linked Surface-Confined Molecular Dyads of Zn-Porphyrin-Metallo-Terpyridine: An Experimental and Theoretical Study. *RSC Adv.* **2017**, *7* (3), 1290–1298.

(45) Northrop, B. H.; Frayne, S. H.; Choudhary, U. Thiol-Maleimide "Click" Chemistry: Evaluating the Influence of Solvent, Initiator, and Thiol on the Reaction Mechanism, Kinetics, and Selectivity. *Polym. Chem.* **2015**, *6* (18), 3415–3430.

(46) Homaei, A. A.; Sariri, R.; Vianello, F.; Stevanato, R. Enzyme Immobilization: An Update. *J. Chem. Biol.* **2013**, *6* (4), 185–205.

(47) Wang, Y.; Cai, J.; Rauscher, H.; Behm, R. J.; Goedel, W. A. Maleimido-Terminated Self-Assembled Monolayers. *Chem. - A Eur. J.* **2005**, *11* (13), 3968–3978.

(48) Strother, T.; Hamers, R. J.; Smith, L. M. Covalent Attachment of Oligodeoxyribonucleotides to Amine-Modified Si (001) Surfaces. *Nucleic Acids Res.* **2000**, *28* (18), 3535–3541.

(49) Zhang, X.; Kumar, S.; Chen, J.; Teplyakov, A. V. Covalent Attachment of Shape-Restricted DNA Molecules on Amine-Functionalized Si(111) Surface. *Surf. Sci.* **2009**, *603* (16), 2445–2457.

(50) Zhang, X.; Antonopoulos, I. H.; Kumar, S.; Chen, J.; Teplyakov, A. V. Tuning the Geometry of Shape-Restricted DNA Molecules on the Functionalized Si(111). *Appl. Surf. Sci.* **2009**, *256* (3), 815–818.

(51) Cai, W.; Peck, J. R.; van der Weide, D. W.; Hamers, R. J. Direct Electrical Detection of Hybridization at DNA-Modified Silicon Surfaces. *Biosens. Bioelectron.* **2004**, *19* (9), 1013–1019.

(52) Liu, Y.; Chen, J.; Teplyakov, A. V. Chemical Passivation Processes for Biofunctionalization Schemes on Semiconductor Surfaces. *Langmuir* **2012**, *28* (44), 15521–15528.

(53) Ishibashi, K. I.; Tanaka, K.; Hirano-Iwata, A.; Miyamoto, K. I.; Kimura, Y.; Niwano, M. In Situ Study of DNA Attachment and Hybridization at Silicon Surfaces by Infrared Absorption Spectroscopy. *Jpn. J. Appl. Phys.* **2008**, *47* (4), 3204–3208.

(54) Cha, T.; Boiadjiev, V.; Lozano, J.; Yang, H.; Zhu, X. Immobilization of Oligonucleotides on Poly(Ethylene Glycol) Brush-Coated Si Surfaces. *Anal. Biochem.* **2002**, *311*, 27–32.

(55) Wong, A. K. Y.; Krull, U. J. Surfaces for Tuning of Oligonucleotide Biosensing Selectivity Based on Surface-Initiated Atom Transfer Radical Polymerization on Glass and Silicon Substrates. *Anal. Chim. Acta* **2009**, *639* (1–2), 1–12.

(56) Cattani-Scholz, A.; Pedone, D.; Dubey, M.; Neppl, S.; Nickel, B.; Feulner, Ḱ. P.; Schwartz, J.; Abstreiter, G.; Tornow, M. Organophosphonate-Based PNA-Functionalization of Silicon Nanowires for Label-Free DNA Detection. *ACS Nano* **2008**, *2* (8), 1653–1660.

(57) Cattani-Scholz, A.; Pedone, D.; Blobner, F.; Abstreiter, G.; Schwartz, J.; Tornow, M.; Andruzzi, L. PNA-PEG Modified Silicon Platforms as Functional Bio-Interfaces for Applications in DNA Microarrays and Biosensors. *Biomacromolecules* **2009**, *10* (3), 489–496.

(58) Böcking, T.; James, M.; Coster, H. G. L. L.; Chilcott, T. C.; Barrow, K. D. Structural Characterization of Organic Multilayers on Silicon(111) Formed by Immobilization of Molecular Films on Functionalized Si-C Linked Monolayers. *Langmuir* **2004**, *20* (21), 9227–9235.

(59) Kim, J.; Cho, J.; Seidler, P. M.; Kurland, N. E.; Yadavalli, V. K. Investigations of Chemical Modifications of Amino-Terminated Organic Films on Silicon Substrates and Controlled Protein Immobilization. *Langmuir* **2010**, *26* (4), 2599–2608.

(60) Seto, H.; Takara, M.; Yamashita, C.; Murakami, T.; Hasegawa, T.; Hoshino, Y.; Miura, Y. Surface Modification of Siliceous Materials Using Maleimidation and Various Functional Polymers Synthesized by Reversible Addition-Fragmentation Chain Transfer Polymerization. *ACS Appl. Mater. Interfaces* **2012**, *4* (10), 5125–5133.

(61) Sun, G.; Hovestädt, M.; Zhang, X.; Hinrichs, K.; Rosu, D. M.; Lauermann, I.; Zielke, C.; Vollmer, A.; Löchel, H.; Ay, B.; Holzhütter, H.-G. G.; Schade, U.; Esser, N.; Volkmer, R.; Rappich, J. Infrared Spectroscopic Ellipsometry (IRSE) and X-Ray Photoelectron Spectroscopy (XPS) Monitoring the Preparation of Maleimide-Functionalized Surfaces: From Au Towards Si (111). *Surf. Interface Anal.* **2011**, *43* (9), 1203–1210.

(62) Zhang, X.; Tretjakov, A.; Hovestaedt, M.; Sun, G.; Syritski, V.; Reut, J.; Volkmer, R.; Hinrichs, K.; Rappich, J. J. Electrochemical Functionalization of Gold and Silicon Surfaces by a Maleimide Group as a Biosensor for Immunological Application. *Acta Biomater.* **2013**, *9* (3), 5838–5844.

(63) Kanyong, P.; Sun, G.; Rösicke, F.; Syritski, V.; Panne, U.; Hinrichs, K.; Rappich, J. Maleimide Functionalized Silicon Surfaces for Biosensing Investigated by In-Situ IRSE and EQCM. *Electrochem. commun.* **2015**, *51*, 103–107.

(64) Streifer, J. A.; Kim, H.; Nichols, B. M.; Hamers, R. J. Covalent Functionalization and Biomolecular Recognition Properties of DNA-Modified Silicon Nanowires. *Nanotechnology* **2005**, *16* (9), 1868–1873.

(65) Lin, Z.; Strother, T.; Cai, W.; Cao, X.; Smith, L. M.; Hamers, R. J. DNA Attachment and Hybridization at the Silicon (100) Surface. *Langmuir* **2002**, *18* (3), 788–796.

(66) Perrine, K. A.; Teplyakov, A. V. Reactivity of Selectively Terminated Single Crystal Silicon Surfaces. *Chem. Soc. Rev.* **2010**, *39* (8), 3256.

(67) Zhang, A.; Lieber, C. M. Nano-Bioelectronics. *Chem. Rev.* **2016**, *116* (1), 215–257.

(68) Yu, K. J.; Kuzum, D.; Hwang, S. W.; Kim, B. H.; Juul, H.; Kim, N. H.; Won, S. M.; Chiang, K.; Trumpis, M.; Richardson, A. G.; Cheng, H.; Fang, H.; Thompson, M.; Bink, H.; Talos, D.; Seo, K. J.; Lee, H. N.; Kang, S. K.; Kim, J. H.; Lee, J. Y.; Huang, Y.; Jensen, F. E.; Dichter, M. A.; Lucas, T. H.; Viventi, J.; Litt, B.; Rogers, J. A. Bioresorbable Silicon Electronics for Transient Spatiotemporal Mapping of Electrical Activity from the Cerebral Cortex. *Nat. Mater.* **2016**, *15* (7), 782–791.

(69) Dasog, M.; Kehrle, J.; Rieger, B.; Veinot, J. G. C. Silicon Nanocrystals and Silicon-Polymer Hybrids: Synthesis, Surface Engineering, and Applications. *Angew. Chemie - Int. Ed.* **2016**, *55* (7), 2322–2339.

(70) Cui, Y.; Wei, Q.; Park, H.; Lieber, C. M. Nanowire Nanosensors for Highly Sensitive and

Selective Detection of Biological and Chemical Species. *Science* **2001**, *293* (5533), 1289–1292.

(71) Heni, W.; Kutuvantavida, Y.; Haffner, C.; Zwickel, H.; Kieninger, C.; Wolf, S.; Lauermann, M.; Fedoryshyn, Y.; Tillack, A. F.; Johnson, L. E.; Elder, D. L.; Robinson, B. H.; Freude, W.; Koos, C.; Leuthold, J.; Dalton, L. R. Silicon-Organic and Plasmonic-Organic Hybrid Photonics. *ACS Photonics* **2017**, *4* (7), 1576–1590.

(72) Chen, J.; Ge, K.; Zhang, C.; Guo, J.; Yang, L.; Song, D.; Li, F.; Xu, Z.; Xu, Y.; Mai, Y. Vacuum-Free, Room-Temperature Organic Passivation of Silicon: Toward Very Low Recombination of Micro-/Nanotextured Surface Structures. *ACS Appl. Mater. Interfaces* **2018**, *10* (51), 44890–44896.

(73) Neergaard Waltenburg, H.; Yates, J. T. Surface Chemistry of Silicon. *Chem. Rev.* **1995**, *95* (5), 1589–1673.

(74) Harada, Y.; Koitaya, T.; Mukai, K.; Yoshimoto, S.; Yoshinobu, J. Spectroscopic Characterization and Transport Properties of Aromatic Monolayers Covalently Attached to Si(111) Surfaces. *J. Phys. Chem. C* **2013**, *117* (15), 7497–7505.

(75) Rozlosnik, N.; Gerstenberg, M. C.; Larsen, N. B. Effect of Solvents and Concentration on the Formation of a Self-Assembled Monolayer of Octadecylsiloxane on Silicon (001). *Langmuir* **2003**, *19* (4), 1182–1188.

(76) Wang, Y.; Lieberman, M. Growth of Ultrasmooth Octadecyltrichlorosilane Self-Assembled Monolayers on SiO2. *Langmuir* **2003**, *19* (4), 1159–1167.

(77) Buriak, J. M. Silicon-Carbon Bonds on Porous Silicon Surfaces. *Adv. Mater.* **1999**, *11* (3), 265–267.

(78) Linford, M. R.; Fenter, P.; Eisenberger, P. M.; Chidsey, C. E. D. Alkyl Monolayers on Silicon Prepared from 1-Alkenes and Hydrogen-Terminated Silicon. *J. Am. Chem. Soc.* **1995**, *117* (11), 3145–3155.

(79) Walsh, R. Bond Dissociation Energy Values in Silicon-Containing Compounds and Some of Their Implications. *Acc. Chem. Res.* **1981**, *14* (8), 246–252.

(80) Anglin, E. J.; Cheng, L.; Freeman, W. R.; Sailor, M. J. Porous Silicon in Drug Delivery Devices and Materials. *Adv. Drug Deliv. Rev.* **2008**, *60* (11), 1266–1277.

(81) Sano, H.; Maeda, H.; Ichii, T.; Murase, K.; Noda, K.; Matsushige, K.; Sugimura, H. Alkyl and Alkoxyl Monolayers Directly Attached to Silicon: Chemical Durability in Aqueous Solutions. *Langmuir* **2009**, *25* (10), 5516–5525.

(82) Fabre, B. Functionalization of Oxide-Free Silicon Surfaces with Redox-Active Assemblies.

Chem. Rev. **2016**, *116* (8), 4808–4849.

(83) Linford, M. R.; Chidsey, C. E. D. Alkyl Monolayers Covalently Bonded to Silicon Surfaces. *J. Am. Chem. Soc.* **1993**, *115* (26), 12631–12632.

(84) Sieval, A. B.; van den Hout, B.; Zuilhof, H.; Sudhölter, E. J. R. Molecular Modeling of Covalently Attached Alkyl Monolayers on the Hydrogen-Terminated Si(111) Surface. *Langmuir* **2001**, *17* (7), 2172–2181.

(85) Lee, M. V.; Guo, D.; Linford, M. R.; Zuilhof, H. Molecular Modeling of Alkyl Monolayers on the Si(100)-2×1 Surface. *Langmuir* **2004**, *20* (21), 9108–9113.

(86) Adongo, J. O.; Neubert, T. J.; Sun, G.; Janietz, S.; Lauermann, I.; Rademann, K.; Rappich, J. Fabrication and Characterization of Surfaces Modified with Carboxymethylthio Ligands for Chelate-Assisted Trapping of Copper. *ACS Appl. Mater. Interfaces* **2017**, *9* (28), 24273–24281.

(87) Yang, F.; Roodenko, K.; Hunger, R.; Hinrichs, K.; Rademann, K.; Rappich, J. Near-Ideal Complete Coverage of CD3 onto Si(111) Surfaces Using One-Step Electrochemical Grafting: An IR Ellipsometry, Synchrotron XPS, and Photoluminescence Study. *J. Phys. Chem. C* **2012**, *116* (35), 18684–18690.

(88) Hahm, J.; Lieber, C. M. Direct Ultrasensitive Electrical Detection of DNA and DNA Sequence Variations Using Nanowire Nanosensors. *Nano Lett.* **2004**, *4* (1), 51–54.

(89) Wayner, D. D. M.; Wolkow, R. A. Organic Modification of Hydrogen Terminated Silicon Surfaces. *J. Chem. Soc. Perkin Trans. 2* **2002**, *1* (1), 23–34.

(90) Chazalviel, J.-N. (Allesandro Volta Award Presentation) Facts and Challenges in the Electrochemistry and Wet Surface Chemistry of Silicon. *ECS Trans.* **2013**, *53* (6), 3–22.

(91) Mobarok, M. H.; Purkait, T. K.; Veinot, J. G. C. A Nanoscale Adventure with Silicon: Synthesis, Surface Chemistry, and Other Surprises. *Solid State Phenom.* **2015**, *242* (d), 383–390.

(92) Chen, B. M. L.; Tulinsky, A. Redetermination of the Structure of Porphine. *J. Am. Chem. Soc.* **1972**, *94* (12), 4144–4151.

(93) Gottfried, J. M. Surface Chemistry of Porphyrins and Phthalocyanines. *Surf. Sci. Rep.* **2015**, *70* (3), 259–379.

(94) Thomas, D. W.; Martell, A. E. Tetraphenylporphine and Some Para-Substituted Derivatives. **1956**, *78*.

(95) Lukasczyk, T.; Flechtner, K.; Merte, L. R.; Jux, N.; Maier, F.; Gottfried, J. M.; Steinrück, H. P. Interaction of Cobalt(II) Tetraarylporphyrins with a Ag(111) Surface Studied with Photoelectron Spectroscopy. *J. Phys. Chem. C* **2007**, *111* (7), 3090–3098.

(96) Weber-Bargioni, A.; Eichberger, M.; Schiffrin, A.; Kreuzer, H. J.; Barth, J. V.; Marschall, M.; Wang, R. L. C.; Auwärter, W.; Pennec, Y.; Reichert, J. Dimerization Boosts One-Dimensional Mobility of Conformationally Adapted Porphyrins on a Hexagonal Surface Atomic Lattice. *Nano Lett.* **2008**, *8* (12), 4608–4613.

(97) Liu, Z. Molecular Memories That Survive Silicon Device Processing and Real-World Operation. *Science (80-.).* **2003**, *302* (5650), 1543–1545.

(98) Roth, K. M.; Dontha, N.; Dabke, R. B.; Gryko, D. T.; Clausen, C.; Lindsey, J. S.; Bocian, D. F.; Kuhr, W. G. Molecular Approach toward Information Storage Based on the Redox Properties of Porphyrins in Self-Assembled Monolayers. *J. Vac. Sci. Technol. B Microelectron. Nanom. Struct.* **2000**, *18* (5), 2359.

(99) Roth, K. M.; Gryko, D. T.; Clausen, C.; Li, J.; Lindsey, J. S.; Kuhr, W. G.; Bocian, D. F. Comparison of Electron-Transfer and Charge-Retention Characteristics of Porphyrin-Containing Self-Assembled Monolayers Designed for Molecular Information Storage. *J. Phys. Chem. B* **2002**, *106* (34), 8639–8648.

(100) Roth, K. M.; Yasseri, A. A.; Liu, Z.; Dabke, R. B.; Malinovskii, V.; Schweikart, K. H.; Yu, L.; Tiznado, H.; Zaera, F.; Lindsey, J. S.; Kuhr, W. G.; Bocian, D. F. Measurements of Electron-Transfer Rates of Charge-Storage Molecular Monolayers on Si(100). Toward Hybrid Molecular/Semiconductor Information Storage Devices. *J. Am. Chem. Soc.* **2003**, *125* (2), 505–517.

(101) Pop, S.-F.; Ion, R.-M. Kinetic Parameters and Thermal Stability of Metalloporphyrins. In *Proc.SPIE, Advanced Topics in Optoelectronics, Microelectronics, and Nanotechnologies*; Constanta, 2012; Vol. 8411.

(102) Berezin, D. B.; Karimov, D. R.; Barannikov, V. P.; Semeikin, A. S. Thermal Stability of Porphyrins with Chemicaly Active NH Bond and Their Associates with Electron-Donor Solvents. *Russ. J. Phys. Chem. A* **2011**, *85* (12), 2171–2176.

(103) Cook, L. P.; Brewer, G.; Wong-Ng, W. Structural Aspects of Porphyrins for Functional Materials Applications. *Crystals* **2017**, *7* (7), 223.

(104) Tanaka, T.; Osuka, A. Conjugated Porphyrin Arrays: Synthesis, Properties and Applications for Functional Materials. *Chem. Soc. Rev.* **2015**, *44* (4), 943–969.

(105) Giuntini, F.; Alonso, C.; Boyle, R. W. Synthetic Approaches for the Conjugation of Porphyrins and Related Macrocycles to Peptides and Proteins. *Photochem. Photobiol. Sci.* **2011**, *10* (5), 759.

(106) Vilan, A.; Cahen, D. How Organic Molecules Can Control Electronic Devices. *Trends Biotechnol.* **2002**, *20* (1), 22–29.

(107) Koiry, S. P.; Jha, P.; Aswal, D. K.; Nayak, S. K.; Majumdar, C.; Chattopadhyay, S.; Gupta, S. K.; Yakhmi, J. V. Diodes Based on Bilayers Comprising of Tetraphenyl Porphyrin Derivative and Fullerene for Hybrid Nanoelectronics. *Chem. Phys. Lett.* **2010**, *485* (1–3), 137–141.

(108) Kuhr, W. G.; Gallo, A. R.; Manning, R. W.; Rhodine, C. W. Molecular Memories Based on a CMOS Platform. *MRS Bull.* **2004**, 838–842.

(109) Anderson, H. L. Building Molecular Wires from the Colours of Life: Conjugated Porphyrin Oligomers. *Chem. Commun.* **1999**, No. 23, 2323–2330.

(110) Al-Warhi, T. I.; Al-Hazimi, H. M. A.; El-Faham, A. Recent Development in Peptide Coupling Reagents. *J. Saudi Chem. Soc.* **2012**, *16* (2), 97–116.

(111) Valeur, E.; Bradley, M. Amide Bond Formation: Beyond the Myth of Coupling Reagents. *Chem. Soc. Rev.* **2009**, *38* (2), 606–631.

(112) Liu, H.; Duclairoir, F.; Fleury, B.; Dubois, L.; Chenavier, Y.; Marchon, J.-C. Porphyrin Anchoring on Si(100) Using a β-Pyrrolic Position. *Dalt. Trans.* **2009**, No. 19, 3793.

(113) Yamashige, H.; Matsuo, S.; Kurisaki, T.; Perera, R. C. C.; Wakita, H. Local Structure of Nitrogen Atoms in a Porphine Ring of Meso-Phenyl Substituted Porphyrin with an Electron-Withdrawing Group Using X-Ray Photoelectron Spectroscopy and X-Ray Absorption Spectroscopy. *Anal. Sci.* **2005**, *21* (6), 635–639.

(114) Lu, M.; Chen, B.; He, T.; Li, Y.; Tour, J. M. Synthesis, Grafting, and Film Formation of Porphyrins on Silicon Surfaces Using Triazenes. *Chem. Mater.* **2007**, *19* (18), 4447–4453.

(115) Stewart, M. P.; Maya, F.; Kosynkin, D. V.; Dirk, S. M.; Stapleton, J. J.; McGuiness, C. L.; Allara, D. L.; Tour, J. M. Direct Covalent Grafting of Conjugated Molecules onto Si, GaAs, and Pd Surfaces from Aryldiazonium Salts. *J. Am. Chem. Soc.* **2004**, *126* (1), 370–378.

(116) Huang, K.; Duclairoir, F.; Pro, T.; Buckley, J.; Marchand, G.; Martinez, E.; Marchon, J.-C.; De Salvo, B.; Delapierre, G.; Vinet, F. Ferrocene and Porphyrin Monolayers on Si(100) Surfaces: Preparation and Effect of Linker Length on Electron Transfer. *ChemPhysChem* **2009**, *10* (6), 963–971.

(117) Anariba, F.; Schmidt, I.; Muresan, A. Z.; Lindsey, J. S.; Bocian, D. F. Metal-Molecule Interactions upon Deposition of Copper Overlayers on Reactively Functionalized Porphyrin Monolayers on Si(100). *Langmuir* **2008**, *24* (13), 6698–6704.

(118) Liu, Z.; Yasseri, A. A.; Loewe, R. S.; Lysenko, A. B.; Malinovskii, V. L.; Zhao, Q.; Surthi, S.; Li, Q.; Misra, V.; Lindsey, J. S.; Bocian, D. F. Synthesis of Porphyrins Bearing Hydrocarbon Tethers and Facile Covalent Attachment to Si(100). *J. Org. Chem.* **2004**, *69* (17), 5568–5577.

(119) Anariba, F.; Tiznado, H.; Diers, J. R.; Schmidt, I.; Muresan, A. Z.; Lindsey, J. S.; Zaera, F.;

Bocian, D. F. Comprehensive Characterization of Hybrid Junctions Comprised of a Porphyrin Monolayer Sandwiched Between a Coinage Metal Overlayer and a Si(100) Substrate. *J. Phys. Chem. C* **2008**, *112* (25), 9474–9485.

(120) Padmaja, K.; Youngblood, W. J.; Wei, L.; Bocian, D. F.; Lindsey, J. S. Triple-Decker Sandwich Compounds Bearing Compact Triallyl Tripods for Molecular Information Storage Applications. *Inorg. Chem.* **2006**, *45* (14), 5479–5492.

(121) Gunnoo, S. B.; Madder, A. Chemical Protein Modification through Cysteine. *ChemBioChem* **2016**, *17* (7), 529–553.

(122) Stenzel, M. H. Bioconjugation Using Thiols: Old Chemistry Rediscovered to Connect Polymers with Nature's Building Blocks. *ACS Macro Lett.* **2013**, *2* (1), 14–18.

(123) Nair, D. P.; Podgórski, M.; Chatani, S.; Gong, T.; Xi, W.; Fenoli, C. R.; Bowman, C. N. The Thiol-Michael Addition Click Reaction: A Powerful and Widely Used Tool in Materials Chemistry. *Chem. Mater.* **2014**, *26* (1), 724–744.

(124) Singh, A. K.; Flounders, A. W.; Volponi, J. V; Ashley, C. S.; Wally, K.; Schoeniger, J. S. Development of Sensors for Direct Detection of Organophosphates. Part I: Immobilization, Characterization and Stabilization of Acetylcholinesterase and Organophosphate Hydrolase on Silica Supports. *Biosens. Bioelectron.* **1999**, *14*, 703–713.

(125) Chang, J.; Li, H.; Hou, T.; Duan, W.; Li, F. Paper-Based Fluorescent Sensor via Aggregation Induced Emission Fluorogen for Facile and Sensitive Visual Detection of Hydrogen Peroxide and Glucose. *Biosens. Bioelectron.* **2018**, *104*, 152–157.

(126) Achadu, O. J.; Nyokong, T. Graphene Quantum Dots Decorated with Maleimide and Zinc Tetramaleimido-Phthalocyanine: Application in the Design of " OFF-ON " Fluorescence Sensors for Biothiols. *Talanta* **2017**, *166*, 15–26.

(127) Cha, T.; Boiadjiev, V.; Lozano, J.; Yang, H.; Zhu, X. Immobilization of Oligonucleotides on Poly (Ethylene Glycol) Brush-Coated Si Surfaces. *Anal. Biochem.* **2002**, *311*, 27–32.

(128) Cattani-Scholz, A.; Pedone, D.; Dubey, M.; Neppl, S.; Nickel, B.; Feulner, Ḱ. P.; Schwartz, J.; Abstreiter, G.; Tornow, M. Organophosphonate-Based PNA-Functionalization of Silicon Nanowires for Label-Free DNA Detection. *ACS Nano* **2008**, *2* (8), 1653–1660.

(129) Strother, T.; Cai, W.; Zhao, X.; Hamers, R. J.; Smith, L. M. Synthesis and Characterization of DNA-Modified Silicon (111) Surfaces. *J. Am. Chem. Soc.* **2000**, *122* (6), 1205–1209.

(130) Haensch, C.; Hoeppener, S.; Schubert, U. S. Chemical Modification of Self-Assembled Silane Based Monolayers by Surface Reactions. *Chem. Soc. Rev.* **2010**, *39* (6), 2323–2334.

(131) Wang, A.; Tang, H.; Cao, T.; Salley, S. O.; Ng, K. Y. S. In Vitro Stability Study of

Organosilane Self-Assemble Monolayers and Multilayers. *J. Colloid Interface Sci.* **2005**, *291* (2), 438–447.

(132) Pujari, S. P.; Scheres, L.; Marcelis, A. T. M.; Zuilhof, H. Covalent Surface Modification of Oxide Surfaces. *Angew. Chem. Int. Ed. Engl.* **2014**, *53* (25), 6322–6356.

(133) Krasnoslobodtsev, A. V.; Smirnov, S. N. Effect of Water on Silanization of Silica by Trimethoxysilanes. *Langmuir* **2002**, *18* (8), 3181–3184.

(134) Silberzan, P.; Leger, L.; Ausserre, D.; Benattar, J. J. Silanation of Silica Surfaces. A New Method of Constructing Pure or Mixed Monolayers. *Langmuir* **1991**, *7* (8), 1647–1651.

(135) Jakša, G.; Štefane, B.; Kovač, J. Influence of Different Solvents on the Morphology of APTMS-Modified Silicon Surfaces. *Appl. Surf. Sci.* **2014**, *315* (1), 516–522.

(136) Kim, J.; Seidler, P.; Wan, L. S.; Fill, C. Formation, Structure, and Reactivity of Amino-Terminated Organic Films on Silicon Substrates. *J. Colloid Interface Sci.* **2009**, *329* (1), 114–119.

(137) Pasternack, R. M.; Rivillon Amy, S.; Chabal, Y. J. Attachment of 3-(Aminopropyl)Triethoxysilane on Silicon Oxide Surfaces: Dependence on Solution Temperature. *Langmuir* **2008**, *24* (22), 12963–12971.

(138) Kim, J.; Seidler, P.; Fill, C.; Wan, L. S. Investigations of the Effect of Curing Conditions on the Structure and Stability of Amino-Functionalized Organic Films on Silicon Substrates by Fourier Transform Infrared Spectroscopy, Ellipsometry, and Fluorescence Microscopy. *Surf. Sci.* **2008**, *602* (21), 3323–3330.

(139) Kim, J.; Holinga, G. J.; Somorjai, G. A. Curing Induced Structural Reorganization and Enhanced Reactivity of Amino-Terminated Organic Thin Films on Solid Substrates: Observations of Two Types of Chemically and Structurally Unique Amino Groups on the Surface. *Langmuir* **2011**, *27* (9), 5171–5175.

(140) Zhu, M.; Lerum, M. Z.; Chen, W. How to Prepare Reproducible, Homogeneous, and Hydrolytically Stable Aminosilane-Derived Layers on Silica. *Langmuir* **2012**, *28* (1), 416–423.

(141) Asenath Smith, E.; Chen, W. How To Prevent the Loss of Surface Functionality Derived from Aminosilanes. *Langmuir* **2008**, *24* (21), 12405–12409.

(142) Fadeev, A. Y.; McCarthy, T. J. Self-Assembly Is Not the Only Reaction Possible between Alkyltrichlorosilanes and Surfaces: Monomolecular and Oligomeric Covalently Attached Layers of Dichloro- and Trichloroalkylsilanes on Silicon. *Langmuir* **2000**, *16* (18), 7268–7274.

(143) Yu, C. H.; Huang, C. H.; Tan, C. S. A Review of CO2 Capture by Absorption and Adsorption. *Aerosol Air Qual. Res.* **2012**, *12* (5), 745–769.

(144) Acres, R. G.; Ellis, A. V.; Alvino, J.; Lenahan, C. E.; Khodakov, D. A.; Metha, G. F.; Andersson, G. G. Molecular Structure of 3-Aminopropyltriethoxysilane Layers Formed on Silanol-Terminated Silicon Surfaces. *J. Phys. Chem. C* **2012**, *116* (10), 6289–6297.

(145) Zhang, F.; Srinivasan, M. P. Self-Assembled Molecular Films of Aminosilanes and Their Immobilization Capacities. *Langmuir* **2004**, *20* (6), 2309–2314.

(146) Cao, C.; Zhang, Y.; Jiang, C.; Qi, M.; Liu, G. Advances on Aryldiazonium Salt Chemistry Based Interfacial Fabrication for Sensing Applications. *ACS Appl. Mater. Interfaces* **2017**, *9* (6), 5031–5049.

(147) Pinson, J.; Podvorica, F. Attachment of Organic Layers to Conductive or Semiconductive Surfaces by Reduction of Diazonium Salts. *Chem. Soc. Rev.* **2005**, *34* (5), 429.

(148) Allongue, P.; Delamar, M.; Desbat, B.; Fagebaume, O.; Hitmi, R.; Pinson, J.; Savéant, J. M. Covalent Modification of Carbon Surfaces by Aryl Radicals Generated from the Electrochemical Reduction of Diazonium Salts. *J. Am. Chem. Soc.* **1997**, *119* (1), 201–207.

(149) de Villeneuve, C. H.; Pinson, J.; Bernard, M. C.; Allongue, P. Electrochemical Formation of Close-Packed Phenyl Layers on Si(111). *J. Phys. Chem. B* **1997**, *101* (14), 2415–2420.

(150) Chaussé, A.; Chehimi, M. M.; Karsi, N.; Pinson, J.; Podvorica, F.; Vautrin-Ul, C. The Electrochemical Reduction of Diazonium Salts on Iron Electrodes. The Formation of Covalently Bonded Organic Layers and Their Effect on Corrosion. *Chem. Mater.* **2002**, *14* (1), 392–400.

(151) Bélanger, D.; Pinson, J. Electrografting: A Powerful Method for Surface Modification. *Chem. Soc. Rev.* **2011**, *40* (7), 3995.

(152) Buriak, J. M. Organometallic Chemistry on Silicon and Germanium Surfaces. *Chem. Rev.* **2002**, *102* (5), 1271–1308.

(153) Doppelt, P.; Hallais, G.; Pinson, J.; Podvorica, F.; Verneyre, S. Surface Modification of Conducting Substrates. Existence of Azo Bonds in the Structure of Organic Layers Obtained from Diazonium Salts. *Chem. Mater.* **2007**, *19* (18), 4570–4575.

(154) Adenier, A.; Combellas, C.; Kanoufi, F.; Pinson, J.; Podvorica, F. I. Formation of Polyphenylene Films on Metal Electrodes by Electrochemical Reduction of Benzenediazonium Salts. *Chem. Mater.* **2006**, *18* (8), 2021–2029.

(155) Anariba, F.; DuVall, S. H.; McCreery, R. L. Mono-and Multilayer Formation by Diazonium Reduction on Carbon Surfaces Monitored with Atomic Force Microscopy "Scratching." *Anal. Chem.* **2003**, *75* (15), 3837–3844.

(156) Combellas, C.; Jiang, D. E.; Kanoufi, F.; Pinson, J.; Podvorica, F. I. Steric Effects in the

Reaction of Aryl Radicals on Surfaces. *Langmuir* **2009**, *25* (1), 286–293.

(157) Combellas, C.; Kanoufi, F.; Pinson, J.; Podvorica, F. I. Sterically Hindered Diazonium Salts for the Grafting of a Monolayer on Metals Scheme 1. Electrografting of Diazonium Salts and Formation of (a) Multilayer and (b) Monolayer. *J. Am. Chem. Soc* **2008**, *130*, 8576–8577.

(158) Zhang, X.; Rösicke, F.; Syritski, V.; Sun, G.; Reut, J.; Hinrichs, K.; Janietz, S.; Rappich, J. Influence of the Para-Substitutent of Benzene Diazonium Salts and the Solvent on the Film Growth during Electrochemical Reduction. *Zeitschrift fur Phys. Chemie* **2014**, *228* (4–5), 557–573.

(159) Menanteau, T.; Dias, M.; Levillain, E.; Downard, A. J.; Breton, T. Electrografting via Diazonium Chemistry: The Key Role of the Aryl Substituent in the Layer Growth Mechanism. *J. Phys. Chem. C* **2016**, *120* (8), 4423–4429.

(160) Saby, C.; Ortiz, B.; Champagne, G. Y.; Bélanger, D. Electrochemical Modification of Glassy Carbon Electrode Using Aromatic Diazonium Salts. 1. Blocking Effect of 4-Nitrophenyl and 4-Carboxyphenyl Groups. *Langmuir* **1997**, *13* (25), 6805–6813.

(161) Ricci, A. M.; Méndez De Leo, L. P.; Williams, F. J.; Calvo, E. J. Some Evidence for the Formation of an Azo Bond during the Electroreduction of Diazonium Salts on Au Substrates. *ChemPhysChem* **2012**, *13* (8), 2119–2127.

(162) Combellas, C.; Jiang, D.; Kanoufi, F.; Pinson, J.; Podvorica, F. I. Supporting Information Steric Effects in the Reaction of Aryl Radicals on Sufaces. **2009**, No. 31, 1–12.

(163) Korte, E. H.; Röseler, A. Infrared Spectroscopic Ellipsometry: A Tool for Characterizing Nanometer Layers. *Analyst* **1998**, *123* (4), 647–651.

(164) Angermann, H.; Henrion, W.; Rebien, M.; Fischer, D.; Zettler, J.-T.; Röseler, A. H-Terminated Silicon: Spectroscopic Ellipsometry Measurements Correlated to the Surface Electronic Properties. *Thin Solid Films* **1998**, *313–314*, 552–556.

(165) Korte, E. H.; Schade, U.; Peatman, W. B.; Röseler, A.; Tsankov, D.; Hinrichs, K. Infrared Ellipsometric View on Monolayers: Towards Resolving Structural Details. *Anal. Bioanal. Chem.* **2002**, *374* (4), 665–671.

(166) Losurdo, M.; Bergmair, M.; Bruno, G.; Cattelan, D.; Cobet, C.; De Martino, A.; Fleischer, K.; Dohcevic-Mitrovic, Z.; Esser, N.; Galliet, M.; Gajic, R.; Hemzal, D.; Hingerl, K.; Humlicek, J.; Ossikovski, R.; Popovic, Z. V.; Saxl, O. Spectroscopic Ellipsometry and Polarimetry for Materials and Systems Analysis at the Nanometer Scale: State-of-the-Art, Potential, and Perspectives. *J. Nanoparticle Res.* **2009**, *11* (7), 1521–1554.

(167) Hook, F. F.; Vörös, J.; Rodahl, M.; Kurrat, R.; Böni, P.; Ramsden, J. J.; Textor, M.; Spencer, N. D.; Tengvall, P.; Gold, J.; Kasemo, B. A Comparative Study of Protein Adsorption on

Titanium Oxide Surfaces Using in Situ Ellipsometry, Optical Waveguide Lightmode Spectroscopy, and Quartz Crystal Microbalance/Dissipation. *Colloids Surfaces B Biointerfaces* **2002**, *24* (2), 155–170.

(168) Christensen, P. A.; Hamnett, A. In Situ Spectroscopic Investigations of the Growth, Electrochemical Cycling and Overoxidation of Polypyrrole in Aqueous Solution. *Electrochim. Acta* **1991**, *36* (8), 1263–1286.

(169) Arwin, H. Ellipsometry on Thin Organic Layers of Biological Interest: Characterization and Applications. *Thin Solid Films* **2000**, *377–378*, 48–56.

(170) Mikhaylova, Y.; Ionov, L.; Rappich, J.; Gensch, M.; Esser, N.; Minko, S.; Eichhorn, K. J.; Stamm, M.; Hinrichs, K. In Situ Infrared Ellipsometric Study of Stimuli-Responsive Mixed Polyelectrolyte Brushes. *Anal. Chem.* **2007**, *79* (20), 7676–7682.

(171) Gersten, J. I.; Smith, F. W. *The Physics and Chemistry of Materials*; New York, 2001.

(172) Yeh, J. J.; Lindau, I. Atomic Subshell Photoionization Cross Sections And Asymmetry Parameters. *At. Data Nucl. Data Tables* **1985**, *32* (l), 1–155.

(173) Proctor, A.; Sherwood, P. M. A. Data Analysis Techniques in X-Ray Photoelectron Spectroscopy. *Anal. Chem.* **1982**, *54* (1), 13–19.

(174) Aissaoui, N.; Bergaoui, L.; Landoulsi, J.; Lambert, J.-F.; Boujday, S. Silane Layers on Silicon Surfaces: Mechanism of Interaction, Stability, and Influence on Protein Adsorption. *Langmuir* **2012**, *28* (1), 656–665.

(175) White, L. D.; Tripp, C. P. Reaction of (3-Aminopropyl)Dimethylethoxysilane with Amine Catalysts on Silica Surfaces. *J. Colloid Interface Sci.* **2000**, *232* (2), 400–407.

(176) Milekhin, A.; Friedrich, M.; Hiller, K.; Wiemer, M.; Gessner, T.; Zahn, D. R. T. Infrared Study of Si Surfaces and Bonded Si Wafers. *Semicond. Sci. Technol.* **1999**, *14* (1), 70–73.

(177) Asay, D. B.; Kim, S. H. Evolution of the Adsorbed Water Layer Structure on Silicon Oxide at Room Temperature. *J. Phys. Chem. B* **2005**, *109* (35), 16760–16763.

(178) Balakumar, A.; Lysenko, A. B.; Carcel, C.; Malinovskii, V. L.; Gryko, D. T.; Schweikart, K. H.; Loewe, R. S.; Yasseri, A. A.; Liu, Z.; Bocian, D. F.; Lindsey, J. S. Diverse Redox-Active Molecules Bearing O-, S-, or Se-Terminated Tethers for Attachment to Silicon in Studies of Molecular Information Storage. *J. Org. Chem.* **2004**, *69* (5), 1435–1443.

(179) Knorr, D. B.; Williams, K. S.; Baril, N. F.; Weiland, C.; Andzelm, J. W.; Lenhart, J. L.; Woicik, J. C.; Fischer, D. A.; Tidrow, M. Z.; Bandara, S. V.; Henry, N. C. Use of 3-Aminopropyltriethoxysilane Deposited from Aqueous Solution for Surface Modification of III-V Materials. *Appl. Surf. Sci.* **2014**, *320*, 414–428.

(180) Tian, R.; Seitz, O.; Li, M.; Hu, W.; Chabal, Y. J.; Gao, J. Infrared Characterization of Interfacial Si-O Bond Formation on Silanized Flat SiO2/Si Surfaces. *Langmuir* **2010**, *26* (7), 4563–4566.

(181) Bouden, S.; Pinson, J.; Vautrin-Ul, C. Electrografting of Diazonium Salts: A Kinetics Study. *Electrochem. commun.* **2017**, *81* (October), 120–123.

(182) Mangeney, C.; Qin, Z.; Dahoumane, S. A.; Adenier, A.; Herbst, F.; Boudou, J. P.; Pinson, J.; Chehimi, M. M. Electroless Ultrasonic Functionalization of Diamond Nanoparticles Using Aryl Diazonium Salts. *Diam. Relat. Mater.* **2008**, *17* (11), 1881–1887.

(183) Bouriga, M.; Chehimi, M. M.; Combellas, C.; Decorse, P.; Kanoufi, F.; Deronzier, A.; Pinson, J. Sensitized Photografting of Diazonium Salts by Visible Light. *Chem. Mater.* **2013**, *25* (1), 90–97.

(184) Karousis, N.; Economopoulos, S. P.; Iizumi, Y.; Okazaki, T.; Liu, Z.; Suenaga, K.; Tagmatarchis, N. Microwave Assisted Covalent Functionalization of C60@SWCNT Peapods. *Chem. Commun.* **2010**, *46* (48), 9110–9112.

(185) Masheter, A. T.; Wildgoose, G. G.; Crossley, A.; Jones, J. H.; Compton, R. G. A Facile Method of Modifying Graphite Powder with Aminophenyl Groups in Bulk Quantities. *J. Mater. Chem.* **2007**, *17* (29), 3008–3014.

(186) Mévellec, V.; Roussel, S.; Tessier, L.; Chancolon, J.; Mayne-L'Hermite, M.; Deniau, G.; Viel, P.; Palacin, S. Grafting Polymers on Surfaces: A New Powerful and Versatile Diazonium Salt-Based One-Step Process in Aqueous Media. *Chem. Mater.* **2007**, *19* (25), 6323–6330.

(187) Mesnage, A.; Esnouf, S.; Jégou, P.; Deniau, G.; Palacin, S. Understanding the Redox-Induced Polymer Grafting Process: A Dual Surface-Solution Analysis. *Chem. Mater.* **2010**, *22* (23), 6229–6239.

(188) Adenier, A.; Cabet-Deliry, E.; Chaussé, A.; Griveau, S.; Mercier, F.; Pinson, J.; Vautrin-Ul, C. Grafting of Nitrophenyl Groups on Carbon and Metallic Surfaces without Electrochemical Induction. *Chem. Mater.* **2005**, *17* (3), 491–501.

(189) Cullen, R. J.; Jayasundara, D. R.; Soldi, L.; Cheng, J. J.; Dufaure, G.; Colavita, P. E. Spontaneous Grafting of Nitrophenyl Groups on Amorphous Carbon Thin Films: A Structure-Reactivity Investigation. *Chem. Mater.* **2012**, *24* (6), 1031–1040.

(190) Shi, L.; Sun, T.; Yan, Y.; Zhao, J.; Dong, S. Fabrication of Functional Structures at Si (100) Surface by Mechanical Scribing in the Presence of Aryl Diazonium Salts. *J. Vac. Sci. Technol. B Microelectron. Nanom. Struct. Process. Meas. Phenom.* **2009**, *27* (3), 1399–1402.

(191) Mesnage, A.; Lefèvre, X.; Jégou, P.; Deniau, G.; Palacin, S. Spontaneous Grafting of Diazonium Salts: Chemical Mechanism on Metallic Surfaces. *Langmuir* **2012**, *28* (32), 11767–

11778.

(192) Berisha, A.; Combellas, C.; Kanoufi, F.; Decorse, P.; Oturan, N.; Médard, J.; Seydou, M.; Maurel, F.; Pinson, J. Some Theoretical and Experimental Insights on the Mechanistic Routes Leading to the Spontaneous Grafting of Gold Surfaces by Diazonium Salts. *Langmuir* **2017**, *33* (35), 8730–8738.

APPENDIX 1: SUPPLEMENTARY FIGURES TO CHAPTER 5 (S5.1 - S5.2)

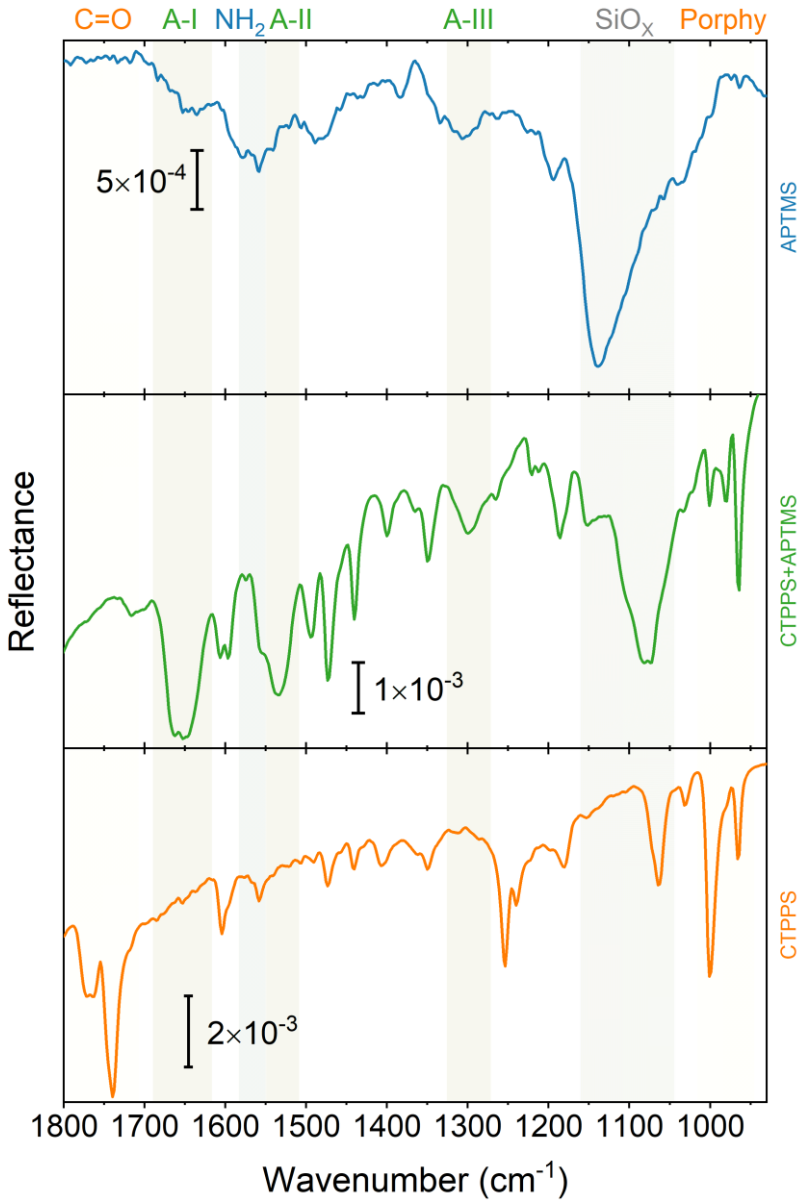

Figure S5.1: *Spectra of solution reaction of CTTPS and APTMS compared with the spectra of all starting materials.*

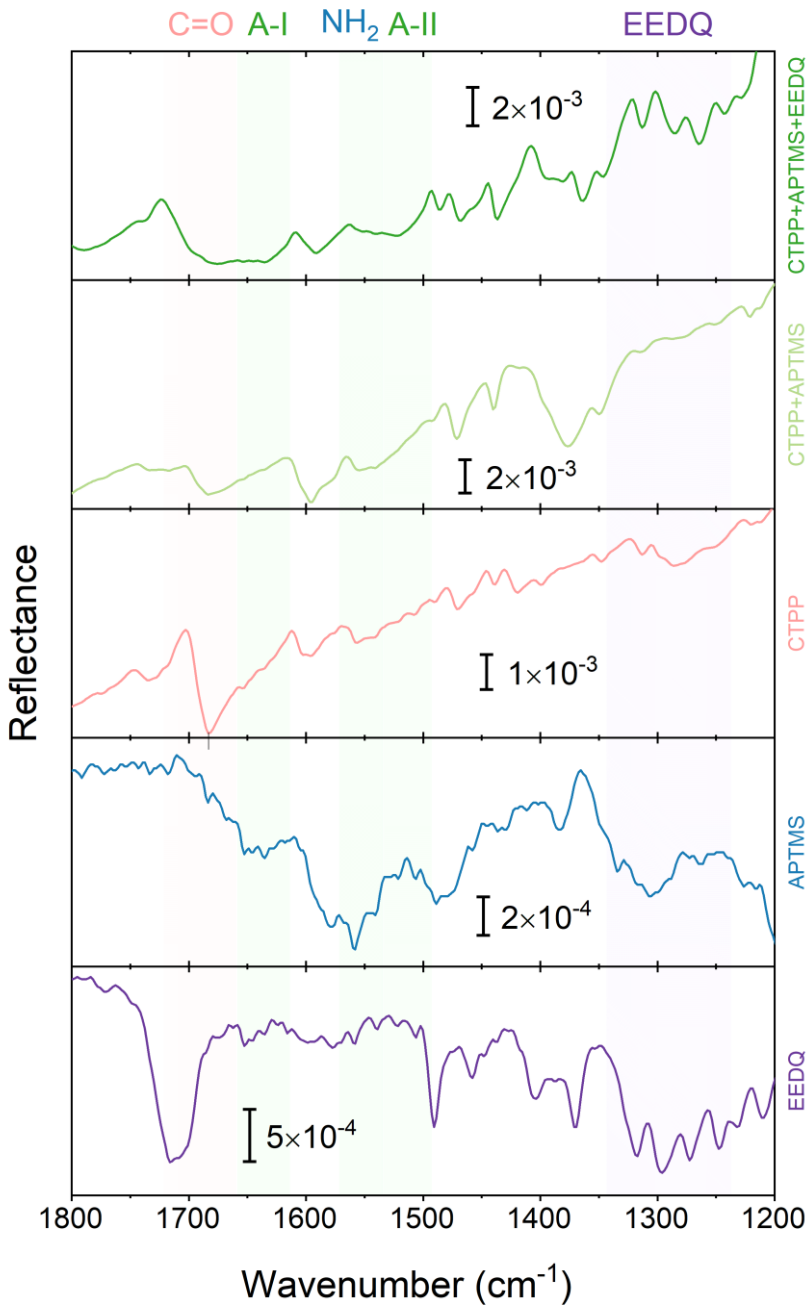

Figure S5.2: *Spectra of solution reaction of CTTP and APTMS, with and without the use of EEDQ compared with the spectra of all starting materials.*

APPENDIX 2: SUPPLEMENTARY FIGURES TO CHAPTER 6 (A6.1 - A6.6)

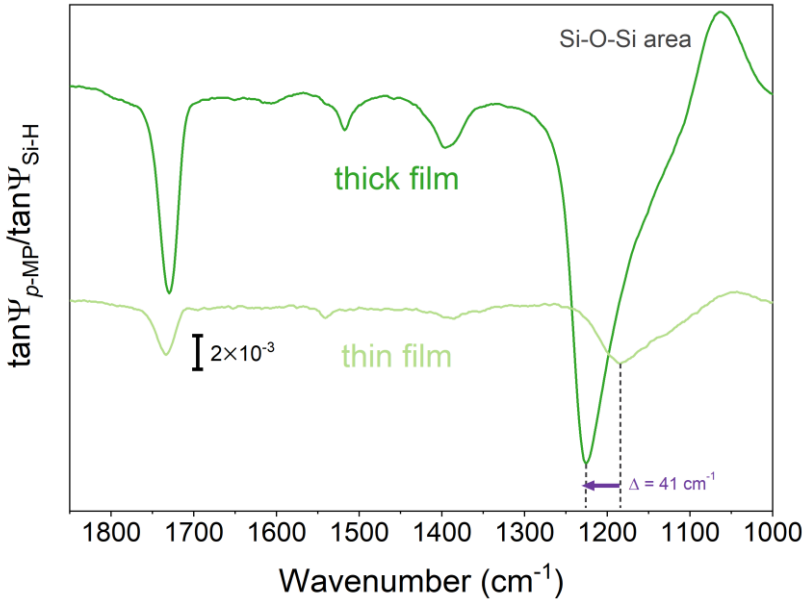

Figure S6.1: *Comparison of LO bands in thick (deposition time, t = 600 s) and thin (t = 10 s) p-MP layers on a silicon substrate.*

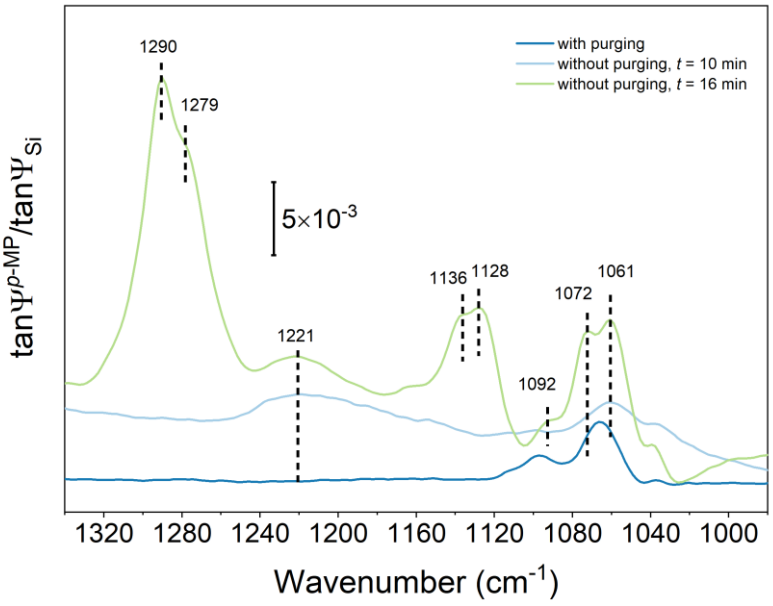

Figure S6.2: *Changes in Si-O-Si area depending on deposition times and with deposition time purging conditions of an electrochemical cell. a) Si-O-Si area when the cell is purged for two hours with dry air before pumping in of the reactive solution; b) and c) Si-O-Si area without cell purging with deposition times, t = 10 min and 16 min, respectively.*

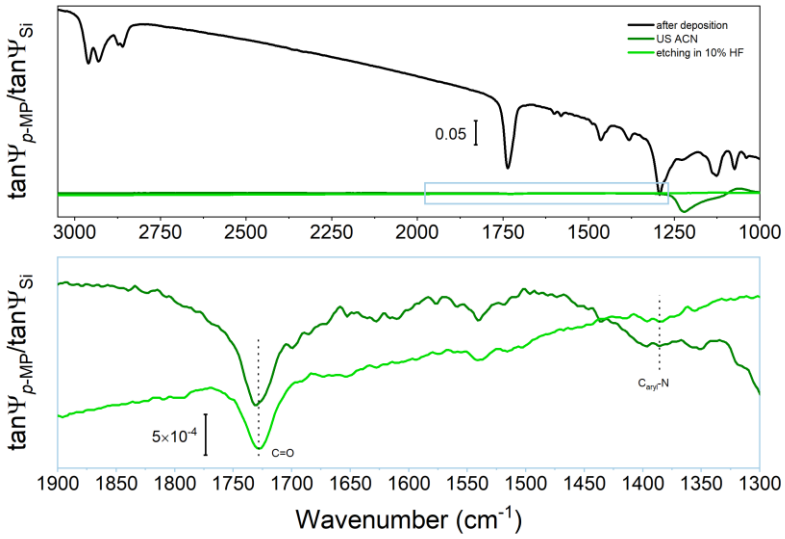

Figure S6.3: *a) p-MP spectra after deposition; b) solvent wash; c) etching in 10% HF.*

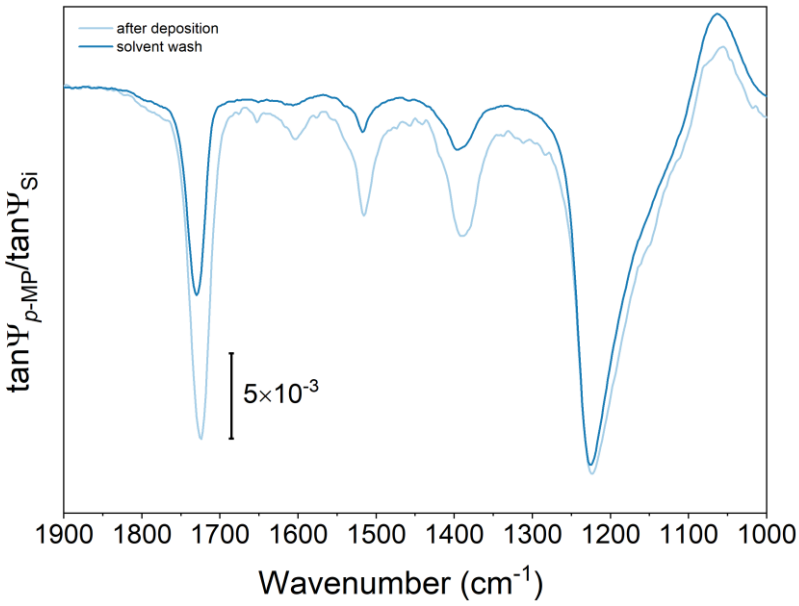

Figure S6.4: *The solvent wash of p-MP-modified substrate (water, ACN, and isopropanol).*

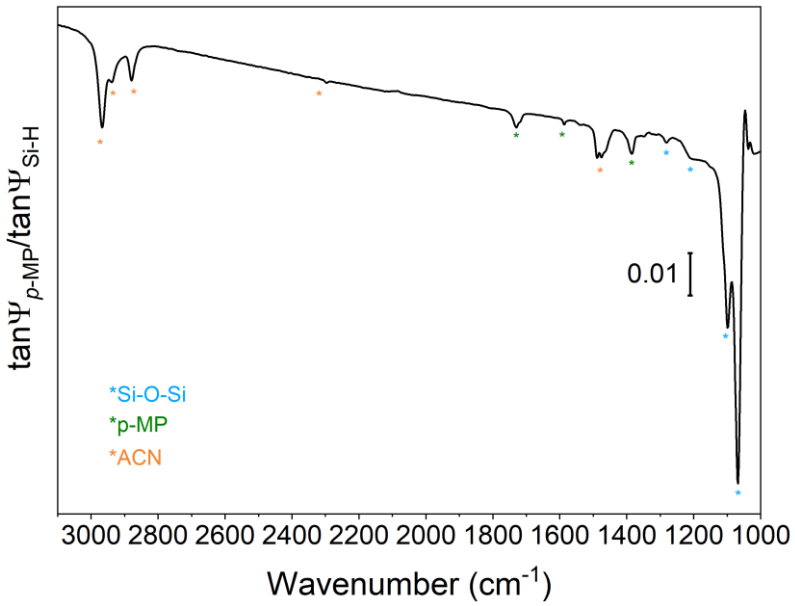

Figure S6.5: *Spectral bands of acetonitrile on p-MP modified Si.*

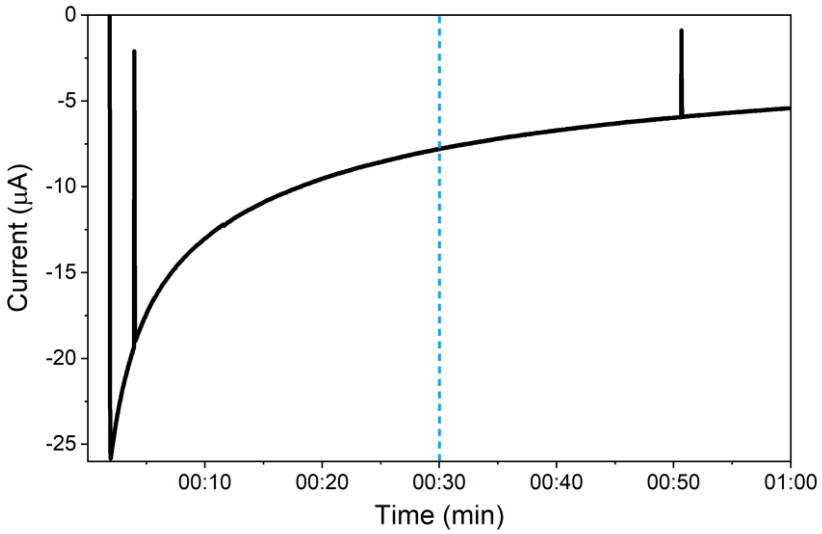

Figure S6.6: *Chronoamperometry of p-MPDS.*

PUBLICATIONS

1) K. Lovrek, K. Rademann, *Covalently attached maleimide and porphyrin on silicon for use in sensing and microelectronics*, Advanced Functional Materials, 2019 (currently under peer review)

CONTRIBUTIONS AT ACADEMIC CONFERENCES

1) 2016 (**Poster**), SALSA Poster Session, K. Lovrek, K. Rademann, et al., *Deposition of small anchor molecules for binding of porphyrin thin films*, Berlin, Germany

2) 2016 (**Poster**), 10th International Summer School on Nanosciences and Nanotechnologies, K. Lovrek, K. Rademann, et al., *Deposition of small linker molecules for binding of porphyrin thin films*, Thessaloniki, Greece

3) 2016 (**Talk**), K. Lovrek, K. Rademann, et al., *Optical and structural properties of electrochemically prepared porphyrin thin films*, 80th Annual Meeting of DPG, Regensburg, Germany

ACKNOWLEDGMENTS

I want to express my deepest gratitude and admiration to my supervisor, Prof. Dr. Klaus Rademann, for his continuous support throughout my doctoral studies. His expert guidance and patience helped me throughout this challenging experience. I am truly indebted to him and humbled for his commitment and kindness at the toughest of times, and the faith he had in me to complete this journey.

I extend my appreciation to Prof. Dr. Kannan Balasubramanian and Prof. Dr. Norbert Esser for acting as reviewers of my thesis, as well as Dr. Franziska Emmerling and Prof. Dr. Emil List-Kratochvil for accepting the roles of committee members.

I want to thank PD Dr. Karsten Hinrichs for giving me the opportunity to conduct my research at ISAS Berlin, for his expert advice, and support he has given me throughout the experimental phase of the project.

I want to thank the German Excellence Initiative of the German Research Society (project GSC 1013) for financial support.

I want to give my thanks to our collaborators at Fraunhofer Institute for Applied Polymer Research for providing the samples of maleimidophenyldiazonium salt, Fritz-Haber Institute of Max Planck Society for the XPS measurements, and Institute for Silicon Photovoltaics of Helmholtz Zentrum Berlin for supplying equipment for electrochemical experiments. Special thanks go to Dr. Jörg Rappich of HZB for engaging discussions about chemistry and for providing his expertise on all things electrochemistry.

I gratefully acknowledge the team at SALSA for their continuous support and being there every step of the way, and for kindly providing me with professional support, as well as the office space. I very much enjoyed my time at grad school, and the immersive experience of interdisciplinarity and internationality it provided for their students.

Many thanks go to the in situ IR spectroscopy group at ISAS: Dr. Andreas Furchner, Dr. Dimitra Gkogkou, Özgür Savaş, Dr. Timur Shaykhutdinov, Dr. Christoph Kratz, Dr. Cordula Walder, and Ilona Engler for a great working atmosphere, helpful discussions, and technical support in the laboratory. I would also like to thank the technical staff and all my colleagues at ISAS Berlin for a friendly atmosphere.

I sincerely thank my family and close friends for support and kindness throughout the entire journey of my higher education. Words cannot describe the appreciation I have for knowing that I have in my life, people who are always there no matter what, and whose priority above all is my well-being.

I am especially grateful to my SALSA peers for many interesting discussions, shared laughs and anxieties, and being the only people who "get it." To my *Salsitas*, Vesna Živanović, Marija Vranić, Melissa-Jane Monks, Christine Querebillo, and Clara Marshall, thank you for all the laughing sessions, many coffees, and understanding for missing out on coffees. Special thanks to my "big sister" and a "work wife," Dimitra Gkogkou, for keeping me on track, while also matching my sense of humor.

Above all, I am grateful to the person who has been there for me every step of the way and, therefore, should be given an honorary doctorate, Matko Smoljan. I thank you for your constant support, undying patience, and growing up and figuring out life together.

STATEMENT OF AUTHORSHIP

I declare that I have completed the thesis independently, using only the aids and tools specified. I have not applied for a doctor's degree in the doctoral subject elsewhere and do not hold a corresponding doctor's degree. I have taken due note of the Faculty of Mathematics and Natural Sciences Ph.D. Regulations, published in the Official Gazette of Humboldt-Universität zu Berlin no. 126/2014 on 18/11/2014.